



# THE UNIVERSITY *of* EDINBURGH

This thesis has been submitted in fulfilment of the requirements for a postgraduate degree (e.g. PhD, MPhil, DClinPsychol) at the University of Edinburgh. Please note the following terms and conditions of use:

This work is protected by copyright and other intellectual property rights, which are retained by the thesis author, unless otherwise stated.

A copy can be downloaded for personal non-commercial research or study, without prior permission or charge.

This thesis cannot be reproduced or quoted extensively from without first obtaining permission in writing from the author.

The content must not be changed in any way or sold commercially in any format or medium without the formal permission of the author.

When referring to this work, full bibliographic details including the author, title, awarding institution and date of the thesis must be given.



---

ELUCIDATING THE RNA-  
BINDING MECHANISMS  
AND FUNCTIONS OF E3  
UBIQUITIN LIGASE TRIM25  
IN CELL BIOLOGY AND  
INNATE IMMUNITY

---

Gregory Heikel



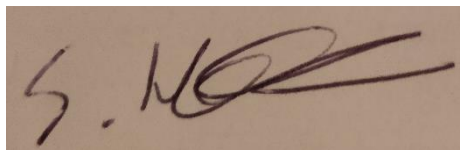
THE UNIVERSITY  
*of* EDINBURGH

JUNE 1, 2019

## Declarations

I declare that the thesis has been composed by myself and that the work has not been submitted for any other degree or professional qualification. I confirm that the work submitted is my own, except where work which has formed part of jointly-authored publications has been included. My contribution and those of the other authors to this work have been explicitly indicated in the text. I confirm that appropriate credit has been given within this thesis where reference has been made to the work of others

The data presented in Results Chapter 1, figures 8-12 and Results Chapter 2, figures 14 and 15 have previously been published in BioMed Central Biology **15**:105 (11/17) as article “RNA-binding activity of TRIM25 is mediated by its PRY/SPRY domain and is required for ubiquitination” by authors Nila Roy Choudhury, **Gregory Heikel**, Maryia Trubitsyna, Peter Kubik, Jakub Stanislaw Nowak, Shaun Webb, Sander Granneman, Christos Spanos, Juri Rappsilber, Alfredo Castello and Gracjan Michlewski.

A handwritten signature in dark ink on a light brown background. The signature is stylized and appears to read 'G. Heikel'.

Gregory Heikel

June 2019

## Acknowledgements

I would like to thank my supervisor Dr Gracjan Michlewski for his support and supervision, as well as for being a constant source of ideas and advice on where to take my research. I would also like to thank the other members of the Michlewski group; Dr Nila Roy Choudhury for her constant help and abnormal patience and Angela Downie for cheering me up when things were difficult.

I would like to thank Paul Digard and all of the members of his lab, especially Eleanor Gaunt, Rute Maria Pinto and Nikki Smith for their help and ideas. In addition, I would also like to thank our collaborator Alfredo Castello.

I would like to acknowledge the Wellcome Trust for their financial contribution to this project.

*“That just goes to show that you never know, although what it is we never know I suspect we’ll never know.”*

*Terry Pratchett, Snuff*

# Table of Contents

|   |    |
|---|----|
| <b>Declarations</b> .....   | 1  |
| <b>Acknowledgements</b> .....   | 2  |
| <b>Abstract</b> .....   | 7  |
| <b>Lay Summary</b> .....  | 8  |
| <b>Glossary of Abbreviations</b> .....  | 9  |
| <b>Introduction</b> .....   | 12 |
| The innate immune system is the first line of defence against viral infection .....                             | 12 |
| <i>Viruses have a large impact on human health and society</i> .....  | 12 |
| <i>Influenza A is an RNA virus with a large impact on human health</i> .....                                    | 14 |
| <i>The innate immune system defends against viral pathogens</i> .....   | 18 |
| RIG-I is a key PRR in the recognition of RNA viruses.....   | 24 |
| <i>RIG-I and MDA5 are cytosolic PRRs that recognise viral RNA</i> .....   | 24 |
| <i>RIG-I signalling is activated upon binding to 5'ppp-RNA</i> .....  | 27 |
| <i>K63-linked polyubiquitination of the RIG-I 2CARD may be performed by multiple E3 ubiquitin ligases</i> ..... | 29 |
| <i>RIG-I signalling is targeted for inhibition by many viruses</i> .....  | 32 |
| The E3 ubiquitin ligase TRIM25 has many different roles .....   | 37 |
| <i>TRIM family proteins are E3 ubiquitin ligases</i> .....  | 37 |
| <i>Many TRIM family proteins are involved in innate immune responses</i> .....                                  | 38 |
| <i>TRIM25 has other cellular roles and has been implicated in some cancers</i> .....                            | 40 |
| <i>TRIM25 is an RNA-binding protein</i> .....   | 45 |
| Aims .....  | 50 |
| <b>Materials and Methods</b> .....  | 52 |
| Primers .....   | 52 |
| <i>Templates for In Vitro Transcription</i> .....   | 52 |
| <i>Sequencing</i> .....   | 52 |
| <i>qRT-PCR</i> .....  | 53 |
| RNA Sequences .....   | 54 |
| Antibodies .....  | 55 |
| Buffers .....   | 55 |
| <i>In Vitro</i> Transcription and RNA Purification.....   | 56 |
| Cell culture and transfections .....  | 57 |

|  |    |
|--|----|
| Protein extraction .....   | 58 |
| RNA extraction .....   | 58 |
| Western blots.....   | 59 |
| quantitative Real Time Polymerase Chain Reaction (qRT-PCR).....  | 60 |
| RNA pulldown .....   | 60 |
| Protein purification .....   | 62 |
| <i>Buffers</i> .....   | 62 |
| <i>Method</i> .....  | 62 |
| RNA Footprinting/Structure Probing .....   | 63 |
| EMSA.....  | 64 |
| Thermal Denaturation Assays.....   | 64 |
| RNA Immunoprecipitation (RIP).....   | 64 |
| SEC-MALS .....   | 65 |
| Immunoprecipitation (IP).....  | 65 |
| <i>In Vitro</i> Ubiquitination .....   | 66 |
| Generation of Knockout Cell Lines.....   | 66 |
| Gene Sequencing .....  | 67 |
| RNA Stability Assays.....  | 67 |
| RNAseq.....  | 68 |
| IAV Reverse Genetics .....   | 68 |
| Plaque Assays.....   | 70 |
| Infection of Cells with IAV .....  | 70 |
| 3p-hpRNA Assays .....  | 71 |
| <i>Western Blot and HEKBlue Assays</i> .....   | 71 |
| <i>Luciferase Assays</i> .....   | 71 |
| Minireplicon Assays .....  | 72 |
| <b>Results</b> .....   | 73 |
| Chapter 1 - Determining the mechanism of TRIM25 binding to RNA.....                                    | 73 |
| <i>Aims</i> .....  | 73 |
| <i>The GGAGAU motif of pre-let-7a is not necessary for TRIM25 RNA-binding</i> .....                    | 74 |
| <i>Mutating a potential TRIM25 binding site on pre-let-7a-1 does not reduce binding</i> ....           | 75 |
| <i>Amino acids 470-508 in the PRY/SPRY domain of TRIM25 contribute to RNA binding</i> .                | 80 |
| <i>Two intact TRIM25-PRY/SPRY domains in a dimer are likely important for TRIM25 RNA binding</i> ..... | 84 |
| <i>TRIM25 requires RNA binding for efficient auto-ubiquitination</i> .....                             | 89 |

|  |     |
|--|-----|
| <i>Conclusions</i> .....   | 94  |
| Chapter 2 – Generation of TRIM25 KO HeLa and HEK293 cells.....   | 96  |
| <i>Aims</i> .....  | 96  |
| <i>HeLa TRIM25 KO cells were generated by CRISPR</i> .....   | 98  |
| <i>HEK293 TRIM25 KO cells were generated by CRISPR</i> .....   | 103 |
| <i>TRIM25 was reintegrated into the HEK293 TRIM25 KO genome using the Flp-In system</i><br>.....                                 | 103 |
| <i>Conclusions</i> .....   | 107 |
| Chapter 3 – Analysis of changes in RNA and protein levels in HeLa TRIM25 KO cells.....   | 109 |
| <i>Aims</i> .....  | 109 |
| <i>Stability of cMyc and ZAP mRNAs is not affected by loss of TRIM25</i> .....   | 110 |
| <i>Levels of SUB1 mRNA decrease upon loss of TRIM25 in HeLa cells</i> .....  | 112 |
| <i>RNAseq identifies changes in RNA levels in HeLa TRIM25 KO cells</i> .....   | 112 |
| <i>Abundance of very few proteins is changed by loss of TRIM25</i> .....   | 120 |
| <i>Expression of SERPINB5 is substantially reduced in HeLa TRIM25 KO cells</i> .....   | 121 |
| <i>Conclusions</i> .....   | 126 |
| Chapter 4 – The role of TRIM25 in viral infection.....   | 128 |
| <i>Aims</i> .....  | 128 |
| <i>HEK293 TRIM25 KO cells are more permissive to an NS1 deficient IAV than HEK293 WT cells</i> .....                             | 129 |
| <i>PR8 NS1 R38K41A restriction is rescued by TRIM25 WT, TRIM25<math>\Delta</math>RBD and TRIM25<math>\Delta</math>RING</i> ..... | 132 |
| <i>Deletion of TRIM25 does not reduce activation of RIG-I signalling upon 5'ppp-RNA transfection in HEK293 cells</i> .....       | 135 |
| <i>TRIM25 deletion compromises RIG-I activity in response to 5'pppRNA transfection in MEF, but not HeLa, cells</i> .....         | 138 |
| <i>TRIM25 does not inhibit IAV RNA polymerase in HEK293 cells</i> .....  | 140 |
| <i>Conclusions</i> .....   | 145 |
| <b>Discussion</b> .....  | 147 |
| <i>The PRY/SPRY domain is the main determinant of TRIM25 RNA binding</i> .....   | 147 |
| <i>Other PRY/SPRY containing proteins could bind to RNA</i> .....  | 149 |
| <i>TRIM25 requires RNA binding for its E3 ubiquitin ligase activity</i> .....  | 150 |
| <i>TRIM25 binding to mRNAs at steady state does not have a general effect on RNA or protein stability</i> .....                  | 152 |
| <i>TRIM25 is not required for RIG-I signalling in HEK293 cells</i> .....   | 153 |
| <i>TRIM25 and direct restriction of IAV</i> .....  | 155 |

|                                 |     |
|---------------------------------|-----|
| <i>Concluding Remarks</i> ..... | 157 |
| <b>References</b> .....         | 159 |



## Abstract

Pathogenic viruses have a huge impact on human health and have caused numerous major epidemics both in the past and during the 21st century. The innate immune system is the body's first line of defence against viruses, with pattern recognition receptors recognising molecules unique to viruses and triggering the expression of interferons and other anti-viral cytokines, leading to the formation of an anti-viral state. The Tripartite Motif Containing 25 (TRIM25) is an E3 ubiquitin ligase thought to be a key component in the activation of signalling by the pattern recognition receptor Retinoic Acid-Inducible Gene I Protein (RIG-I), which recognises viral RNAs with a 5'-triphosphate moiety. TRIM25 has recently been identified as an RNA-binding protein, raising the question of whether its RNA-binding activity is important for its role in innate immunity. In this thesis, I demonstrated that TRIM25's RNA-binding activity is mediated by its C-terminal PRY/SPRY domain and is required for its E3 ligase activity. I also generated TRIM25 knockout cells using a CRISPR/Cas9 strategy in HeLa and HEK293 cell lines and showed that deletion of TRIM25 does not generally affect levels of the mRNA binding partners of TRIM25 identified by a genome-wide Cross-Linking Immunoprecipitation (CLIP) screen. Finally, I showed that although deletion of TRIM25 in HEK293 cells reduced their ability to restrict Influenza A virus infection, it did not affect activation of RIG-I signalling pathway in response to 5'-triphosphate RNA. This suggests that TRIM25 is redundant for RIG-I signalling in HEK293 cells and its role in restricting Influenza A virus infection is unrelated to its role in the RIG-I pathway. These findings have opened new lines of investigations into functional and molecular roles of TRIM25 in cell biology and control of pathogenic infections and I have generated tools to aid in these investigations.

## Lay Summary

Infections by pathogens such as viruses or bacteria have a huge impact on global health. Viruses are an enormous class of pathogens, and millions die every year from a variety of viral infections. Some of the worst epidemics in recent years have been caused by viruses such as Ebola and Influenza. The body has developed many ways of protecting itself from viruses and other pathogens and together these are known as the immune system, which is further divided into adaptive and innate immunity. This project focused on innate immunity. This consists of a group of specialist 'receptor' proteins that can recognise molecules that are present in pathogens but not in humans. One of these molecules is called 5 prime triphosphate ribonucleic acid (5'ppp-RNA). RNA is present and plays an important role in the body's processes, but human RNA does not have the 5 prime triphosphate that is present on RNA from many viruses including Influenza virus. The receptor protein for 5'ppp-RNA is called RIG-I, when RIG-I recognises 5'ppp-RNA it sends a multi-step signal that tells the cell that it has been infected with a virus and to turn on its defences to protect against the virus.

A key step in the RIG-I signalling process is thought to require a protein called TRIM25. TRIM25 is known to bind to RNAs so we wanted to find out if this was important for its role in RIG-I signalling. In addition to this, we wanted to find out how TRIM25 binds to RNA as it does not contain any parts similar to other proteins that can bind to RNA. By deleting parts of the TRIM25 protein, we determined which part was necessary for binding to RNA. We also found that when TRIM25 is not bound to RNA it cannot function properly. Finally, by deleting TRIM25 from cells we discovered that it is not required for RIG-I signalling but it may still play a role in inhibiting replication of Influenza virus. This implies that there is another role for TRIM25 in innate immunity that is as yet unknown. This work increases our understanding of how the body defends against viruses and may lead to development of novel medicines in the future.

## Glossary of Abbreviations

|                              |  |
|------------------------------|--|
| <b>5'-ppp</b>                | 5'-triphosphate  |
| <b>aa</b>                    | amino acid   |
| <b>ActD</b>                  | Actinomycin D  |
| <b>AIDS</b>                  | Acquired Immune Deficiency Syndrome                        |
| <b>APOBEC</b>                | Apolipoprotein B mRNA Editing enzyme Catalytic polypeptide |
| <b>ATBF1</b>                 | AT-Binding Transcription Factor 1                          |
| <b>ATP</b>                   | Adenosine Triphosphate                                     |
| <b>CARD</b>                  | Caspase Recruitment Domain                                 |
| <b>CCD</b>                   | Coiled-coil Domain   |
| <b>cDNA</b>                  | complementary Deoxyribonucleic Acid                        |
| <b>CLIP-seq</b>              | Cross-linking Immunoprecipitation and Sequencing           |
| <b>CLR</b>                   | C-type Lectin Receptor                                     |
| <b>Co-IP</b>                 | Co-immunoprecipitation                                     |
| <b>CRISPR</b>                | Clustered Regularly Interspaced Short Palindromic Repeats  |
| <b>CTD</b>                   | C-Terminal Domain  |
| <b>DHX9</b>                  | DExH-Box Helicase 9  |
| <b>DMEM</b>                  | Dulbecco's Modified Eagle Medium                           |
| <b>DNA</b>                   | Deoxyribonucleic Acid                                      |
| <b>ds</b>                    | double-stranded  |
| <b>ED</b>                    | Effector Domain  |
| <b>EMCV</b>                  | Encephalomyocarditis Virus                                 |
| <b>EMSA</b>                  | Electromobility Shift Assay                                |
| <b>ER<math>\alpha</math></b> | Oestrogen Receptor $\alpha$                                |
| <b>FBS</b>                   | Fetal Bovine Serum   |
| <b>FRT</b>                   | Flippase Recognition Target                                |
| <b>G3BP2</b>                 | GTPase-Activating Protein-Binding Protein 2                |
| <b>GST</b>                   | Glutathione S Transferase                                  |
| <b>GTP</b>                   | Guanosine Triphosphate                                     |
| <b>HA</b>                    | Haemagglutinin   |
| <b>HEK</b>                   | Human Embryonic Kidney                                     |
| <b>HIV</b>                   | Human Immunodeficiency Virus                               |
| <b>HnRNP</b>                 | Heterogeneous Nuclear Ribonucleoprotein                    |
| <b>HRP</b>                   | Horseradish Peroxidase                                     |
| <b>IAV</b>                   | Influenza A Virus  |
| <b>IBV</b>                   | Influenza B Virus  |
| <b>iE-DAP</b>                | $\gamma$ -D-glutamyl-meso-diaminopimelic acid              |
| <b>IFIT</b>                  | Interferon Induced protein with Tetratricopeptide repeats  |
| <b>IFN</b>                   | Interferon   |
| <b>IFNAR</b>                 | Interferon-alpha/beta Receptor                             |
| <b>Ig</b>                    | Immunoglobulin   |
| <b>IKK</b>                   | Inhibitor of $\kappa$ B Kinase                             |
| <b>IL</b>                    | Interleukin  |
| <b>IP</b>                    | Immunoprecipitation  |

|                                |  |
|--------------------------------|--|
| <b>IPTG</b>                    | Isopropyl $\beta$ -D-1-thiogalactopyranoside                   |
| <b>IRF</b>                     | Interferon Regulatory Factor                                   |
| <b>ISG</b>                     | Interferon-Stimulated Gene                                     |
| <b>ISGF3</b>                   | Interferon-Stimulated Gene Factor 3                            |
| <b>ISRE</b>                    | Interferon-Sensitive Response Element                          |
| <b>I<math>\kappa</math>B</b>   | Inhibitor of $\kappa$ B  |
| <b>JAK1</b>                    | Janus Kinase 1   |
| <b>KLF5</b>                    | Kruppel-Like Factor 5  |
| <b>KO</b>                      | Knockout   |
| <b>LGP2</b>                    | Laboratory of Genetics and Physiology 2                        |
| <b>lncRNA</b>                  | long non-coding Ribonucleic Acid                               |
| <b>LPS</b>                     | Lipopolysaccharide   |
| <b>LUBAC</b>                   | Linear Ubiquitin Assembly Complex                              |
| <b>M1</b>                      | Matrix 1 protein   |
| <b>M2</b>                      | Matrix 2 protein   |
| <b>MAPK</b>                    | Mitogen-Activated Protein Kinase                               |
| <b>MAVS</b>                    | Mitochondrial Antiviral Signalling protein                     |
| <b>MDA5</b>                    | Melanoma Differentiation-Associated gene 5                     |
| <b>MDCK</b>                    | Madin-Darby Canine Kidney                                      |
| <b>MDP</b>                     | Muramyl Dipeptide  |
| <b>MEF</b>                     | Mouse Embryonic Fibroblast                                     |
| <b>MEX3C</b>                   | Mex-3 RNA Binding Family Member C                              |
| <b>MHC</b>                     | Major Histocompatibility Complex                               |
| <b>miRNA</b>                   | micro Ribonucleic Acid   |
| <b>MOI</b>                     | Multiplicity of Infection                                      |
| <b>mRNA</b>                    | messenger Ribonucleic Acid                                     |
| <b>MS</b>                      | Mass Spectroscopy  |
| <b>NA</b>                      | Neuraminidase  |
| <b>NEP</b>                     | Nuclear Export Protein   |
| <b>NF-<math>\kappa</math>B</b> | Nuclear Factor kappa-light-chain-enhancer of activated B cells |
| <b>NLR</b>                     | Nod-Like Receptor  |
| <b>NLS</b>                     | Nuclear Localisation Sequence                                  |
| <b>NP</b>                      | Nucleoprotein  |
| <b>NS1</b>                     | Non-structural protein 1                                       |
| <b>NS2</b>                     | Non-structural protein 2                                       |
| <b>nts</b>                     | nucleotides  |
| <b>OAS</b>                     | 2'-5'-Oligoadenylate Synthetases                               |
| <b>OD</b>                      | Optical Density  |
| <b>PA</b>                      | Polymerase Acidic protein                                      |
| <b>PAMP</b>                    | Pathogen-Associated Molecular Pattern                          |
| <b>PB1</b>                     | Polymerase Basic protein 1                                     |
| <b>PB2</b>                     | Polymerase Basic protein 2                                     |
| <b>PBS</b>                     | Phosphate-Buffered Saline                                      |
| <b>PCR</b>                     | Polymerase Chain Reaction                                      |
| <b>PCR</b>                     | Polymerase Chain Reaction                                      |
| <b>PKR</b>                     | Protein Kinase R   |

|                               |   |
|-------------------------------|---|
| <b>PLB</b>                    | Passive Lysis Buffer  |
| <b>PP1</b>                    | Protein Phosphatase 1   |
| <b>PR8</b>                    | Influenza A/Puerto Rico/8/1934(H1N1)                                  |
| <b>PRR</b>                    | Pattern Recognition Receptor  |
| <b>qRT-PCR</b>                | quantitative Real Time Polymerase Chain Reaction                      |
| <b>RBD</b>                    | RNA-Binding Domain  |
| <b>RBP</b>                    | RNA-Binding Protein   |
| <b>RIG-I</b>                  | Retinoic Acid-Inducible Gene I  |
| <b>RING</b>                   | Really Interesting New Gene   |
| <b>RIP</b>                    | RNA Immunoprecipitation   |
| <b>RLR</b>                    | RIG-I-Like Receptor   |
| <b>RNA</b>                    | Ribonucleic Acid  |
| <b>RNAi</b>                   | RNA interference  |
| <b>rRNA</b>                   | ribosomal Ribonucleic Acid  |
| <b>RSV</b>                    | Respiratory Syncytial Virus   |
| <b>SARS-CoV</b>               | Severe Acute Respiratory Syndrome Coronavirus                         |
| <b>SDS</b>                    | Sodium Dodecyl Sulfate  |
| <b>SEAP</b>                   | Secreted Alkaline Phosphatase   |
| <b>SEC-MALS</b>               | Size Exclusion Chromatography Multi-Angle Light Scattering            |
| <b>sgRNA</b>                  | short guide Ribonucleic Acid  |
| <b>SILAC</b>                  | Stable Isotope Labelling by Amino Acids in Cell Culture               |
| <b>siRNA</b>                  | small interfering Ribonucleic Acid                                    |
| <b>ss</b>                     | singe-stranded  |
| <b>STAT</b>                   | Signal Transducer and Activator of Transcription                      |
| <b>TANK</b>                   | TRAF Family Member Associated NF- $\kappa$ B Activator                |
| <b>TBK</b>                    | TRAF Family Member Associated NF- $\kappa$ B Activator Binding Kinase |
| <b>TBS-T</b>                  | Tris-Buffered Saline with Tween                                       |
| <b>TDA</b>                    | Thermal Denaturation Assay  |
| <b>TIP60</b>                  | Tat Interacting Protein, 60kDa  |
| <b>TK</b>                     | Thymidine Kinase  |
| <b>TYK2</b>                   | Tyrosine Kinase 2   |
| <b>TLR</b>                    | Toll-Like Receptor  |
| <b>TNF<math>\alpha</math></b> | Tumour Necrosis Factor $\alpha$                                       |
| <b>TPCK</b>                   | Tosyl Phenylamyl Chloromethyl Ketone                                  |
| <b>TRAF</b>                   | Tumour Necrosis Factor Receptor Associated Factor                     |
| <b>TRIM</b>                   | Tri-partite Motif   |
| <b>Ub</b>                     | Ubiquitin   |
| <b>UV</b>                     | Ultraviolet   |
| <b>VGM</b>                    | Virus Growth Medium   |
| <b>vRNA</b>                   | viral Ribonucleic Acid  |
| <b>vRNP</b>                   | viral Ribonuclear Protein   |
| <b>VSV</b>                    | Vesicular Stomatitis Virus  |
| <b>WB</b>                     | Western Blot  |
| <b>XPO1</b>                   | Exportin 1  |
| <b>ZAP</b>                    | Zinc-finger Antiviral Protein   |

## Introduction

The innate immune system is the first line of defence against viral infection

*Viruses have a large impact on human health and society*

Viruses are an incredibly diverse and abundant class of obligate intracellular parasites that are the causes of a myriad of diseases or defects in every cellular organism. At their most basic, they are composed of a nucleic acid genome (either ribonucleic acid (RNA) or deoxyribonucleic acid (DNA)) surrounded by a protein coat (capsid) and can range in size from 20 nm (parvovirus) to just under 1  $\mu\text{m}$  (Ebola virus). Some viruses can infect all types of cellular organisms including bacteria, archaea, fungi, plants and metazoans, although they cannot replicate autonomously. Viral infections of cells often have deleterious effects on the host organism as normal cellular processes are disrupted by the virus, which hijacks the host cell machinery in order to propagate.

Viral human pathogens have an enormous impact on human health around the globe and have been the cause of the deadliest pandemics in the last 100 years. These include the 'Spanish flu' outbreak of 1918 that killed an estimated 50,000,000 people<sup>1</sup> and the Human Immunodeficiency Virus/Acquired Immune Deficiency Syndrome (HIV/AIDS) pandemic of the 1980s and 1990s that resulted in over 30,000,000 people living with HIV/AIDS worldwide by 1999<sup>2</sup>. Viral pathogens have also caused more recent epidemics such as the West African Ebola virus outbreak of 2014-2016 that killed more than 11,000 in Guinea, Liberia and Sierra Leone<sup>3</sup>. In addition to mortality, viral infections cause a massive socioeconomic burden, with viral infections being a major cause of loss in agricultural industries and having a large impact on health systems worldwide.

Viruses can be classified according to their morphology, genetic material, replication strategy and host organism. Viruses exist in four main general forms; icosahedral (or isometric), filamentous, 'head and tail' and enveloped. The complexity of viral morphology bears no relation to the complexity of their hosts, with bacteriophages, some of the most complex viruses, infecting the simplest cellular organisms, bacteria. Viral genomes can consist of single-stranded (ss) or double-stranded (ds), linear or circular DNA or RNA. Most viruses have genomes that consist of a single DNA or RNA molecule encoding all the proteins the virus needs to survive and replicate although some viruses, for example Influenza virus, have a genome consisting of several separate nucleic acid molecules termed segments. Some RNA viruses, for example HIV, must reverse transcribe their genome to DNA so that it can be replicated by the host machinery and these are termed retroviruses. Since the early 1970s, viruses have been most commonly classified using the Baltimore classification system which distinguishes viruses based on how messenger RNAs (mRNAs) are produced during their life cycle<sup>4</sup>. The different classes of the Baltimore system are described in Table 1. The rise of genetic sequencing has led to challenges in the classification of viruses, particularly in the absence of information about host organisms and morphology of viruses that have been identified from large scale sequencing<sup>5</sup>.

| Group | Nucleic Acid | ds or ss | Sense | Retrovirus? (Y or N) | Example Family                    |
|-------|--------------|----------|-------|----------------------|-----------------------------------|
| I     | DNA          | ds       | N/A   | N                    | Herpesviruses                     |
| II    | DNA          | ss       | +     | N                    | Parvoviruses                      |
| III   | RNA          | ds       | N/A   | N                    | Reoviruses                        |
| IV    | RNA          | ss       | +     | N                    | Picornaviruses                    |
| V     | RNA          | ss       | -     | N                    | Orthomyxoviruses                  |
| VI    | RNA          | ss       | +     | Y – DNA intermediate | Retroviruses (e.g. HIV)           |
| VII   | DNA          | ds       | N/A   | Y – RNA intermediate | Hepadnaviruses (e.g. Hepatitis B) |

**Table 1** – The Baltimore Classification of virus groups.

### *Influenza A is an RNA virus with a large impact on human health*

Influenza viruses are negative sense RNA viruses with both protein and lipid envelopes that belong to the *Orthomyxoviridae* family, a schematic of the virus is shown in Figure 1. The primary disease-causing influenza viruses in humans, Influenza A and B viruses (IAV and IBV), have a genome comprised of 8 segments that encodes for 9 primary proteins, as well as several accessory proteins. In IAV, these include the three subunits of the influenza RNA polymerase, polymerase basic protein 2 (PB2), polymerase basic protein 1 (PB1) and polymerase acidic protein (PA) encoded by segments 1, 2 and 3, respectively<sup>6</sup>. In addition to this the nucleoprotein (NP) is encoded by segment 5 and associates with virus genomic RNA and the influenza RNA polymerase to form viral ribonuclear proteins (vRNPs)<sup>7</sup>. The viral entry factor haemagglutinin (HA) is encoded by segment 4<sup>8</sup> and neuraminidase (NA), required for virus release from non-functional host cell receptors, is encoded by segment 6<sup>9</sup>. Segment 7 encodes the matrix 1 protein (M1) and matrix 2 protein (M2) which can both be produced from the same transcript due to alternative splicing. M1 aids in maintaining the structure of the virion and regulating membrane trafficking of virus components in the host cell<sup>10</sup>, M2 is a proton ion channel required for viral entry and exit from host cells<sup>11</sup>.



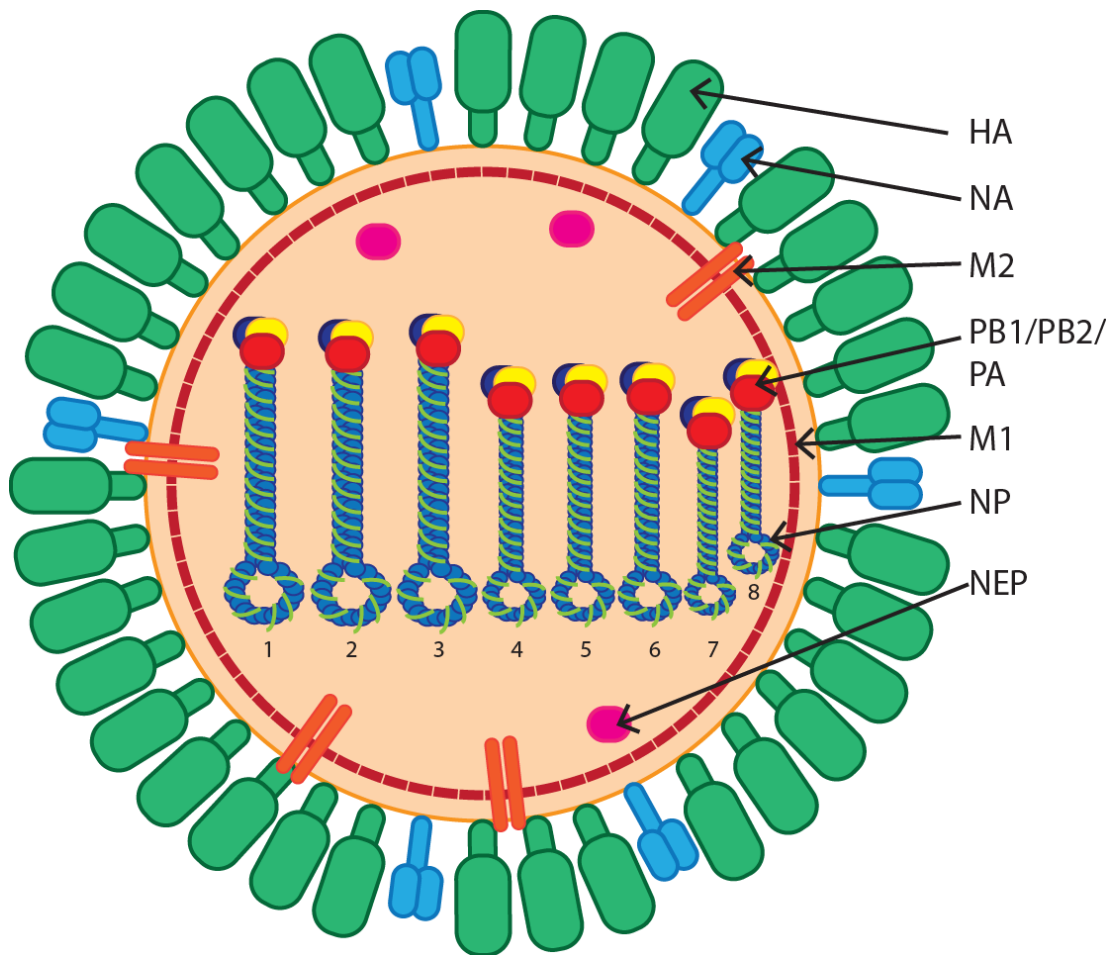


**Figure 1** – Schematic of the structure of an IAV virion.

Segment 8 encodes non-structural protein 1 (NS1), which inhibits host cell immune defences and non-structural protein 2 (NS2) also known as nuclear export protein (NEP) which allows viral RNA to leave the host cell nucleus<sup>12,13</sup>.

Influenza virions enter cells through receptor-mediated endocytosis, triggered by HA binding to sialic acid on the surface of host cells<sup>8</sup>. Virions enter the cell in endosomes, the membranes of which fuse with the virion lipid membrane. The acidic environment of the endosome triggers opening of the M2 ion channel, leading to acidification of the viral core and allowing the release of vRNPs from M1 and entry into the host cell cytoplasm<sup>11</sup>. The protein components of the vRNP (PA, PB1, PB2 and NP) each have nuclear localisation sequences (NLSs) which allow their import into the host cell nucleus<sup>14</sup>. Once in the nucleus, transcription and replication of the viral genome can occur. The viral genome must first be transcribed from negative sense RNA to positive sense RNA (known as complementary RNA, cRNA) by the viral polymerase to provide a template for replication. 5' methylated caps from host cell mRNAs are 'snatched' and added to the viral negative sense RNA. PB2 cleaves host mRNAs 10-15 nucleotides (nts) 3' of the 5' cap and this fragment is used to prime the viral RNA for transcription to positive sense RNA<sup>15,16</sup>. At this stage capped and polyadenylated positive sense viral mRNAs are also generated and are exported to the cytoplasm for translation into viral proteins. Once negative sense viral genomic RNA has been replicated, vRNPs are exported from the nucleus via the exportin 1 (XPO1) dependent pathway in a process mediated by NS2<sup>13,14,17</sup>. The exported vRNPs contain packaging signals to allow them to be packaged into newly synthesised virions<sup>18</sup>. Complete virions can subsequently leave the host cell by budding from the lipid membrane, using the host lipid membrane to form the new virion lipid membrane<sup>19</sup>. This process is dependent on cleavage of sialic acid on host cell membrane glycoproteins and glycolipids by NA<sup>20</sup>.

IAV strains capable of infecting humans are further classified by which of the 16 subtypes of HA and 9 subtypes of NA that they contain<sup>21</sup>. For example, a strain of H1N1 (containing HA1 and NA1) is currently endemic in humans and is the cause of seasonal flu, which causes around 500,000 deaths worldwide each year, with very young children and the elderly being most at risk<sup>22,23</sup>. HA and NA are the most antigenically variable proteins of influenza and are the main targets of protective antibodies produced by the body<sup>21</sup>. Mutations accumulated by HA and NA through genetic drift help the virus to escape immune surveillance<sup>24</sup>. IAV has the capability to swap genome segments between different strains co-infecting the same cell (reassortment). Unlike other influenza viruses, IAV is capable of circulating in domestic animals such as pigs and chickens in addition to humans. This provides a 'reservoir' of antigenically diverse IAV strains that can reassort with strains circulating in humans, generating new IAV strains that may not be covered by seasonal influenza vaccines<sup>21,24</sup>. An example of this occurring is the 2009 'swine flu' pandemic in which a new IAV H1N1 strain emerged from pigs<sup>25</sup>.

Infections with IAV or IBV can cause a variety of symptoms in humans. Most IAV infections in humans target the epithelial cells of the respiratory tract and result in a mild respiratory disease with symptoms such as fever, fatigue, sore throat and muscle pain that passes in 1-2 weeks. However, infections with influenza viruses can lead to complications, especially in immunocompromised individuals, including potentially fatal respiratory diseases such as pneumonia as well as a range of non-respiratory complications that can vary in severity<sup>21,26</sup>. Between 2010 and 2017, influenza virus infections resulted in up to 35,000,000 illnesses and 700,000 hospitalisations in the USA and each year 3-5,000,000 cases of severe disease due to influenza are reported worldwide, exemplifying the ubiquity of influenza as a hazard to human health<sup>21</sup>.

Vaccines are available that attempt to protect against seasonal influenza, however they are narrow and strain specific and have to be updated each year to protect against circulating influenza strains which will be antigenically diverged from the previous year due to antigenic drift<sup>27</sup>. In addition to this, the vaccine will not cover newly arising pandemic strains of influenza and it is extremely difficult to produce, distribute and administer a vaccine against the new strain within a timeframe in which it can make an impact. This occurred during the 2009 swine flu pandemic, with the vaccine being distributed after new infections had already peaked. Due to these issues, work is ongoing to develop a universal influenza vaccine that can protect against all strains of influenza A and B viruses<sup>27</sup>. In addition to vaccines, antiviral drugs are also used to treat influenza infections. Currently there are four recommended treatments for influenza infection, three of which are inhibitors of NA activity and one that is an endonuclease inhibitor that blocks viral replication<sup>28</sup>. Development of resistance to antiviral drugs is prevalent and a challenge in treating the disease. For example, adamantanes, a class of drugs targeting the M2 ion channel, are now resisted by the vast majority of circulating influenza strains<sup>28,29</sup>.

### *The innate immune system defends against viral pathogens*

Humans, as well as other organisms, must protect themselves from infection by viruses and other pathogens. To do this, they developed a robust means of distinguishing self from non-self and responding accordingly. Their primary means of doing so is through the immune system. The immune system is divided into two parts, the adaptive and innate immune systems. Adaptive immunity consists of antigen-specific receptor-mediated responses to specific pathogens, while innate immunity consists of pathways for the detection of factors

common to many pathogens as well as physical barriers such as the skin. In general, the innate immune system is fast-acting, involving elements that are ubiquitously expressed in somatic cells and acts in early infection. In contrast, the adaptive immune response is slower, acting in late infection, as there are only small numbers of each antigen-specific receptor and the cells expressing these must undergo clonal expansion before an effective response can be mounted<sup>30</sup>.

Of the two, adaptive immunity is more complex. It involves the recognition of antigens by antigen-specific receptors on the surface of B (immunoglobulins, Igs<sup>31</sup>) and T (T cell receptors<sup>32</sup>) lymphocytes. The antigen-specific receptors are generated by a process known as somatic rearrangement: rearrangement of the antigen-specific receptor genes to form complete receptors with a very high affinity for their antigen<sup>33</sup>. This process can potentially generate millions of antigen-specific receptors, each with a different specificity. Upon infection, cells will present antigens on their surface. These are then recognised by a complementary antigen-specific receptor, triggering a cytokine response that leads to the propagation of the cell encoding the receptor<sup>30</sup>. T cells that have undergone this process can propagate and can differentiate into other cell types including T-helper cells and T-killer cells. T-killer cells proceed to kill infected host cells by inducing apoptosis, helping to prevent the spread of the pathogen. T-helper cells perform a variety of roles, including recruiting other immune cells such as macrophages and neutrophils as well as presenting antigen to B lymphocytes. B lymphocytes are generally activated after binding to antigen present by T-helper cells, however they are capable of being activated without this<sup>30</sup>. Activated B lymphocytes secrete antibodies, which can induce neutralisation of infected cells or the pathogen itself, for example by opsonisation leading to recruitment of phagocytes and natural killer cells or by inducing the complement cascade<sup>31</sup>. Activation of

both types of lymphocytes also leads to the propagation of memory cells, which allow a rapid adaptive immune response to a second infection by the pathogen<sup>34</sup>.

The innate immune system involves non-antigen-specific pattern recognition receptors (PRRs) that recognise pathogen associated molecular patterns (PAMPs) that are common to many pathogens, but not found in host cells. An overview of PRR pathways in human cells is shown in Figure 2. Upon detection of PAMPs by PRRs, a signalling cascade is initiated that results in the expression of various anti-pathogenic molecules such as interferons (IFNs) and other cytokines, resulting in activation of host defences such as inflammation and recruitment of the adaptive immune system. Importantly, no single pathogen is recognised by a single PRR and biologically unrelated pathogens can be recognised by the same PRR, allowing for a fast and efficient response to any pathogen<sup>35</sup>. Different classes of pathogens are recognised by different PAMPs, for example viruses are recognised through glycoproteins and various DNA and RNA species<sup>36</sup>. Bacteria through lipoproteins<sup>37</sup>, peptidoglycan and derivatives<sup>38</sup>, CpG DNA<sup>39</sup>, lipopolysaccharides (LPS)<sup>40</sup> and proteins such as flagellin<sup>41</sup>. Fungi are generally recognised through cell wall or cell surface components such as phospholipomannan<sup>42</sup> or  $\beta$ -glucan<sup>43</sup>.

There are a wide variety of PRRs found in humans that recognise different classes of PAMPs. PRRs are generally classed into the membrane-bound Toll-like receptors (TLRs) and C-type lectin receptors (CLRs) as well as the cytoplasmic RIG-I like receptors (RLRs), Nod-like receptors (NLRs) and cytosolic DNA sensors such as cGAS. There are 10 distinct TLRs in humans, recognising a diverse range of PAMPs. Cell surface TLRs mainly recognise microbial membrane components such as LPS (TLR4)<sup>40</sup>, flagellin (TLR5)<sup>41</sup>, peptidoglycans and glycoproteins (TLR2 in complex with TLR1 or TLR6)<sup>44</sup>. Intracellular TLRs are often found on the endosomal membrane and generally recognise bacterial or viral nucleic acids such as

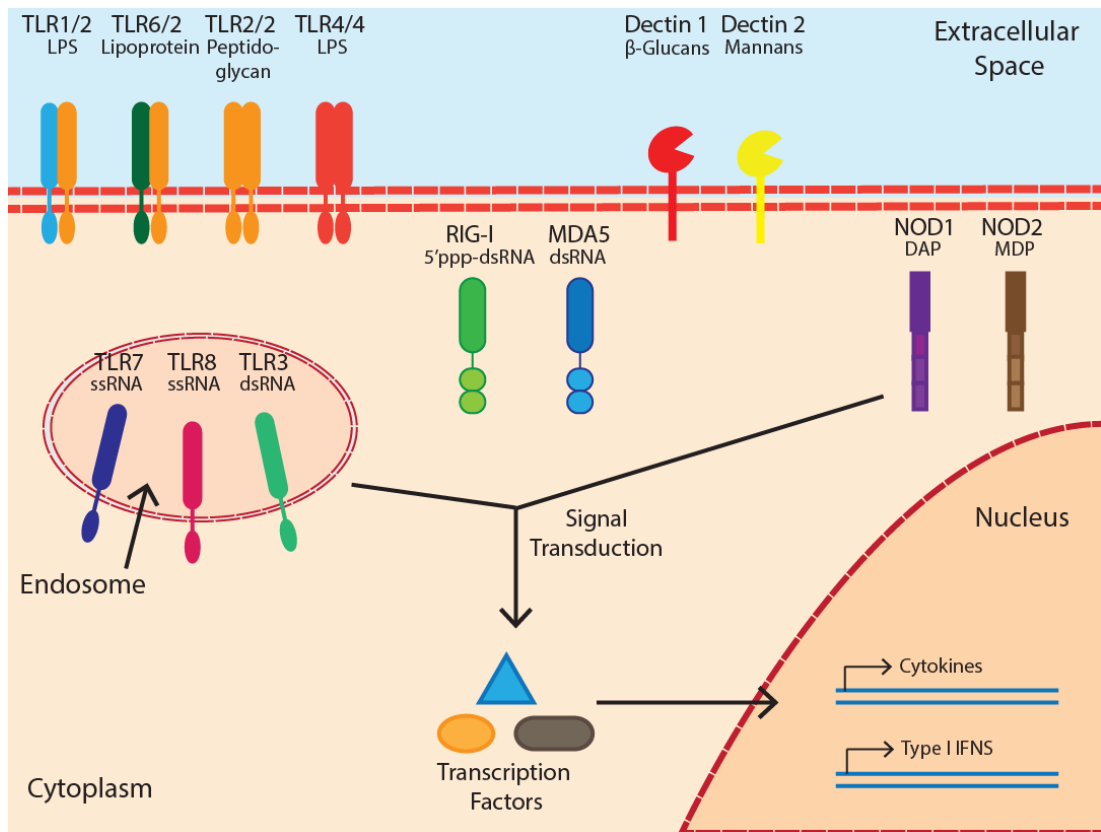


**Figure 2 - Overview of PRRs in human cells.** Upon detection of their PAMP, PRRs initiate signal transduction pathways that converge on the activation of various transcription factors including IRF-3, IRF-7 and NF-κB. The transcription factors enter the nucleus where they induce expression of type I IFNs and other pro-inflammatory cytokines.

dsRNA (TLR3)<sup>45</sup>, ssRNA (TLR7/8)<sup>46</sup> or CpG DNA (TLR9)<sup>47</sup>. The ligand for TLR10 is not yet known, however it has been shown to induce cytokine production in response to *Listeria monocytogenes*<sup>48</sup> and influenza<sup>49</sup> infection. TLRs signal downstream through MyD88 and TRIF, resulting in activation of the transcription factors Interferon Regulatory Factor 3 (IRF-3) and Nuclear Factor kappa-light-chain-enhancer of activated B cells (NF-κB) which enter the nucleus and induce expression of type I IFNs and other pro-inflammatory cytokines<sup>44</sup>.

CLRs are a large family of PRRs that primarily function in immunity against fungal pathogens, however some family members have roles in immunity against other organisms<sup>50,51</sup>. NLRs are divided into four subfamilies based on their structure; NLRA, NLRB, NLRC and NLRP. The best characterised NLRs are NOD1 and NOD2, both caspase recruitment domain (CARD)-containing NLRCs. NOD1 recognises γ-D-glutamyl-meso-diaminopimelic acid (iE-DAP) which is a component of peptidoglycans from Gram negative bacteria<sup>52</sup> while NOD2 recognises muramyl dipeptide (MDP) found in both Gram positive and Gram negative bacteria<sup>53</sup>. Both of these NLRs signal through activation of NF-κB. The RLR family consists of three members; Retinoic Acid-Inducible Gene I (RIG-I), Melanoma Differentiation-Associated gene 5 (MDA5) and Laboratory of Genetics and Physiology 2 (LGP2). The RLRs primarily recognise viral RNAs, with RIG-I recognising RNAs with a 5'-triphosphate (5'ppp) moiety and MDA5 recognising long dsRNAs. LGP2 is less well characterised, with studies suggesting it is capable of both positive and negative regulation of RIG-I<sup>54,55</sup>. The mechanisms of RLR activation will be explained in more detail later in this introduction.

Signalling through PRR pathways generally results in the activation of transcriptional activators such as IRF-3, IRF-7 and NF-κB in the cytoplasm. These transcription factors translocate to the nucleus where they induce expression of various proteins that contribute



to the establishment of an anti-pathogenic state such as IFNs and pro-inflammatory cytokines. The IRF proteins primarily activate expression of type I IFNs, consisting of 13 subtypes of IFN $\alpha$  and a single IFN $\beta$  as well as the poorly characterised IFN $\epsilon$ , IFN $\omega$  and IFN $\kappa$ <sup>56</sup>. IFN $\alpha/\beta$  secreted from cells and are recognised by the Interferon-alpha/beta Receptor alpha/beta chain heterodimer (IFNAR1/2), which is present on the cell membranes of all nucleated cells<sup>57</sup>. IFN $\alpha/\beta$  bind to IFNAR2 with a much higher affinity than IFNAR1 (0.2-200nm compared to 1-5 $\mu$ m)<sup>58,59</sup>. Upon IFNAR2 binding to IFN $\alpha/\beta$ , the receptor homodimer undergoes phosphorylation on its cytoplasmic domain and the associated Janus family kinases Janus Kinase 1 (JAK1) and Tyrosine Kinase 2 (TYK2) are also activated by reciprocal trans-phosphorylation<sup>60</sup>. JAK1 and TYK2 phosphorylate Signal Transducer and Activator of Transcription 1 and 2 (STAT1 and STAT2) which in turn form a complex with IRF-9 called Interferon-Stimulated Gene Factor 3 (ISGF3)<sup>61</sup>. ISGF3 enters the nucleus and activates transcription of thousands of target ISGs by binding to the Interferon-Sensitive Response Element (ISRE)<sup>62</sup>. In addition to this canonical pathway of IFN $\alpha/\beta$  action, IFNAR can also activate other STAT proteins as well as other signal transduction proteins such as the Mitogen-Activated Protein Kinases (MAPKs). This means an even greater variety of ISGs can be induced and the cellular response to IFN $\alpha/\beta$  can vary by cell type as well as other context-dependent factors. Among the best characterised ISGs are the 2'-5'-Oligoadenylate Synthetases (OAS), which synthesise 2',5'-oligoadenylates that activate RNase L<sup>63</sup>, and Protein Kinase R (PKR), which performs many roles including inhibition of mRNA translation and activation of NF- $\kappa$ B<sup>64</sup>. Others include the Interferon Induced proteins with Tetratricopeptide repeats (IFIT proteins), which inhibit translation and bind to viral RNAs<sup>65</sup>, the Apolipoprotein B mRNA Editing enzyme Catalytic polypeptide proteins (APOBECs), which edit viral mRNAs<sup>66</sup> and MX1, which specifically inhibits assembly of the influenza ribonucleoprotein<sup>67</sup>. In addition to these, IFN $\alpha/\beta$  can induce expression of pro-

inflammatory and pro-apoptotic cytokines and can help to activate the adaptive immune response, particularly through dendritic cells and CD8<sup>+</sup> T cells<sup>68,69</sup>.

The other primary transcription factor activated by PRR pathways is NF- $\kappa$ B, which represents 5 closely related proteins which act as homo- or heterodimers to activate transcription of a number of target genes<sup>70</sup>. Induction of gene expression by NF- $\kappa$ B varies by cell type but induced genes include many pro-inflammatory cytokines such as Tumour Necrosis Factor  $\alpha$  (TNF $\alpha$ ) and interleukins (ILs) as well as other immunoregulatory proteins such as Major Histocompatibility Complex (MHC) proteins and complement cascade proteins<sup>71</sup>.

Overall, innate immune responses triggered by PRR recognition of PAMPs are a key part of the initial host defences against virus infection, resulting in large-scale gene expression changes and the formation of an antiviral state. Genes stimulated by these pathways perform a variety of roles from the direct inhibition of viral replication to the initiation of inflammation and the priming of the adaptive immune system. Further underlining the importance of these processes, most pathogenic viruses have evolved strategies to evade or dampen host innate immune responses and these can be key for viral proliferation. Therefore, further understanding of the mechanisms of activation of PRR pathways and their inhibition by viruses is key for protecting human health.

## RIG-I is a key PRR in the recognition of RNA viruses

### *RIG-I and MDA5 are cytosolic PRRs that recognise viral RNA*

The RIG-I-like receptor family consists of three members; RIG-I, MDA5 and LGP2. Each has a DExD/H-box RNA helicase domain and a C-terminal Domain (CTD), while RIG-I and MDA5

both have N-terminal tandem Caspase Recruitment Domains (2CARD)<sup>72</sup>. RIG-I recognises RNAs with a 5'- di- or triphosphate (5'pp/5'ppp) moiety while MDA5 recognises long, double-stranded RNA (dsRNA)<sup>73-77</sup>. Upon binding to their substrates, both RIG-I and MDA5 trigger downstream signalling pathways via the adaptor Mitochondrial Antiviral Signalling protein (MAVS, also known as Interferon Beta Promoter Stimulator Protein 1 (IPS1), CARD Adapter Inducing Interferon Beta (CARDIF) or Virus-Induced-Signalling Adapter (VISA)), leading to activation of IRF-3, IRF-7 and NF- $\kappa$ B<sup>72</sup>. The role of LGP2 is less well characterised but as it does not have the N-terminal CARDS needed for interaction with MAVS, it does not seem to act as a PRR<sup>75</sup>. It has been shown to both positively and negatively regulate RIG-I and MDA5 signalling in mice in response to infection by different viruses<sup>54,78</sup>. More recent work has elucidated the mechanism of LGP2 enhancement of MDA5 signalling. LGP2 increases the rate of MDA5 binding to RNA and induces the formation of more numerous, shorter MDA5 filaments that exhibit an increased signalling activity compared to the filaments produced in the absence of LGP2<sup>79</sup>.

Both RIG-I and MDA5 recognise RNA from a multitude of RNA viruses, as well as RNA intermediates produced by some DNA viruses<sup>80</sup>. There are several viruses that have been shown to trigger innate immune signalling via both RLRs. For example, negative sense ssRNA paramyxoviridae such as Sendai virus<sup>75,81,82</sup>, Newcastle disease virus<sup>82</sup> and Respiratory Syncytial virus<sup>83</sup>. In addition to this positive sense ssRNA flaviviridae such as Dengue and West Nile viruses<sup>83</sup> as well as Hepatitis C virus<sup>84</sup> are recognised by both MDA5 and RIG-I. Double stranded RNA replicative intermediates from positive sense ssRNA picornaviridae are generally recognised by MDA5 rather than RIG-I<sup>85</sup>. RIG-I, but not MDA5, generally recognises RNA from other negative sense ssRNA viruses that are not paramyxoviridae including the filoviridae Ebola virus<sup>86</sup>, the rhabdoviridae Rabies virus and

Vesicular Stomatitis Virus (VSV)<sup>76,82</sup> and negative sense RNA viruses with a segmented genome such as Rift Valley fever virus and Lassa virus<sup>87</sup>.

RNA from IAV and IBV is recognised by RIG-I but not MDA5<sup>84,88,89</sup>. RIG-I<sup>-/-</sup> mice showed reduced production of IFN $\beta$  compared to WT mice in response to infection with IAV lacking NS1, while MDA5<sup>-/-</sup> mice showed no change<sup>84</sup>. In addition to this, IAV NS1 was shown to interact with human RIG-I, but not MDA5 in co-immunoprecipitation experiments. Also, Transfection of IAV vRNA in human cell lines was shown to induce innate immune activity in a RIG-I dependent manner<sup>89</sup>. Further work found that activation of RIG-I signalling in IAV infection was dependent on replication of the IAV genome with the agonist for RIG-I being full-length IAV genome segments. After infection with IAV, RNA associated with RIG-I was isolated and IAV genome segments, but no smaller RNAs, were identified<sup>88</sup>. More recent work has suggested that replication of IAV is not necessary and rather RIG-I can recognise and bind to vRNA upon nucleocapsid entry into the cell. This work also identified the 'panhandle' RNA structure as possibly being important for RIG-I recognition of nucleocapsid-associated RNA<sup>90</sup>. Further studies using synthetic viral RNAs determined that 5'ppp-ssRNA was not on its own sufficient for activation of RIG-I signalling and a stretch of dsRNA, as found in the panhandle structure of negative sense RNA virus genomes, was required for efficient signalling<sup>91,92</sup>.

RIG-I recognises 5'ppp-RNA through its DExD/H-box RNA helicase domain and its CTD. The CTD of RIG-I contains a basic stretch that binds 5'ppp and this interaction is enhanced by the presence of a blunt ended dsRNA stretch compared to ssRNA<sup>93</sup>. Crystallisation of the RIG-I CTD with short 5'ppp-dsRNA indicated that the side chain of Phe853 in the CTD stacks over both bases at the terminal end of the RNA duplex, explaining this increase in affinity<sup>93</sup>. Affinity for the 5' phosphate groups on the RNA is mostly due to the highly basic nature of

the CTD loop spanning residues 847-888, with multiple lysine and histidine residues forming hydrogen bonds with the phosphate groups<sup>93</sup>. MDA5 does not have this basic stretch in its CTD and as such does not interact with the 5' phosphate groups, explaining its lower affinity for 5'ppp-RNAs<sup>94,95</sup>. The DExD/H-box RNA helicase domain of RIG-I is made up of three sub-domains; Hel1, Hel2i and Hel2. Crystal structures of the helicase domain and CTD in complex with dsRNA indicated that all three helicase sub-domains, as well as the CTD, surround dsRNA in a ring-like structure with the 5' end of the RNA covered and the opposite end exposed<sup>96</sup>. The RIG-I helicase/CTD encircles roughly 8 base pairs of RNA, with interactions primarily with the RNA phosphate backbone.

### *RIG-I signalling is activated upon binding to 5'ppp-RNA*

To prevent inappropriate activation of innate immune responses, RIG-I signalling must be repressed in the absence of 5'ppp-RNA. This is achieved by several auto-repression mechanisms. For example, crystal structures of ligand-free RIG-I indicated that RIG-I is kept in an inactive conformation through interactions between the helicase 2i and the second CARD<sup>97</sup>. Mutational analysis of RIG-I also identified the linker between the helicase and C-terminal domains as necessary for auto-repression as transfection of a RIG-I construct lacking this linker induced type I IFN signalling even in the absence of RIG-I agonists<sup>98</sup>. In addition to this, phosphorylation of the RIG-I 2CARD by Protein Kinase C- $\alpha$  and  $\beta$  (PKC- $\alpha$  and PKC- $\beta$ ) has been shown to significantly inhibit RIG-I signalling and dephosphorylation of the 2CARD by Protein Phosphatase 1- $\alpha$  (PP1 $\alpha$ ) and PP1 $\gamma$  is required for efficient activation of signalling<sup>99,100</sup>. Upon binding to 5'ppp-RNA, RIG-I undergoes an ATP-dependent conformational change that results in the helicase and C-terminal domain packing with the

RNA and the 2CARD being released from auto-repression<sup>97,101</sup>. It has been suggested that K63-linked polyubiquitination of the RIG-I CTD and helicase-CTD linker by the E3 ubiquitin ligase Riplet is also necessary for release of the 2CARD<sup>102,103</sup>.

Upon binding to 5'ppp-RNA, RIG-I translocates down the dsRNA stem, allowing multiple RIG-I molecules to form a 'beads-on-a-string' complex on the RNA<sup>104,105</sup>. This oligomerisation activity is ATP hydrolysis-dependent and increases the strength of the resulting type I IFN response<sup>106</sup>. Oligomerisation of RIG-I is also important for the formation of tetramers of the 2CARD, which is required for activation of downstream signalling via MAVS through interaction with MAVS' own CARD<sup>107</sup>. A critical process in the formation of the 2CARD tetramer and the activation of MAVS is the K63-linked polyubiquitination of the 2CARD, which has been shown to stabilise the 2CARD tetramer and enhance the formation of MAVS filaments that are required for signalling<sup>108,109</sup>. Upon filament formation, MAVS can act as a scaffold for the recruitment of downstream signalling factors including Tumour Necrosis Factor Receptor Associated Factor proteins (TRAFs) such as TRAF3 and TRAF5 through a TRAF binding motif<sup>110-112</sup>. TRAFs in turn recruit and activate the Inhibitor of  $\kappa$ B ( $\kappa$ B) Kinases (IKKs) IKK $\alpha/\beta/\gamma$  that phosphorylate  $\kappa$ B, causing it to dissociate from NF- $\kappa$ B and allowing NF- $\kappa$ B to translocate to the nucleus and induce expression of pro-inflammatory cytokines. TRAFs also recruit and activate IKK $\epsilon$  and TRAF Family Member Associated NF- $\kappa$ B Activator (TANK) Binding Kinase 1 (TBK1) that can phosphorylate and activate the transcription factors IRF-3 and IRF-7 which enter the nucleus and induce expression of type I IFNs<sup>72</sup>.

## *K63-linked polyubiquitination of the RIG-I 2CARD may be performed by multiple E3 ubiquitin ligases*

Initially, Tri-partite Motif 25 (TRIM25) was identified as the key E3 ubiquitin ligase for the ubiquitination of the RIG-I 2CARD in both mice and humans by Gack *et al.*<sup>113</sup>. In this report, 6 lysine residues on the RIG-I 2CARD that underwent K63-linked polyubiquitination were identified by mass spectrometry (MS); K99, K169, K172, K181, K190 and K193. Of these, only mutation of K172 to arginine resulted in a reduction in polyubiquitination of the 2CARD and a concomitant reduction in activation of the NF- $\kappa$ B and IFN $\beta$  promoters when the 2CARD was transfected into HEK293 cells. This suggested that polyubiquitination of this residue is key for RIG-I 2CARD-mediated signalling. However, later work suggested that a RIG-I K172R mutant was fully functional and could efficiently trigger innate immune signalling in response to Sendai virus infection, suggesting that K172 may not be required for signalling<sup>114</sup>. Gack *et al.* also identified TRIM25 as a binding partner of the 2CARD in co-immunoprecipitation (Co-IP) experiments and demonstrated that this interaction was mediated by the C-terminal SPRY domain of TRIM25. Furthermore, knockdown of TRIM25 using RNA interference (RNAi) resulted in a reduction of RIG-I 2CARD polyubiquitination and IFN $\beta$  promoter activity in response to 2CARD transfection. Finally, production of IFN $\beta$  in TRIM25 knockout (KO) mouse embryonic fibroblast (MEF) cells upon Sendai virus infection was reduced compared to WT cells, while replication of VSV was increased in the TRIM25 KO cells compared to WT<sup>113</sup>.

Further work has underlined the role that TRIM25 plays in ubiquitination of the RIG-I 2CARD. Mutation of T55 in the first RIG-I CARD was found to abolish the TRIM25-2CARD interaction and this was required for TRIM25-mediated polyubiquitination of the 2CARD<sup>115</sup>. *In vitro* reconstitution of the human RIG-I pathway suggested that direct conjugation of

K63-linked polyubiquitin chains to the 2CARD was not necessary for activation of signalling as unanchored K63-linked chains generated by TRIM25 can be bound by the 2CARD and this is sufficient for activation of signalling<sup>116</sup>. Transfection of TRIM25 into HEK293T KO cells enhanced IFN $\beta$  promoter activity by about 2-fold compared to TRIM25 KO cells alone in response to transfection of the RIG-I 2CARD. However, a roughly 20-fold induction of IFN $\beta$  promoter activity when compared to cells not transfected with the RIG-I 2CARD was seen in the TRIM25 KO HEK293T cells, suggesting that there may be some redundancy in the role of TRIM25 in RIG-I signalling<sup>117</sup>. The same work reported that IAV replication was restricted upon TRIM25 transfection in the TRIM25 KO cells when compared to the TRIM25 KO cells alone.

Importantly, other E3 ubiquitin ligases have also been implicated in the ubiquitination of the RIG-I 2CARD. In addition to its role in ubiquitinating the RIG-I helicase-CTD linker, Riplet (also known as RIG-I E3 Ubiquitin Ligase (REUL)) was found to polyubiquitinate the RIG-I 2CARD at lysines 154, 164 and 172. Knockdown of Riplet was shown to inhibit IFN $\beta$  expression in response to Sendai virus infection and resulted in increased replication of VSV<sup>118</sup>. Knockdown of TRIM4 was found to inhibit activation of the IFN $\beta$  promoter in response to overexpression of RIG-I or infection with Sendai virus<sup>119</sup>. This study also found that TRIM4 primarily targeted K164 and K172 of the RIG-I 2CARD for polyubiquitination. A systems biology approach combined with experimental validation identified the ubiquitination of K164 and K172 by TRIM25 and TRIM4 as being key for RIG-I signalling activation, with TRIM25 and TRIM4 working synergistically to optimise activation<sup>120</sup>.

Another E3 ubiquitin ligase, Mex-3 RNA Binding Family Member C (MEX3C), was found to co-localise with RIG-I in antiviral stress granules and ubiquitinate the RIG-I 2CARD at K48, K99 and K169. Cells derived from MEX3C KO mice were shown to have impaired activation of the IFN $\beta$  promoter in response to infection with VSV and Newcastle Disease Virus (NDV)



while activation after infection with Encephalomyocarditis Virus (EMCV, recognised by MDA5) was unaffected<sup>121</sup>. Shi *et al.* showed that in a HEK293T cell-free system knockout of Riplet abrogates RIG-I mediated aggregation of MAVS in response to VSV genomic RNA while knockout of TRIM25, MEX3C or TRIM4 did not abrogate aggregation. However, MAVS aggregation could still be triggered in response to addition of the RIG-I 2CARD even in the absence of Riplet<sup>122</sup>. This may suggest that activation of full-length RIG-I signalling in response to viral RNA requires Riplet activity, but Riplet is redundant with the other E3 ubiquitin ligases in the ubiquitination of the RIG-I 2CARD alone.

More recent work has underlined the importance of Riplet in RIG-I signalling and indicated that TRIM25 is dispensable for activation of signalling by full-length RIG-I. TRIM25, Riplet and RIG-I were knocked out of HEK293T cells before the cells were stimulated with a 42bp 5'ppp-dsRNA or Sendai virus (SeV). Riplet and RIG-I KO cells, but not TRIM25 KO, showed a reduction in expression of ISGs or luciferase under the IFN $\beta$  promoter upon stimulation<sup>123</sup>. Expression of exogenous Riplet in the Riplet KO cells restored IFN activity, confirming that Riplet is required for efficient RIG-I signalling. These findings were repeated with an expanded range of stimulants (5'ppp-dsRNA, SeV, Rift Valley fever virus and IAV) and in other cell lines from independent sources including mouse embryonic fibroblasts (MEFs) and A549 lung carcinoma cells<sup>123</sup>. Interestingly, stimulation of TRIM25 KO cells with GST-2CARD resulted in a 50% reduction in signalling activity compared to WT cells, while Riplet KO had no effect. This further suggests a difference in the activation mechanisms of full-length RIG-I and isolated 2CARD and helps to explain the earlier findings of Gack *et al.* This study also looked at the abilities of Riplet and TRIM25 to ubiquitinate RIG-I *in vitro* by performing ubiquitination assays with purified RIG-I, ubiquitin and E1 and E2 ubiquitin ligases in the presence or absence of 42bp 5'ppp-dsRNA. This showed that Riplet, but not TRIM25, could robustly ubiquitinate RIG-I in a 5'ppp-dsRNA-dependent manner<sup>123</sup>. Another

study, by Hayman *et al.*, similarly showed that Riplet, and not TRIM25, was essential for RIG-I signalling<sup>124</sup>. As shown by Cadena *et al.*, knock-out of TRIM25 in A549 cell lines was shown to have no effect on RIG-I signalling in response to several RIG-I-stimulating viruses or ligands while Riplet knock-out abolished RIG-I signalling. Interestingly, deletion of TRIM25 in mice resulted in higher virus titres after infection with IAV, with levels of IFN $\gamma$  in the lungs being unaffected<sup>124</sup>. This implies that TRIM25 may be playing a RIG-I-independent role in the restriction of IAV in mice.

Okamoto *et al.* proposed a 'sequential ubiquitination' mechanism to explain the activation of RIG-I by polyubiquitination by different E3 ubiquitin ligases (Figure 3)<sup>125</sup>. In this model, Riplet first ubiquitinates the helicase-CTD linker at K788 upon RIG-I RNA binding to release the 2CARD from auto-repression and this step is required for the E3 ligases to access the 2CARD. This is followed by ubiquitination at various sites on the 2CARD by Riplet, TRIM25, TRIM4 and MEX3C. This would fit with the observations of Shi *et al.*, Cadena *et al.* and Hayman *et al.* that Riplet is absolutely required for efficient RIG-I signalling activation, as well as explaining why there is seemingly redundancy between the other E3 ligases.

### *RIG-I signalling is targeted for inhibition by many viruses*

In order to be able to replicate efficiently, most human viruses have evolved mechanisms for avoiding the triggering of innate immune signalling. Many RNA viruses that can be recognised by RIG-I have developed mechanisms of inhibiting RIG-I signalling at different stages of the pathway. In addition to this, RIG-I signalling must be tightly controlled by host cells to avoid aberrant activation that could lead to inappropriate inflammation and IFN

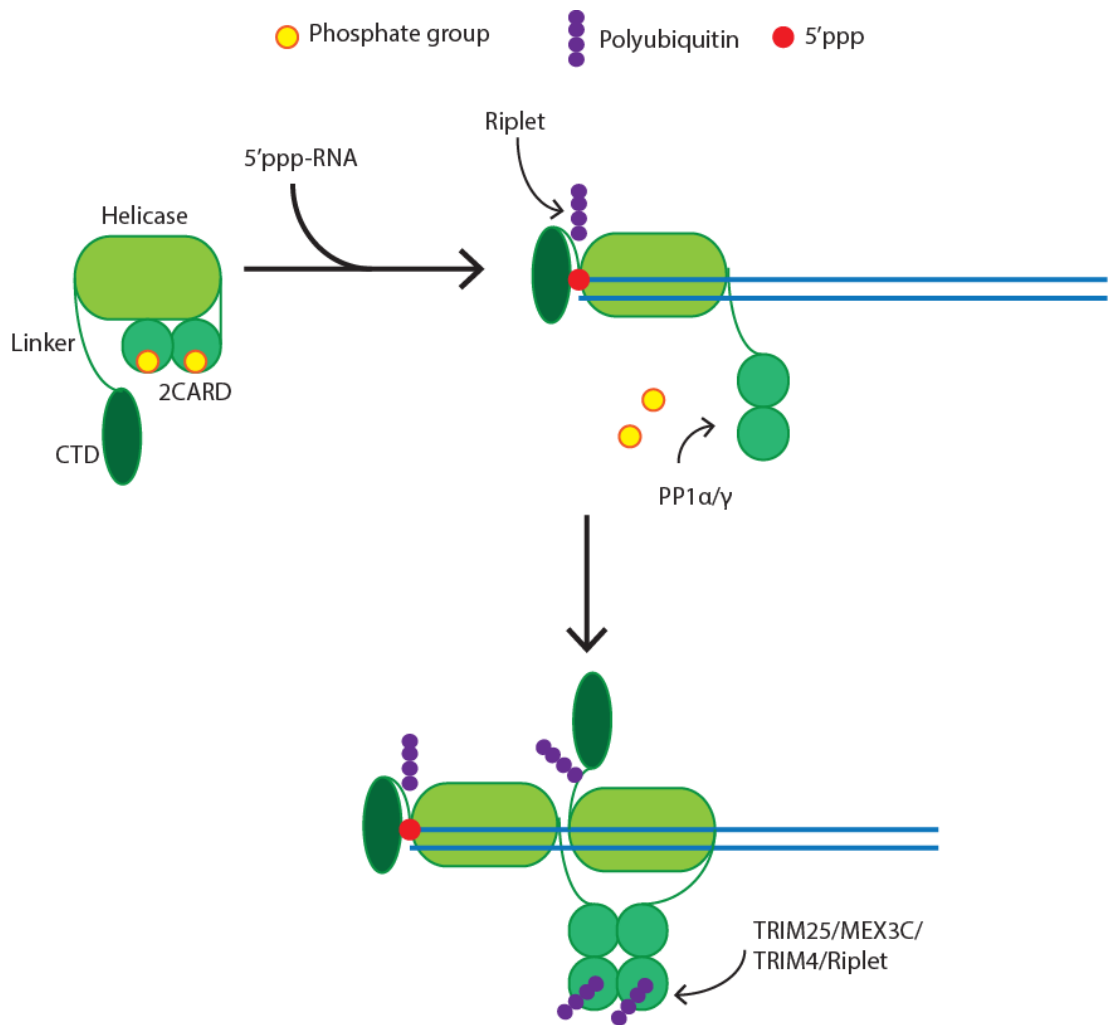


**Figure 3** - Model of activation of RIG-I based on the sequential ubiquitination model proposed by Okamoto et al. Upon recognition of 5'ppp-dsRNA, RIG-I undergoes a conformational change and the Helicase-CTD linker can be ubiquitinated by Riplet. This releases the 2CARDS from auto-repression and allows their dephosphorylation by PP1α/γ. Ubiquitination of the linker also promotes the assembly of other RIG-I molecules along the dsRNA, although the CTD of only one molecule can bind the 5'ppp moiety. The 2CARDS from RIG-I molecules assembled along the dsRNA can form 'tetramer' structures that are stabilised by K63-linked polyubiquitination of the 2CARD. This tetramer structure interacts with the CARDS of MAVS and promotes its oligomerisation, leading to further downstream signalling.

expression. Examples of this include the mechanisms for RIG-I auto-repression as explained previously. RIG-I must also avoid signalling upon recognition of self RNA. This is reliant on hydrolysis of ATP, which leads to displacement of RIG-I from self RNA which is bound less stably than non-self RNA<sup>126</sup>. A mutant of RIG-I that could bind to, but not hydrolyse, ATP was found to stably associate with 60S rRNA, triggering innate immune signalling while WT RIG-I rapidly dissociated<sup>127</sup>.

A common viral strategy for avoiding recognition by RIG-I is by post-transcriptionally removing or sequestering the 5'ppp moiety on genomic RNAs. For example, the Crimean-Congo hemorrhagic fever, Hanta and Borna disease viruses all remove 5'ppp from their genomic RNA<sup>87</sup> and Polioviruses cap the 5' end of their RNAs<sup>128</sup>. Arenavirus has an unpaired 5'ppp nucleotide overhang that prevents recognition by RIG-I<sup>129</sup>. The VP35 proteins from both Ebola and Marburg viruses sequester vRNA from RIG-I and mask the 5'ppp by end-capping<sup>130,131</sup>. IAV NS1 also prevents RIG-I binding to its RNA through its dsRNA binding activity<sup>132</sup>. Another strategy used by several viruses is the targeting of RIG-I or MAVS for degradation or mislocalisation. Proteins encoded by Hepatitis A virus cleave MAVS while Hepatitis B virus targets it for degradation<sup>133,134</sup>. EMCV and Respiratory Syncytial virus (RSV) both target RIG-I for degradation via the proteasome<sup>135,136</sup>, while RSV, as well as Dengue virus, cause mislocalisation of MAVS and RIG-I respectively<sup>133,137</sup>. In addition to strategies targeting upstream factors in RIG-I signalling, viruses also target downstream factors. For example, Dengue virus inhibits the phosphorylation of TBK1 and IRF-3<sup>138</sup>, Severe Acute Respiratory Syndrome Coronavirus (SARS-CoV) disrupts the TANK-TBK1/IKK $\epsilon$  complex<sup>139</sup> and Herpes Simplex virus type 1 (HSV-1) targets IRF-3<sup>140</sup>.

As ubiquitination of the RIG-I 2CARD is a key process in RIG-I signalling activation it is also targeted for inhibition by several viruses. Some viruses have been reported to encode

deubiquitinases that remove polyubiquitin chains from the RIG-I 2CARD including SARS-CoV, arterivirus, nairovirus, foot-and-mouth disease virus (FMDV) and herpesvirus<sup>141-143</sup>. Hepatitis C virus (HCV) NS3-4A targets Riplet to prevent it from ubiquitinating RIG-I by disrupting their association<sup>102</sup>. The NS1 protein of IAV is known to block ubiquitination of RIG-I through interactions with TRIM25, Riplet and RIG-I itself<sup>144-146</sup>.

IAV NS1 binds to the coiled-coil domain of TRIM25, preventing its multimerisation which it requires for its catalytic activity<sup>145</sup>. The interaction between NS1 and TRIM25 requires the E96 and E97 residues in the NS1 effector domain (ED) as well as R38 and K41 in the RNA binding domain (RBD) and recombinant IAVs with the mutant NS1 E96E97A or R38K41A lose their ability to block type I IFN expression as well as their virulence in mice<sup>145</sup>. A later study indicated that NS1s from IAV strains adapted to multiple organisms including humans, mouse, swine and birds efficiently interacted with and blocked the activity of human, but not mouse, TRIM25<sup>146</sup>. In mouse cells, IAV NS1 interacted with and blocked the activity of Riplet and this was sufficient to inhibit RIG-I signalling<sup>146</sup>. In human cells, NS1 from a human adapted IAV strain was also capable of inhibiting Riplet activity and this is likely important for the overall inhibitory effect of NS1 on RIG-I signalling<sup>146</sup>. A crystal structure of the TRIM25 coiled-coil and PRY/SPRY domains in complex with IAV NS1 indicated that E96 and E97 of NS1 are likely needed for overall structural integrity of the NS1 protein rather than direct interactions with the TRIM25 coiled-coil and instead critical interactions were formed with NS1 L95 and S99<sup>147</sup>. This study also showed that only the ED of NS1 was necessary for the interaction with TRIM25 and the RBD was not required as had been previously reported. In addition, the inhibitory effect of NS1 on TRIM25 activity was shown to be due to disruption of interactions between the TRIM25 PRY/SPRY and coiled-coil domains that are required for RIG-I ubiquitination activity, not a lack of TRIM25 multimerisation<sup>147</sup>.

Other viruses also target TRIM25-mediated RIG-I ubiquitination for inhibition in order to dampen the innate immune response. The V proteins of several paramyxoviruses (Nipah, measles, Sendai and parainfluenza viruses) were found to interact with both the RIG-I 2CARD and the SPRY domain of TRIM25, preventing TRIM25-mediated ubiquitination of RIG-I<sup>148</sup>. Similarly, RSV NS1 and N protein from SARS-CoV were also found to interfere with TRIM25 activity<sup>149,150</sup>. Inhibition of TRIM25 was also found to be a factor in the replacement of an endemic clade of Dengue virus by a new clade<sup>151</sup>. The new clade showed increased expression of a subgenomic flavivirus RNA (sfRNA) that bound to and inhibited TRIM25, increasing the epidemiological fitness of the new clade compared to the previous one<sup>151</sup>. TRIM25 can be targeted for inhibition by the host cell in order to downregulate RIG-I signalling to prevent excessive inflammation and IFN responses. The Linear Ubiquitin Assembly Complex (LUBAC), composed of Heme-Oxidized IRP2 Ubiquitin Ligase 1 (HOIL-1) and HOIL-1 Interacting Protein (HOIP), competes with TRIM25 for binding to RIG-I and also targets TRIM25 for degradation via the proteasome<sup>152</sup>.

The wide variety of viruses and mechanisms that target RIG-I signalling for inhibition underlines the importance of RIG-I signalling as a means of restricting virus infection. As RIG-I 2CARD ubiquitination is a commonly targeted step of this pathway, this suggests that it is critical for efficient RIG-I signalling. Due to the large amount of similarity between TRIM25 and Riplet (around 60% sequence homology), it is possible that some of the mechanisms mentioned will also inhibit Riplet activity, as is the case with IAV NS1. However, despite its seeming importance in the activation of RIG-I signalling, Riplet remains less studied than TRIM25 so more work is needed to further elucidate the extent of Riplet inhibition by different viruses.

## The E3 ubiquitin ligase TRIM25 has many different roles

### *TRIM family proteins are E3 ubiquitin ligases*

The Tri-partite Motif (TRIM) family is a large (>80 members in humans) group of E3 ubiquitin ligase proteins that share a common domain structure. Almost all TRIM family proteins consist of an N-terminal Really Interesting New Gene (RING) domain, responsible for their E3 ubiquitin ligase activity, 1 or 2 B-box domains and a coiled-coil domain (CCD), responsible for homo and heterodimerisation<sup>117,153–155</sup>. Most TRIM family proteins have one or a combination of several types of C-terminal domain generally responsible for protein-protein interactions. C-terminal domains include the PRY (~61aa) and SPRY (~140aa) domains, that can be found individually or combined as a single unit, known as a PRY/SPRY or B30.2 domain. Other C-terminal domains include the plant homeodomains (PHDs), fibronectin type 3 domains (FN3s) and COS boxes<sup>153,154,156,157</sup>.

The primary role of TRIM E3 ubiquitin ligases is to catalyse the addition of polyubiquitin chains or single ubiquitin monomers (monoubiquitination) to lysine residues on their target proteins. Ubiquitin is a 76 aa, 8.5 kDa protein and polyubiquitin chains are made by the formation of isopeptide bonds between the ubiquitin C-terminal glycine and one of the 7 lysine residues present in the protein<sup>158,159</sup>. It has also been shown that polyubiquitin chains can form in a 'head-to-tail' manner via the N-terminal methionine residue<sup>160</sup>. The addition of ubiquitin monomers to a target protein or extension of a polyubiquitin chain involves three types of proteins; E1, E2 and E3. The E1 activating enzyme forms a thioester bond with the ubiquitin C-terminal glycine and the ubiquitin is transferred to the E2 conjugating enzyme via a trans-thiolation reaction so that it is bound to a cysteine in the active site of the E2 protein. The E3 ubiquitin ligase then interacts with the E2 and the target protein to

catalyse the transfer of the ubiquitin from the former to the latter. The E2 is the main determinant of the type of ubiquitin chain formed (i.e. which lysine residue the new monomer is added to) while the E3 determines the target protein and the target residue on that protein<sup>161</sup>.

The multiple lysines present in ubiquitin allow the formation of several different types of polyubiquitin chains, each of which has different functionality. Chains can vary significantly in length and can be homogenous or mixed (a chain of different ubiquitin linkages) and straight or branched. The most well studied are straight, homogenous K48-linked polyubiquitination, which leads to targeting of proteins for degradation via the proteasome, and K63-linked polyubiquitination which is used in many intracellular signalling pathways<sup>162</sup>. The proteasome recognises I44 of K48-linked polyubiquitin<sup>163</sup> and ubiquitin-mediated degradation of an inhibitor is a common mechanism for the activation of proteins, for example the NF- $\kappa$ B inhibitor I $\kappa$ B $\alpha$  is degraded following K48-linked polyubiquitination in order to allow NF- $\kappa$ B activation<sup>164</sup>. K63-linked polyubiquitination can have many different functions on the target protein including modulating protein:protein interactions, common in the DNA damage response, and regulation of protein activity as is seen in innate immune signalling<sup>162</sup>.

### *Many TRIM family proteins are involved in innate immune responses*

As discussed previously, TRIM25 and TRIM4 have both been shown to be able to activate downstream signalling from RIG-I by ubiquitinating the RIG-I 2CARD. Many other TRIM family proteins have been shown to play a role in host immune defences, particularly in the pathways initiated by the RLRs RIG-I and MDA5. TRIM genes, especially those that are



closely related to each other, are often clustered together in the genome, suggesting they may have arisen from gene duplications and several TRIMs are ISGs, underlining their importance in innate immune responses<sup>165,166</sup>. Around half of human TRIMs were found to enhance innate immune responses to RIG-I 2CARD expression when overexpressed<sup>167</sup>.

Some TRIM proteins in addition to TRIM25 and TRIM4 directly regulate RIG-I signalling through interactions with RIG-I or MAVS. TRIM40 targets both RIG-I and MDA5 for degradation, while TRIM38 stabilises both through addition of the ubiquitin-like protein SUMO, suppressing their K48-linked polyubiquitination<sup>168,169</sup>. TRIM14 promotes the translocation of RIG-I to the mitochondria and its interaction with MAVS by recruiting Werner Helicase Interacting Protein (WHIP) and Protein Phosphatase 6 Catalytic Subunit (PPP6C) which aid the MAVS/RIG-I interaction and dephosphorylation of RIG-I respectively<sup>170</sup>. TRIM14 also recruits IKK $\gamma$  and NF- $\kappa$ B Essential Modulator (NEMO) to MAVS to aid downstream signalling<sup>171</sup>. TRIM31 was found to promote the aggregation of MAVS in response to RIG-I stimulation, required for efficient downstream signalling, through K63-linked polyubiquitination<sup>172</sup>. TRIM44 interacts with MAVS through its B-box domains and stabilises it by preventing its K48-linked polyubiquitination<sup>173</sup>. In addition to these proteins, several more TRIMs act downstream of MAVS to positively regulate innate immune responses including TRIM9<sup>174</sup>, TRIM26<sup>175</sup> and TRIM23<sup>176</sup>, while some negatively regulate these responses including TRIM11<sup>177</sup>. TRIM proteins are also involved in innate immune signalling through cGAS-STING, TLRs and in IFN signalling through IFNAR<sup>154</sup>.

Apart from their roles in PRR signalling, TRIM proteins are also known to directly restrict viruses. TRIM5 $\alpha$  from monkeys is able to efficiently restrict HIV-1, however human TRIM5 $\alpha$  is less efficient in this<sup>178,179</sup>. TRIM5 $\alpha$  binds directly to the virus capsid proteins and TRIM5 $\alpha$ -mediated restriction of HIV-1 is seemingly proteasome-dependent, suggesting that TRIM5 $\alpha$

is ubiquitinating the capsid protein and targeting it for degradation<sup>180,181</sup>. TRIM11 promotes premature uncoating of HIV-1 and restricts the virus in a proteasome-independent manner<sup>182,183</sup>. TRIM19, TRIM22 and TRIM37 have also been shown to restrict HIV-1, although the mechanisms for this are poorly understood<sup>153</sup>. Two TRIMs have also been shown to restrict IAV by targeting components of the virus for degradation via the proteasome. TRIM22 targets NP<sup>184</sup> and TRIM32<sup>185</sup> targets PB1 for K48-linked polyubiquitination. In addition to this, TRIM56 has been shown to restrict IAV and IBV in a ubiquitination-independent manner, possibly through blocking transcription by binding to vRNAs<sup>186</sup>. TRIM56 expression was found to restrict IAV and IBV, but not Sendai virus or Monkeypox virus, and this restriction was not dependent on the presence of the RING, B-box or CCD but rather a 63 amino acid stretch in the CTD. This region of the CTD was also shown to be sufficient to inhibit transcription of a luciferase reporter construct by the IAV RNA polymerase, implying that transcription by the polymerase is being blocked<sup>186</sup>. Similar ubiquitination-independent blocking of IAV RNA polymerase transcription was also seen for TRIM25 and this will be discussed in further detail later<sup>187</sup>.

### *TRIM25 has other cellular roles and has been implicated in some cancers*

Human TRIM25 is a 630 amino acid, 71 kDa E3 ubiquitin ligase that is widely expressed across human cell types and is conserved among vertebrates including fish, birds and mammals<sup>188–192</sup>. Like other TRIM family proteins, it consists of a zinc-finger RING domain, two B-box domains and a CCD with a linker domain leading to a C-terminal PRY/SPRY (B30.2) domain. TRIM25 forms an antiparallel dimer mediated by its CCD, with the RING domain of each monomer at opposite ends of the dimer and the PRY/SPRY domains

positioned at the centre via the CCD-PRY/SPRY linker<sup>193</sup>. Further work indicated that the RING domain of TRIM25 must dimerise in order to catalyse polyubiquitin chain formation, implying that higher-order assembly of TRIM25 dimers is required for its activity<sup>117</sup>. Two separate mechanisms of higher-order assembly were proposed. Firstly, an 'end-to-end' model in which RING domains on each end of the dimer interact with RING domains from separate dimers. Secondly, a 'tetramer' model in which TRIM25 dimers effectively stack on top of each other with RING domains on either end of one dimer interacting with both RING domains from another dimer (Figure 4)<sup>117</sup>. When human TRIM25 RING domain was crystallised with an ubiquitin-charged E2 conjugating enzyme, UBE2D1, it was shown to form a dimer with both RING monomers contacting the ubiquitin molecule<sup>194</sup>. Crystal structures have also been generated for the PRY/SPRY domain of mouse TRIM25, showing that its overall structure is that of two anti-parallel  $\beta$ -sheets in a sandwich type conformation, similarly to PRY/SPRY domains found in other proteins<sup>195</sup>. By comparing the TRIM25 PRY/SPRY structure to other PRY/SPRY domains, a putative binding site was identified. Three solvent-exposed phenylalanine residues (F528, F559 and F623) and a 'ladder' of arginine and tryptophan residues in close proximity, all of which are conserved across species, form a pocket of hydrophobic and hydrogen bonding-capable residues and were identified as one potential binding site. Conserved residues in loop regions that do not contribute to overall domain architecture were also tested. Mutational analysis revealed that D488 and W621 were key residues for the binding of the PRY/SPRY domain to the RIG-I 2CARD<sup>195</sup>. A recent study identified a second putative 2CARD binding site in the TRIM25 PRY/SPRY on the opposite surface of the domain to the previously identified one<sup>196</sup>. This study also showed that the linker between the CCD and the PRY/SPRY is flexible, allowing the two PRY/SPRY domains in a dimer to be positioned in many ways<sup>196</sup>.

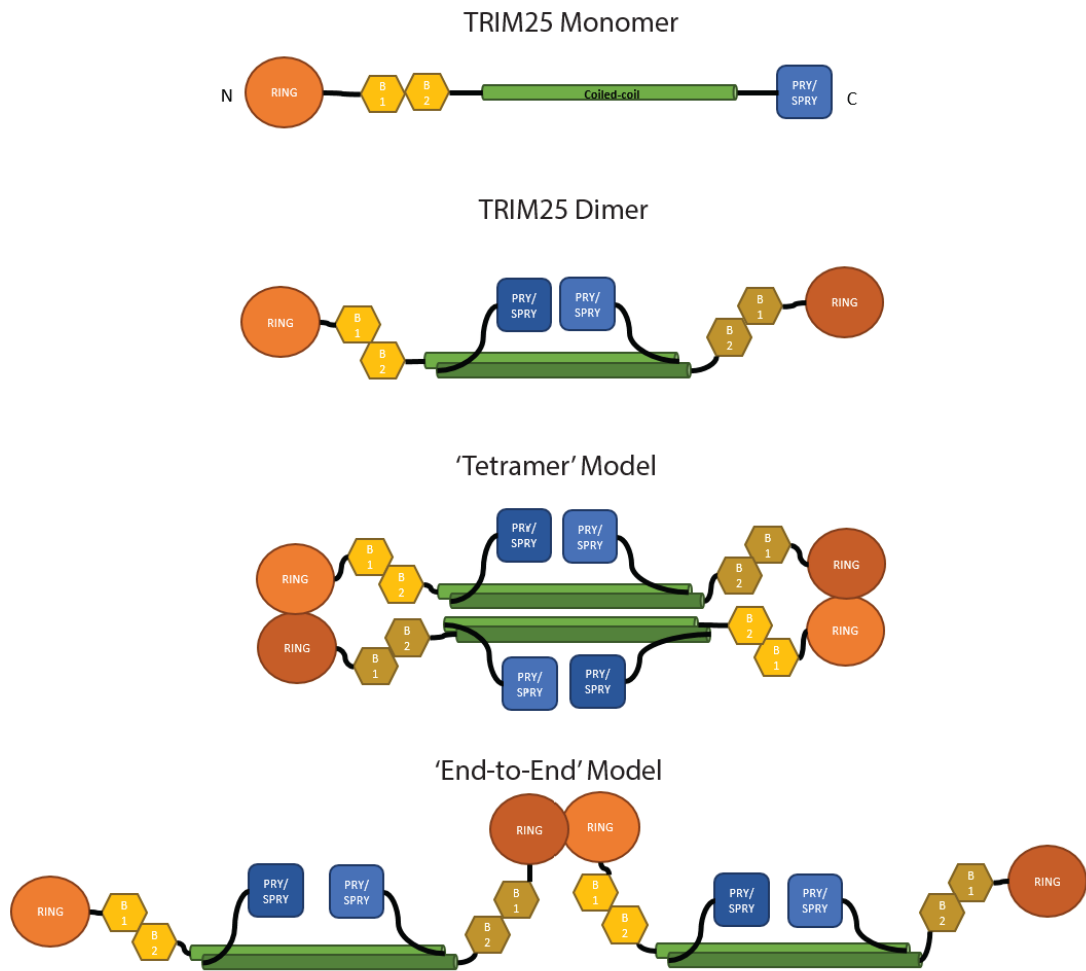


**Figure 4** – Possible models of dimerization of the RING domains of TRIM25 dimers as proposed by Sanchez *et al.* Due to the anti-parallel structure of the TRIM25 dimer, RING domains from TRIM25 molecules found in the same dimer cannot dimerise themselves. This implies that higher order oligomerisation is required for TRIM25 catalytic activity.

Apart from its role in the ubiquitination of the RIG-I 2CARD, TRIM25 has been found to perform other roles in the cell and has been implicated in several cancers. TRIM25 was initially identified as a protein responsive to oestrogen in a screen for regions of DNA bound by the oestrogen receptor and was shown to be upregulated in oestrogen receptor-positive mammary cells<sup>197</sup>. Mice with TRIM25 knocked out were shown to be viable and fertile but with a significantly underdeveloped uterus and a dampened response to oestrogen<sup>198</sup>. TRIM25 has subsequently been shown to interact with and ubiquitinate with components of the oestrogen response. In the presence of oestrogen, TRIM25 ubiquitinates oestrogen receptor  $\alpha$  (ER $\alpha$ ), stimulating interactions with co-factors such as Tat Interacting Protein, 60 kDa (TIP60) and increasing ER $\alpha$  activity<sup>199</sup>. However, a mutant TRIM25 lacking the RING domain increased the half-life of ER $\alpha$ , suggesting that this ubiquitination also targets ER $\alpha$  for degradation<sup>199</sup>. TRIM25 can also positively regulate ER $\alpha$  activity by targeting AT-binding transcription factor 1 (ATBF1), which competes with ER $\alpha$  for co-activators, for degradation<sup>200</sup>. TRIM25 also targets another negative regulator of ER $\alpha$ , Kruppel-like factor 5 (KLF5), for degradation<sup>201</sup>.

TRIM25 has been implicated as being important in the progression of several cancers. In breast cancer, TRIM25 targets the scaffold protein 14-3-3 $\sigma$  for degradation<sup>202</sup>. 14-3-3 $\sigma$  is a negative cell cycle regulator and loss of TRIM25 in MEF cells was shown to lead to an accumulation of 14-3-3 and reduced cell growth. In addition, growth of Michigan Cancer Foundation-7 (MCF7) breast cancer cells implanted in athymic mice was attenuated by the targeting of TRIM25 by RNAi<sup>202,203</sup>. Overexpression of TRIM25 in these cells can overcome the cells oestrogen dependency for tumour growth<sup>202</sup>. A systems biology approach identified TRIM25 as a key regulator at both transcriptional and post-transcriptional levels of a network of genes that promote metastasis of breast cancer and it was linked with disease progression and poor survival outcomes<sup>204</sup>. The p53 protein is an important tumour

suppressor that helps to initiate apoptosis in response to DNA damage, among other anti-proliferative activities, and as such is mutated or downregulated in many cancers<sup>205</sup>.

TRIM25 has been shown to regulate p53 in both a negative and positive manner. Upon TRIM25 knockdown in lung cancer cells, p53 levels increased and proliferation, tumorigenesis and migration of the cells was inhibited<sup>206</sup>. However another study showed that p53 levels were upregulated in the presence of TRIM25 but p53 transcriptional activity was lowered, dampening the p53-dependent DNA damage response<sup>207</sup>. In prostate cancer, TRIM25 was shown to stimulate p53 translocation to the cytoplasm through interaction with GTPase-activating protein-binding protein 2 (G3BP2) and TRIM25 knockdown resulted in reduced prostate tumour growth in mouse models<sup>208</sup>. TRIM25 was also shown to play a role in the invasion and migration of both colorectal and gastric cancer cells through the stimulation of Transforming Growth Factor  $\beta$  signalling<sup>209,210</sup>.

Apart from its role in ubiquitination of the RIG-I 2CARD, TRIM25 has been shown to play other roles in innate immunity. TRIM25 has been shown to enhance the activity of Zinc-finger Antiviral Protein (ZAP), which binds to and inhibits translation of viral mRNAs<sup>211,212</sup>. TRIM25 was shown to mediate K63-linked polyubiquitination of ZAP which enhanced its antiviral activity and was also shown to be required for efficient binding of ZAP to its target mRNA<sup>211</sup>. However another study showed that although TRIM25 E3 ligase activity was needed to enhance ZAP-mediated inhibition of Sindbis virus RNA translation and TRIM25 mediated ZAP ubiquitination, ubiquitination of ZAP itself did not directly affect antiviral activity<sup>212</sup>. It is possible that TRIM25 also targets other factors for ubiquitination in a ZAP-dependent manner and these factors aid ZAP-mediated inhibition of translation. TRIM25 can also be involved in the dampening of RIG-I signalling. The ubiquitin-like FAT10 (also known as Ubiquitin D) forms a complex with TRIM25/RIG-I that sequesters RIG-I away from the mitochondria and causes it to form insoluble aggregates to prevent further signal

transduction<sup>213</sup>. TRIM25 stabilises FAT10, which is usually unstable, by preventing its proteasome-mediated degradation<sup>213</sup>.

### *TRIM25 is an RNA-binding protein*

TRIM25 was initially discovered to be an RNA-binding protein (RBP) in a screen of mRNA binding proteins in HeLa cells<sup>214</sup>. Proteins were cross-linked to RNA via UV irradiation and mRNAs were isolated from the cell lysate with oligo(dT) probes before bound proteins were analysed by mass spectroscopy<sup>214</sup>. A similar strategy also identified mouse Trim25 as an RBP in mouse embryonic stem cells<sup>215</sup>. Binding of human TRIM25 to RNA was further validated by immunoprecipitation (IP) of TRIM25 followed by radiolabelling of RNA. Signal from radiolabelled RNA after TRIM25 IP was reduced in cells in which TRIM25 had been knocked-down by RNAi, indicating that TRIM25 was binding to RNA<sup>215</sup>. This study also tested several truncation mutants of TRIM25 for their RNA binding activity. Truncations in which the N-terminal RING and B-box domains, or the C-terminal PRY/SPRY domain, were deleted were capable of binding RNA in this assay as seen by signal from radiolabelled RNA corresponding to the size of the constructs as visualised by western blot. Conversely, any mutants in which the CCD was deleted were incapable of binding RNA, suggesting that the CCD could play a role in TRIM25 RNA binding activity<sup>215</sup>.

Previous work in this lab uncovered a potential RNA binding-dependent function for TRIM25 in the Lin28-mediated degradation of pre-let-7a-1<sup>216</sup>. Two pre-let-7a-1 mutants with minimal loops required for Lin28a binding (pre-let-7a-1@2 and @3) showed differential uridylation when incubated with P19 cell extracts despite equal binding to Lin28a. Uridylation by TuT4 leads to exonuclease-mediated degradation of pre-let-7a-1, an important step in preventing the expression of mature let-7a in undifferentiated cells<sup>217</sup>.

This discrepancy led to the hypothesis that additional Lin28a cofactors were needed for efficient uridylation, which was tested by the use of RNA pulldown coupled to SILAC mass spectroscopy to search for proteins binding differentially to the two pre-let-7a-1 mutants<sup>216,218</sup>. It was found that TRIM25 bound more to pre-let-7a-1@2, which was efficiently uridylated, than two pre-let-7a-1@3 which wasn't and this was confirmed by RNA pulldown followed by western blot<sup>216</sup>. Further to this, knock-down of TRIM25 resulted in decreased uridylation and therefore increased levels of pre-let-7a-1, although the mechanism of this remains unknown<sup>216</sup>. In terms of sequence, pre-let-7a-1@2 and @3 varied by the change of the GGAGAU motif found in the WT pre-let-7a-1 terminal loop and mutant @2 to GGAGUA in mutant @3, suggesting that the GGAGAU motif may be important for TRIM25 binding to pre-let-7a-1<sup>216</sup>.

Further work performed in the lab has suggested that TRIM25 has a broad specificity with a preference for GC-rich regions of RNA<sup>219</sup>. This was determined through cross-linking immunoprecipitation followed by sequencing (CLIP-seq). T7-tagged TRIM25 was transiently expressed in cells that were subsequently exposed to UV radiation in order to induce cross-linking between proteins and RNAs. T7-TRIM25 was then precipitated and subjected to stringent washes to remove non-cross-linked proteins and RNAs before the bound RNAs were isolated and sequenced. This identified a total of 2611 distinct transcripts, with no correlation seen between the abundance of the transcript in the cell and the abundance that associated with TRIM25 in this experiment, suggesting a level of specificity in the interactions. The majority (56%) of the transcripts identified were mRNAs, with most binding sites being in the exons (56%) or 3'-UTR (23%) of these. Comparison of the sequences identified in the experiment showed that there was no single consensus sequence required for TRIM25 binding, although GC-rich sequences were enriched compared to their abundance in the genome<sup>219</sup>. It should be noted, however, that CLIP-seq



does not discriminate between RNAs that are bound directly to TRIM25 and those that associate indirectly, for example via binding by other proteins that interact with TRIM25. As such, care must be taken when interpreting these results as they do not necessarily represent TRIM25's direct RNA-binding activity.

Recent work has identified a role for the RNA binding of TRIM25 in the restriction of IAV<sup>220</sup>. TRIM25s from human and gibbon were overexpressed in Crandell Reese Feline Kidney (CRFK) cells that were subsequently infected with IAV. Levels of viral proteins were reduced in cells overexpressing TRIM25, with gibbon TRIM25 having a greater effect than human TRIM25, and this was rescued by expression of WT NS1 protein. Virus titres and levels of viral RNAs were also reduced upon overexpression of TRIM25, again with gibbon TRIM25 showing a larger effect and this was also seen for TRIM25 mutants lacking ubiquitin ligase activity (TRIM25 C13A/C16A)<sup>220</sup>. Deletion of RIG-I and TRIM25 from human A549 lung cells resulted in increased viral titres, viral protein, and vRNA levels, which could be rescued by expression of human or gibbon TRIM25. Interestingly, deletion of RIG-I alone had no effect, suggesting this function of TRIM25 is RIG-I-independent<sup>220</sup>. Further evidence that RIG-I is not required for this activity was shown by the use of a viral minigenome assay in HEK293T  $\Delta$ RIG-I cells. Overexpression of both human and gibbon TRIM25 in these cells reduced expression of a luciferase reporter that could only be expressed in the context of IAV RNA polymerase activity, indicating that TRIM25 was inhibiting the activity of the IAV polymerase<sup>220</sup>. TRIM25 was subsequently shown to bind to IAV vRNPs in an RNA-dependent manner and that gibbon TRIM25 binds to vRNPs more efficiently than human TRIM25. In addition to this, purified human or gibbon TRIM25 was able to inhibit viral mRNA chain elongation *in vitro*, again with gibbon TRIM25 doing this more efficiently, reflecting its higher ability to restrict viral replication and protein production as well as its stronger binding to vRNPs<sup>220</sup>. The authors of this study proposed a mechanism whereby TRIM25

blocks the IAV RNA polymerase from moving down the vRNA template and prevents the onset of chain elongation, thus restricting the virus (Figure 5).

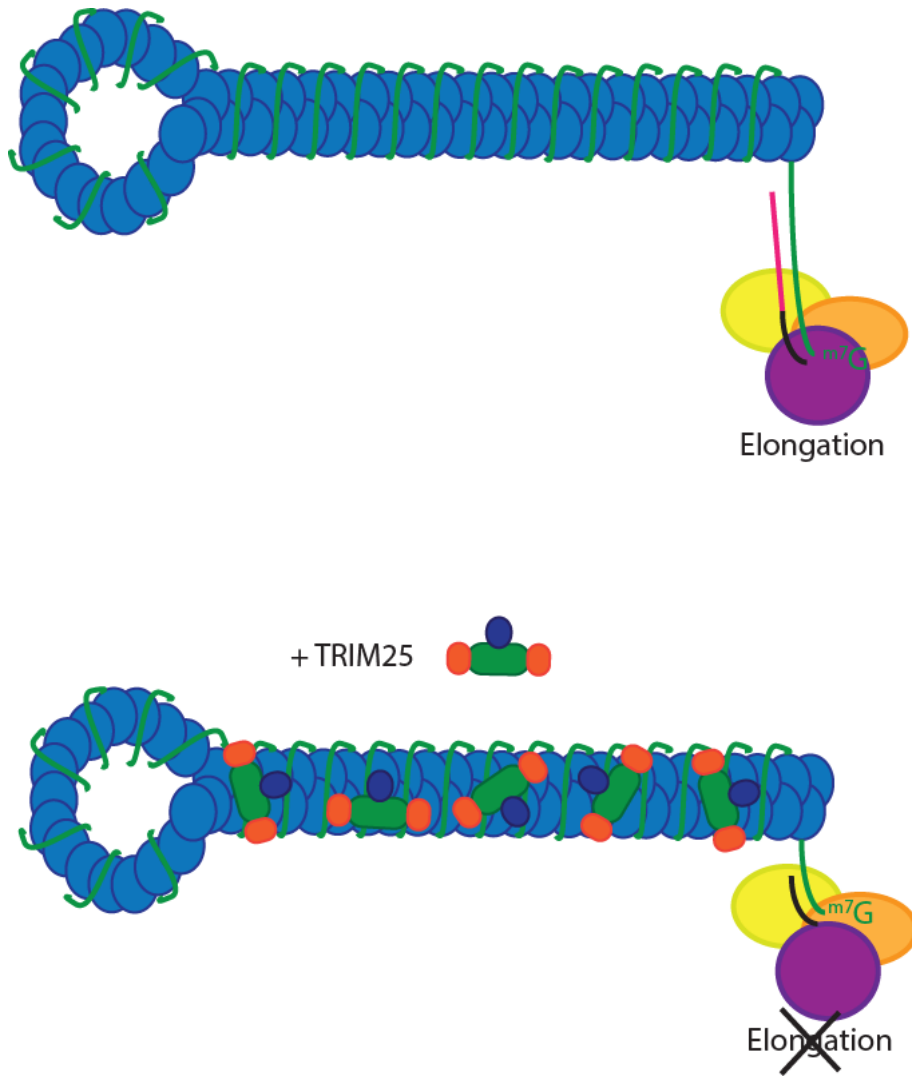


**Figure 5** – A possible mechanism for inhibition of IAV transcription by TRIM25 proposed by Meyerson et al<sup>187</sup>. TRIM25 interacts with IAV vRNPs in an RNA-dependent manner, blocking the onset of RNA chain elongation by the viral polymerase and therefore inhibiting IAV replication. The initiation of RNA replication is suggested not to be affected in this model.

## Aims

The overall aims of this project were to elucidate the mechanism and functions of TRIM25 RNA-binding activity. TRIM25's roles in important disease-related processes such as innate immunity and cancer make it an intriguing and physiologically relevant target to study. It has been shown to bind to RNA despite the lack of a canonical RBD so uncovering the mechanism of this binding may provide insights into a novel method of protein-RNA binding. In addition to this, as TRIM25 is a member of a large family of proteins with similar domain structures, it is possible that this mechanism could be conserved in other members of the same family, many of which have important roles in innate immunity. As TRIM25 is known to function in an innate immune pathway that detects viral RNAs, the obvious question is whether its RNA-binding activity is important for its role in this pathway. It is possible that TRIM25 RNA binding could positively regulate its activity, either through bringing it into close contact with RNA-bound RIG-I or by promoting its E3 ligase activity. Conversely, RNA binding could negatively regulate TRIM25 activity in this pathway, for example through sequestration of TRIM25 away from RIG-I, as has been shown with Dengue virus<sup>151</sup>. The recently uncovered direct restriction of IAV transcription by TRIM25 also underlines the importance of determining the mechanism of TRIM25 RNA binding as TRIM25 interacts with vRNPs in an RNA-dependent manner<sup>220</sup>.

Previous results from our lab have shown that TRIM25 binding to pre-let-7a-1 can influence the stability of the RNA<sup>216</sup>. This raises the question of whether TRIM25 is capable of influencing the stability, or any other properties, of other RNAs. This could prove important in many situations. For example, changes to gene expression are the root of many cancers and if TRIM25 is found to be a possible cause of these changes through its RNA binding activity it could help increase understanding of these cancers. Another possible role for

TRIM25 RNA-binding is that it aids in the targeting of proteins to be ubiquitinated. For example, TRIM25 could use RNA as a scaffold to target other proteins that bind to the same RNA. As TRIM25 is capable of both K48 and K63-linked polyubiquitination, this could be important for targeting proteins for degradation or in modulating protein activity in signalling pathways.

As such, this project had the following aims:

- *Elucidating the mechanism of TRIM25 RNA binding* – This included determining any sequence specificity of the RNAs TRIM25 binds to and identifying the amino acids that are important for binding to RNA.
- *Identifying RNAs and proteins affected by loss of TRIM25* – This included generating TRIM25 knock-out cell lines and analysing the levels of RNAs or proteins that had changed in response to loss of TRIM25.
- *Determining if TRIM25 RNA binding has a function in its role in innate immunity* – This included analysis of TRIM25s roles in both the RIG-I pathway and direct restriction of IAV infection.

## Materials and Methods

### Primers

#### *Templates for In Vitro Transcription*

Primers used for generation of templates for *in vitro* transcription of RNAs are shown in

Table 2.

| Template            | F or R | Sequence  |
|---------------------|--------|---|
| <b>Pre-let-7a-1</b> | F      | 5'-TAATAGGACTCACTATAGGTGAGGTAGTAGGTTCTATA-3'                          |
| <b>Pre-let-7a-1</b> | R      | 5'-GAAAGACAGTAGATTGTATA-3'  |
| <b>5'ppp-79</b>     | F      | 5'-TAATAGGACTCACTATAGGGAGACCATCTGCTACTCGA<br>TCGATATCCTAGCATATTCGT-3' |
| <b>5'ppp-</b>       | R      | 5'-GATTATGCTAGGTACCAGTCAGAAGTGACCTCGAGCG<br>TACGATATGCTAGGATATCG-3'   |
| <b>5'ppp-UA</b>     | F      | 5'-TAATACGACTCACTATAGGGAGACCATCTGCTAC<br>CGATATATAGTTTAAAAGGA-3'      |
| <b>5'ppp-UA</b>     | R      | 5'-GATTATGCTAGGTACCAGTCAGAAGTGTATAGTTTA<br>CTCCTTTTAAACTATATATCG-3'   |
| <b>5'ppp-AU</b>     | F      | 5'-TAATACGACTCACTATAGGGAGACCATCTGCTAC<br>CGATATATAGTTTAAAAGGA-3'      |
| <b>5'ppp-AU</b>     | R      | 5'-GATTATGCTAGGTACCAGTCAGAAGTGTATAGTTAT<br>CTCCTTTTAAACTATATATCG-3'   |

**Table 2** – Primers used for generation of templates for *in vitro* transcription of RNAs. All PCR products contained a promoter for T7 RNA polymerase. Pre-let-7a-1 primers were used for pre-let-7a-1 WT and all mutants.

#### *Sequencing*

Primers used for amplifying regions of genes to be sequenced or for sequencing reactions

are shown in Table 3.

| Name           | F or R | Sequence                    |
|----------------|--------|-----------------------------|
| CMV            | F      | 5'-CGCAAATGGGCGGTAGGCGTG-3' |
| TRIM25 genomic | F      | 5'-TCCTCTCGAGCTAGGTTTCG-3'  |
| TRIM25 genomic | R      | 5'-ATTGTGCTGGGAACATTTCG-3'  |

**Table 3** – Primers used for amplification of genomic regions for sequencing or for sequencing reactions.

### qRT-PCR

Primers used for quantification of RNAs by qRT-PCR are shown in Table 4.

| Name      | F or R | Sequence                      |
|-----------|--------|-------------------------------|
| GAPDH     | F      | 5'-GAGTCAACGGATTTGGTCGT-3'    |
| GAPDH     | R      | 5'-TTGATTTTGGAGGCATCTCG-3'    |
| 18S       | F      | 5'-GTAACCCGTTGAACCCATT-3'     |
| 18S       | R      | 5'-CCATCCAATCGGTAGTAGCG-3'    |
| TRIM25    | F      | 5'-CCAAGAGGGATGAGTTCGAG-3'    |
| TRIM25    | R      | 5'-GCTTCAGCTCGTTTTTGAGG-3'    |
| cMyc      | F      | 5'-TCGGATTCTCTGCTCTCCTC-3'    |
| cMyc      | R      | 5'-CCTGCCTCTTTCCACAGAA-3'     |
| MKMK2     | F      | 5'-GCCAAAGACCTCATCTCAA-3'     |
| MKMK2     | R      | 5'-CAGCTGTTCTCTGCAGGAC-3'     |
| MALAT1    | F      | 5'-CCCACCCCTTAATCAGACT-3'     |
| MALAT1    | R      | 5'-CAACAGCACAGCGGTACACT-3'    |
| LINC00324 | F      | 5'-TGTCAGCACGCAGAGTGTA-3'     |
| LINC00324 | R      | 5'-AGGAAGGCCAAACTCTCCTC-3'    |
| SLC7A5    | F      | 5'-GAAGGCACCAAAGTGGATGT-3'    |
| SLC7A5    | R      | 5'-GGGTCACCTGCCACTCTTTA-3'    |
| ZAP       | F      | 5'-TGCGATAACCTGCATCTCTG-3'    |
| ZAP       | R      | 5'-ATCACTTTGGAGGAGGAGCA-3'    |
| SUB1      | F      | 5'-TCAAGCTCTTCTGGCAGTGA-3'    |
| SUB1      | R      | 5'-AAGATGACAGGGCTCTCGAA-3'    |
| HERC2     | F      | 5'-AAAAATTGCTGCCATTCTG-3'     |
| HERC2     | R      | 5'-TCACCTTAGGCTCCTCCAAA-3'    |
| WDR91     | F      | 5'-GAACACCGTGACAGCATCG-3'     |
| WDR91     | R      | 5'-CCGAGTCAAAAGCGAAGAGT-3'    |
| SYBU      | F      | 5'-CTCCTGGACAGCGCGATG-3'      |
| SYBU      | R      | 5'-TCAAGAGTCAAATGGGCTGTGGC-3' |
| PCDH11X   | F      | 5'-GAAACAACCTCAGCGACTCC-3'    |
| PCDH11X   | R      | 5'-CTCCGGTATGTGATCTGTGGA-3'   |
| SERPIN5   | F      | 5'-ACTAATCAAGCGGCTCTACG-3'    |
| SERPIN5   | R      | 5'-CAAAGTGGCCATCTGTGAGA-3'    |

**Table 4** – Primers used for quantification of RNAs by qRT-PCR.

## RNA Sequences

Sequences of purified RNAs used in this project are shown in Table 5.

| Name                    | Sequence   |
|-------------------------|--|
| <b>Pre-let-7a-1</b>     | 5'-<br>UGGGAUGAGGUAGUAGGUUGUAUAGUUUUAGGGUCACAC<br>CCACCACUGGGAGAUAAACUAUACAAUCUACUGUCUUUCCUA<br>-3'        |
| <b>Pre-let-7a-1/4.2</b> | 5'-<br>UGGGAUGAGGUAGUAGGUUGUAUAGUUUUAGGGUCACAC<br>CCACCACUGGGAGUAAACUAUACAAUCUACUGUCUUUCCUA<br>-3'         |
| <b>Pre-let-7a-1/16</b>  | 5'-<br>UGGGAUGAGGUAGUAGGUUGUAUAGUUUAAGAUUCUAAA<br>AUUAAACUAUACAAUCUACUGUCUUUCCUA-3'                        |
| <b>Pre-let-7a-1/GG</b>  | 5'-<br>UGGGAUGAGGUAGUAGGUUGUAUAGUUUUAGGGUCAGGG<br>GGGGGACUGGGAGAUAAACUAUACAAUCUACUGUCUUUCCU<br>A-3'        |
| <b>Pre-let-7a-1/UU</b>  | 5'-<br>UGGGAUGAGGUAGUAGGUUGUAUAGUUUUAGGGUCAUUU<br>UUUUUACUGGGAGAUAAACUAUACAAUCUACUGUCUUUCCU<br>A-3'        |
| <b>5'ppp-79</b>         | 5'-<br>GGGAGACCAUCUGCUACUCGAUCGAUACCUAGCAUAUCGUA<br>CGCUCGACGUCACUUCUGACUGGUACCUAGCAUAAUC-3'               |
| <b>5'ppp-UA</b>         | 5'-<br>GGGAGACCAUCUGCUACUCGAUCGAUUAUAGUUUAUAAAG<br>GAGUAAACUAUACACUUCUGACUGGUACCUAGCAUAAUC-3'              |
| <b>5'ppp-AU</b>         | 5'-<br>GGGAGACCAUCUGCUACUCGAUCGAUUAUAGUUUAUAAAG<br>GAGUAAACUAUACACUUCUGACUGGUACCUAGCAUAAUC-3'              |
| <b>3p-hpRNA</b>         | 5'-<br>AGCAAAGCAGGGUGACAAAGACAUAUUGGAUCCAAACACU<br>GUGUCAAGCUUUCAGGUAGAUUGC UUUCUUUGGCAUGUCC<br>GCAAAC- 3' |

**Table 5** – Sequences of purified RNAs used in this project.



## Antibodies

Antibodies used in this project are shown in Table 6.

| Target                     | Dilution | Species           | Source                       |
|----------------------------|----------|-------------------|------------------------------|
| <b>TRIM25</b>              | 1:2000   | Rabbit Monoclonal | Abcam                        |
| <b>hnRNPA1</b>             | 1:1000   | Mouse Monoclonal  | Millipore                    |
| <b>hnRNPI</b>              | 1:1000   | Mouse Monoclonal  | Santa Cruz                   |
| <b>DHX9</b>                | 1:2000   | Rabbit Polyclonal | Protein Tech                 |
| <b>T7 (HRP conjugated)</b> | 1:10000  | Mouse Monoclonal  | Millipore                    |
| <b>Tubulin</b>             | 1:40000  | Mouse Monoclonal  | Sigma-Aldrich                |
| <b>SERPINB5</b>            | 1:1000   | Rabbit Polyclonal | GeneTex                      |
| <b>IRF-3</b>               | 1:1000   | Rabbit Polyclonal | Cell Signalling Technologies |
| <b>Phospho-IRF-3</b>       | 1:1000   | Rabbit Polyclonal | Cell Signalling Technologies |

**Table 6** – Antibodies used in this project and their dilutions.

## Buffers

Composition of buffers used in this project are shown in Table 7.

| Buffer                    | Composition  |
|---------------------------|--|
| <b>Buffer G</b>           | 20 mM Tris-HCl pH7.5, 137 mM NaCl, 1 mM EDTA, 1% TritonX-100, 10% glycerol, 1.5 mM MgCl <sub>2</sub> , X mM DTT, 1 mM PMSF |
| <b>BWB</b>                | 1xPBS with 0.02% v/v Tween 20  |
| <b>PXL</b>                | 1xPBS with 1%v/v Igepal, 0.5%wt/v Sodium Deoxycholate, 0.1% wt/v SDS   |
| <b>RNA Elution Buffer</b> | 0.3 M Sodium Acetate pH 5.2, 0.5 mM EDTA, 0.1%SDS  |
| <b>Roeder D</b>           | 100 mM Tris pH8, 100 mM KCl, 200 μM EDTA, 20% Glycerol, X mM DTT, 1 mM PMSF  |
| <b>TBE</b>                | 100 mM Tris, 100 mM Boric Acid, 2 mM EDTA, NaOH to pH  |
| <b>TBS-T (pH7.5)</b>      | 20 mM Tris, 150 mM NaCl, 0.1% Tween 20, HCl to pH  |
| <b>Transfer Buffer</b>    | 200 mM Glycine, 25 mM Tris, 10% Methanol   |
| <b>UEO</b>                | 10 mM EDTA, 3.5 M Urea, Bromophenol Blue, Xylene Cyanol  |

**Table 7** – Compositions of buffers and solutions used in this project. All concentrations shown are final concentrations in 1x solution.

## *In Vitro* Transcription and RNA Purification

DNA templates of pre-let-7a-1 and mutants or sgRNAs with a T7 promoter sequence were generated by PCR through amplification of the sequence of interest from a plasmid using Phusion polymerase (New England Biosciences, NEB). Reagents used for PCR amplification are shown in Table 8. Reactions were run initially at 98°C for 30 seconds before 35 cycles of: 10 seconds at 98°C, 30 seconds at 55°C and 15 seconds at 72°C. Following these cycles reactions ran for a further 5 minutes at 72°C.

| Component              | Volume (µL) |
|------------------------|-------------|
| Phusion Buffer         | 10          |
| 10 µM dNTPs            | 1           |
| F Primer (10 mM)       | 2.5         |
| R Primer (10 mM)       | 2.5         |
| Plasmid                | 2           |
| Phusion RNA Polymerase | 0.5         |
| H <sub>2</sub> O       | 31.5        |
| <b>Total</b>           | <b>50</b>   |

**Table 8** – Reagents used for generation of templates for *in vitro* transcription by PCR.

Templates for 5'ppp-79 and mutants were generated by Klenow extension of two overlapping oligonucleotides using Klenow fragment polymerase. 5 µL of each of the forward and reverse oligonucleotides (100 mM) were mixed with 2 µL Klenow Buffer (New England Bioscience) in a total volume of 20 µL. These were heated to 100°C for 2 minutes before being allowed to cool slowly for 30 minutes to allow annealing. 1 µL 10 µM dNTPs and 1 µL Klenow Polymerase (New England Bioscience) were added and reactions were incubated for a further hour at 37°C.

*In vitro* transcription reactions were set up as follows: 2.5 µL 10x T7 RNA Polymerase buffer (Lucigen), 1.25 µL 20 µM rNTPs, 1 µL NxGen T7 RNA polymerase (Lucigen), 0.5 µL RNase Out

(Invitrogen) and 2  $\mu\text{L}$  template DNA in a total volume of 25  $\mu\text{L}$ . Reactions were incubated for 90 minutes at 37°C. Subsequently, 10 *in vitro* transcription reactions were pooled and 2  $\mu\text{L}$  Turbo DNase (Invitrogen) was added and reactions incubated at 37°C for a further 10 minutes. After this, 25  $\mu\text{L}$  3 M sodium acetate and 800  $\mu\text{L}$  ice cold 100% ethanol were added before the mixture was precipitated for approximately 1 hour on dry ice. The precipitated mixtures were centrifuged for 15 minutes at 13,000rpm, 4°C, washed with 1mL ice cold 70% ethanol and centrifuged for 2 minutes at 13,000rpm, 4°C. Ethanol was removed and the pellet resuspended in 40  $\mu\text{L}$  H<sub>2</sub>O and 40  $\mu\text{L}$  2xUEO buffer before being loaded onto a pre-warmed 10% polyacrylamide, 7.5M Urea gel with TBE running buffer. The gel was then run for approximately 90 minutes at 50mA. After running, gels were stained with RNA staining solution to visualise RNA before RNA bands were excised. Excised RNA bands were incubated overnight in 300  $\mu\text{L}$  RNA elution buffer before buffer was removed from the gel pieces and added to 700  $\mu\text{L}$  100% ethanol. Samples were precipitated either overnight at -20°C or for 1-2 hours on dry ice. Samples were then centrifuged for 15 minutes at 13,000rpm, 4°C, washed with 1mL ice cold 70% ethanol and centrifuged again for 2 minutes at 13,000rpm, 4°C. Ethanol was removed and pellets were allowed to dry to remove residual ethanol before being resuspended in 22  $\mu\text{L}$  H<sub>2</sub>O. RNA concentration was determined using a nanodrop spectrophotometer.

## Cell culture and transfections

Cells were grown in Dulbecco's Modified Eagle Media (DMEM) supplemented with 10% Fetal Bovine Serum (FBS) at 37°C and 5% CO<sub>2</sub> unless otherwise stated. Cells were seeded in

6-well or p100 plates 24 hours before transfection such that they reached a confluency of 70% by the time transfection occurred.

For transfections, DNA or RNA to be transfected was added to 250  $\mu$ L (6-well) or 1.5mL (p100) Optimem serum-free media. 5  $\mu$ L (6-well) or 30  $\mu$ L (p100) Lipofectamine 2000 was also added to a separate tube containing 250  $\mu$ L or 1.5mL Optimem. Both mixtures were incubated for 5 minutes at room temperature before the Lipofectamine mixture was added dropwise to the DNA/RNA mixture. This mixture was then incubated for 30 minutes at room temperature. Meanwhile, cells were washed with Optimem and fresh DMEM was added. After incubation, nucleic acid/Lipofectamine mixtures were added to cells dropwise.

## Protein extraction

Cells were washed twice in PBS and scraped in Roeder D buffer. Cells were lysed by sonication before being centrifuged for 5 minutes at 10,000rpm and 4°C to remove cell debris. Supernatant was removed to a fresh tube and protein concentration was determined using a nanodrop spectrophotometer.

## RNA extraction

Cells were washed twice in PBS before being resuspended in 1mL Tri-Reagent (Invitrogen). 200  $\mu$ L chloroform was added and samples were mixed vigorously by hand for 15 seconds, followed by being allowed to settle for 2-3 minutes at room temperature. Samples were centrifuged for 15 minutes at 12,000 rcf, 4°C and the aqueous phase (approximately 500  $\mu$ L) was removed to a fresh tube. 500  $\mu$ L isopropanol was added and samples were mixed

by inversion before being incubated 10 minutes at room temperature. Following this samples were centrifuged for 10 minutes at 12,000 rcf, 4°C before being washed with ice cold 70% ethanol. Samples were further centrifuged for 5 minutes at 7500 rcf before ethanol was removed and pellets were allowed to dry to remove residual ethanol. Pellets were resuspended in 32  $\mu$ L H<sub>2</sub>O and RNA concentration was determined using a nanodrop spectrophotometer.

## Western blots

Volumes of protein extract corresponding to 80 $\mu$ g protein were mixed with 5  $\mu$ L 4x NuPage LDS Sample Buffer (Invitrogen), 2  $\mu$ L 10x NuPage Sample Reducing Agent (Invitrogen) and Roeder D buffer to a final volume of 20  $\mu$ L. Samples were boiled for 10 minutes at 70°C before being loaded on a NuPage 4-12% Bis Tris Protein Gel (Invitrogen) with NuPage MOPS SDS Running Buffer (Invitrogen). 10  $\mu$ L protein ladder was also loaded. Gels were run for 1 hour at 180V and subsequently transferred to a nitrocellulose membrane using Tris-Glycine transfer buffer. Membranes were blocked overnight in a 1 in 20 dilution of Western Blocking Reagent (Roche) in TBS-T.

After blocking, primary antibodies were diluted as described in Table 6 in TBS-T with a 1 in 20 dilution of Western Blocking Reagent and added to membranes. Membranes were incubated, rocking for one hour at room temperature before being washed with TBS-T 3 times for ten minutes. Corresponding HRP-linked secondary antibodies were diluted as described and incubated, rocking with membranes for 1 hour at room temperature. Membranes were again washed 3 times with TBS-T for ten minutes before addition of SuperSignal West Pico Plus western blotting substrate (ThermoFisher). Membranes were subsequently developed using Radiographic film.

To re-blot membranes for a different protein of interest, they were first stripped for 10 minutes in a 1 in 10 dilution of ReBlot Plus Strong Antibody Stripping Solution (Chemicon) in TBS-T. Following this, blots were blocked for 30 minutes and re-probed with a new antibody as described previously.

## quantitative Real Time Polymerase Chain Reaction (qRT-PCR)

The SuperScript II Platinum One-Step qRT-PCR Kit (Invitrogen) was used for qRT-PCR assays according to manufacturer's instructions. Each reaction was performed with 500ng RNA in a total reaction volume of 25  $\mu$ L with the primers indicated in Table 4. Reactions ran for 40 cycles and were performed on a Roche 480 LightCycler.

## RNA pulldown

In principle, RNA pulldowns seek to identify proteins that associate with a particular RNA by attaching the RNA of interest to agarose beads and incubating with whole cell extract. After washing out unbound proteins, bound proteins can be analysed by western blot or mass spectrometry<sup>221</sup>. Identified proteins do not necessarily bind directly to the RNA in question as they may interact with the RNA via interactions with another protein or RNA molecule. RNAs were covalently attached to adipic-acid coated agarose beads using sodium periodate<sup>222</sup>. A mixture was prepared containing 500 pmol RNA of interest, 100 mM sodium acetate and 5 mM sodium periodate in a total volume of 200  $\mu$ L. A sample without RNA was also prepared at this stage for use as a beads-only control. Samples were wrapped in foil to protect from light and were incubated 1 hour at room temperature while rocking. Subsequently, 15  $\mu$ L 3 M sodium acetate and 600  $\mu$ L ice cold 100% ethanol were added and

RNA was precipitated on dry ice for 30 minutes. Samples were then centrifuged for 15 minutes at 13,000rpm, 4°C, washed with 1mL ice cold 70% ethanol and centrifuged again for 2 minutes at 13,000rpm, 4°C. Ethanol was removed and pellets were allowed to dry to remove residual ethanol before being resuspended in 500 µL 100 mM sodium acetate pH 5. Adipic acid-coated beads were prepared by adding 250 µL resin to a fresh falcon tube per reaction and washing 3 times with 100 mM sodium acetate (spins of 3 minutes at 300rpm). Beads were resuspended in 100 mM sodium acetate such that there was 200 µL total volume per prepared RNA. 200 µL prepared beads were added to each tube of periodate-treated RNA and incubated rocking at 4°C overnight, again wrapped in foil to protect from light.

After incubation, 700 µL 4 M KCl was added to each tube and these were incubated, rocking for 30 minutes at room temperature. Subsequently non-bound RNA was washed out by two washes with 2 M KCl followed by three washes with Buffer G (spins of 2 minutes at 3000rpm, 4°C). To the RNA-coupled beads was added 1mg protein extract, 1.5 mM MgCl<sub>2</sub>, 25 mM Creatine-phosphate, 0.5 mM ATP and 5 µL RNase OUT in a total volume of 650 µL. Samples were incubated, rocking at 37°C for 30 minutes before beads were pelleted by centrifuging 3 minutes at 1000rpm, 4°C. Supernatant at this stage from beads-only controls was kept for use as a loading control (input). Samples were then washed 3 times in Buffer G (spins of 2 minutes at 1000rpm, 4°C). After the last wash, supernatant was removed and beads resuspended in 39 µL H<sub>2</sub>O, 15 µL 4x NuPage LDS Sample Buffer and 6 µL 10x NuPage Sample Reducing Agent. 13 µL Loading control samples were added to 5 µL NuPage LDS Sample Buffer and 2 µL 10x NuPage Sample Reducing Agent. Samples were boiled for 10 minutes at 70°C before 30 µL of pulldown samples and 20 µL loading control was loaded into a protein gel and western blotting proceeded as previously described.

## Protein purification

### Buffers

A list of the buffers used in purification of proteins is found in Table 9. All buffers were passed through a 0.22µm filter before use.

| Buffer                      | Composition   |
|-----------------------------|---|
| <b>Resuspension Buffer</b>  | 20 mM Sodium Pyrophosphate pH7.4, 500 mM NaCl, 5 mM MgCl <sub>2</sub>   |
| <b>Binding Buffer</b>       | 20 mM Sodium Pyrophosphate pH7.4, 500 mM NaCl, 10 mM Imidazole  |
| <b>Elution Buffer</b>       | 20 mM Sodium Pyrophosphate pH7.4, 500 mM NaCl, 500 mM Imidazole   |
| <b>Gel Exclusion Buffer</b> | 10 mM Tris pH8, 300 mM NaCl, 2 mM DTT   |
| <b>Cell Lysis Buffer</b>    | 50mL Resuspension Buffer, 200 µL lysozyme (100mg/mL), 50 µL DNase, 5 µL RNase (100mg/mL), 2 Complete Protease Inhibitor tablets (Roche) |

**Table 9** – Compositions of buffers used for protein purifications.

### Method

The full-length human 6xHis-tagged TRIM25 WT and TRIM25ΔRBD mutant were cloned into the pET30a plasmid, which was transformed into BL21 gold *E. coli* cells. 5mL overnight cultures were grown before expression cultures were set up in 250mL Superbroth with 50 µg/mL kanamycin and 1mL of overnight culture. Cultures were grown to an OD of 0.6-0.8 before 0.5 mM IPTG was added and cultures were incubated 22 hours at 30°C shaking at 180rpm. After incubation, cultures were centrifuged for 15 minutes at 8000 rpm, 4°C and pellets were divided into 5g and snap frozen in liquid nitrogen. 5g pellets were resuspended in 50mL of cell lysis buffer and incubated for 30 minutes at 4°C before being passed through



a 0.6 x 30 mm needle. Samples were then passed through a cell disruptor at 25 kPsi, followed by 30mL lysis buffer and the resulting sample was centrifuged for 1 hour at 50,000 rcf, 4°C. The supernatant was passed through a 5 µm filter, followed by a 0.45 µm filter. Samples were loaded onto an IMAC HiTrap 1 mL FF NiCl<sub>2</sub> column (GE Life Sciences) and passed through with binding buffer before elution with elution buffer.

Samples were concentrated to below 500 µL using a Vivaspin 6 30kD centrifugal concentrator (Sartorius Stedim) before being further purified by size exclusion chromatography. Size exclusion chromatography was performed using a Superdex 200 10/300 GL column (Sigma-Aldrich). The column was primed and run with gel exclusion buffer. Subsequently, samples were further concentrated using a Vivaspin 5 30,000 MWCO centrifugal concentrator (Sartorius Stedim).

## RNA Footprinting/Structure Probing

*In vitro* transcribed and purified pre-let-7a-1 was 5' end-labelled with  $\gamma$ -ATP-32P using T4 polynucleotide kinase (Roche) for 15 minutes at 37°C. End-labelled RNA was purified by gel electrophoresis as previously described. Structure probing reactions took place in a total volume of 8 µL with 1 µL RNA (~100,000 c.p.m) and 7 µL structure probing buffer containing 0.2 mM Pb<sup>2+</sup> or dilutions of 0.5, 0.25 or 0.125 units/ µL T1 RNase in H<sub>2</sub>O. 200ng purified His-TRIM25 WT was added to the indicated reactions. T1 ladder was generated in the same manner with 1 unit/mL T1 RNase. Reactions proceeded for 10 minutes at 37°C before being stopped with 8 µL 2xUEO buffer. Samples were run on a 10% denaturing polyacrylamide-urea gel as previously described before the gel was dried and exposed to a phosphoscreen overnight. The phosphoscreen was subsequently scanned using a Fujifilm FLA 5000 scanner.

## EMSA

EMSAs were performed with end-labelled pre-let-7a-1 probe and 0-2000 ng purified TRIM25 WT or TRIM25 $\Delta$ RBD. 0.1 pmol probe and the indicated amount of purified protein in gel exclusion buffer were supplemented with 3 mM MgCl<sub>2</sub>, 0.5 mM ATP and 37.5 mM creatine phosphate in a total volume of 16  $\mu$ L. Reactions were incubated for 1 hour at 4°C before addition of 16  $\mu$ L 2x native loading buffer. Samples were loaded on a non-denaturing 6% w/v polyacrylamide gel and run in 0.5x TBE buffer at 8 W. The gel was subsequently dried and exposed to a radiographic film that was scanned using a Fujifilm FLA 5000 scanner.

## Thermal Denaturation Assays

Around 4  $\mu$ M purified His-TRIM25 WT or His-TRIM25 $\Delta$ RBD were mixed with 10  $\mu$ L 5x Sypro Orange (ThermoFisher) to a total volume of 50  $\mu$ L. Thermal denaturation assays were then performed on a Bio-Rad iQ5 iCycler, with readings taken at 30 second time points as temperature increased from 20°C to 70°C. The melting temperature was determined from the maximum of the first derivative of the melting curve. The mean melting temperature was determined from the average of three independent replicates.

## RNA-binding Protein Immunoprecipitation (RIP)

HeLa cells were cultured in P100 plates and transfected with a plasmid encoding T7-tagged TRIM25 WT or TRIM25 $\Delta$ RBD, or mock transfected, and incubated for 24 hours. Cells were

resuspended in 1mL PXL buffer and incubated ten minutes on ice before being centrifuged for 20 minutes at 13,000rpm, 4°C to remove cell debris. 50 µL Dynabeads (ThermoFisher) were washed 3 times in BWB buffer before resuspension in 50 µL BWB and addition of 1 µL anti-T7 antibody. Beads were incubated, shaking 30 minutes at room temperature before being washed 3 times in PXL buffer and resuspended in 20 µL PXL. Protein extracts were added to antibody-coupled beads and incubated, rocking 1 hour at 4°C before being washed 3 times with PXL. RNA was isolated by adding 1mL Tri-Reagent to beads and proceeding with RNA extraction as previously described. Levels of bound RNAs were determined by qRT-PCR.

## SEC-MALS

Purified His-TRIM25 WT or His-TRIM25 $\Delta$ RBD were run at 0.75 mg/mL, 1 mL/min on a Superdex200 Increase 10/300 GL column in gel exclusion buffer (Table 9). This was attached to a Viscotek MALS-20 and VE3580 RI detector on which mass measurements took place.

## Immunoprecipitation (IP)

30 µL Protein A beads were washed in Buffer G and resuspended in 500 µL Buffer G before 1 µL anti-T7 antibody was added. Beads were incubated, rocking 30 minutes at room temperature and subsequently washed twice with Buffer G. 20 µL Protein A beads were washed in Roeder D buffer before 500 µg protein extract in a total volume of 500 µL Roeder D was added. Samples were incubated, rocking 30 minutes at room temperature before beads were pelleted by centrifugation for 3 minutes at 4000 rpm, 4°C. Supernatant from this step was added to antibody-coupled beads and incubated, rocking for 1 hour at room

temperature. Beads were washed 3 times in Buffer G before addition of 26  $\mu\text{L}$   $\text{H}_2\text{O}$ , 10  $\mu\text{L}$  4x NuPage LDS Sample Buffer and 4  $\mu\text{L}$  10x NuPage Sample Reducing Agent and boiled for 10 minutes at 70°C. 20  $\mu\text{L}$  of this was run on a gel with 40  $\mu\text{g}$  of the original extract used as a loading control. Gels and western blotting were run as previously described.

## *In Vitro* Ubiquitination

Initially, IP of T7- tagged TRIM25 or mutants was performed as previously described. After the last wash with Buffer G, the components required for ubiquitination, purified Ube1, His-Ube2D3 and ubiquitin (all from UBP-Bio) were added. For TRIM25 auto-ubiquitination, 1 mg/mL Ube1, 2 mg/mL His-Ube2D3 and 50 mg/mL ubiquitin were added. For ZAP ubiquitination 5 mg Ube1, 10 mg/mL His-Ube2D3 and 250 mg/mL ubiquitin were used. Samples were incubated, shaking for 1 hour at 37°C before being prepared for running on a protein gel and western blot as previously described for IPs.

For RNase experiments, 5  $\mu\text{L}$  RNase A/T1 Mix (ThermoFisher) was added to the sample during the initial pre-clearing phase of the IP.

## Generation of Knockout Cell Lines

Two short guide RNAs (sgRNAs) targeting exon 1 of TRIM25 were designed by Nila Roy Choudhury (TRIM25 Left sgRNA – CCACGTTGCACAGCACCGTGTTTC and TRIM25 Right sgRNA CTGCGGTCGCGCCTGGTAGACGG). Purified sgRNAs were produced by *in vitro* transcription as previously described. HeLa or HEK293 Cells were transfected with 50ng of each sgRNA in addition to 200 ng of GeneArt CRISPR Nuclease mRNA (ThermoFisher). Cells were incubated for 24 hours and subsequently seeded to a 96-well plate such that on average one cell was

present in each well. Cells were grown until colonies were visible with the naked eye before cells were split into two more 96-well plates. Once cells had grown, one plate was used for immunoblot (dot-blot) analysis.

Cells were washed twice in PBS before addition of 30  $\mu$ L of Passive Lysis Buffer (Promega). Cells were incubated, rocking for 15 minutes at room temperature. 2  $\mu$ L of protein extract from each well was spotted directly onto a nitrocellulose membrane. Membranes were blocked in Western Blocking Reagent at a 1 in 10 dilution in TBS-T for 1 hour before western blotting proceeded as previously described. Selected clones were picked from corresponding wells of the second 96-well plate and grown in 6-well plates before levels of TRIM25 in each clone were validated by western blot.

## Gene Sequencing

Genomic DNA was isolated from cell lines using the GenElute Mammalian Genomic DNA Miniprep Kit (Sigma-Aldrich) according to manufacturer's instructions. The region surrounding the target sequences of the sgRNAs was amplified by PCR using the primers described in Table 3. The PCR product was gel purified then cloned into a pJET vector using the CloneJET PCR Cloning Kit (ThermoFisher) according to manufacturer's instructions and sequenced using the primer included in the kit.

## RNA Stability Assays

Cells were grown in 6-well plates to 90-95% confluency before addition of 10  $\mu$ g/mL Actinomycin D (Sigma-Aldrich). Total RNA was extracted from cells at the indicated time points as previously described and levels of RNA were assayed by qRT-PCR and normalised

to levels of 18S rRNA. The SuperScript II Platinum One-Step qRT-PCR Kit (Invitrogen) was used for qRT-PCR assays according to manufacturer's instructions. Each reaction was performed with 500ng RNA in a total reaction volume of 25  $\mu$ L with the primers indicated in Table 4. Reactions ran for 40 cycles and were performed on a Roche 480 LightCycler. Reactions for 18S rRNA were first diluted 1 in 100 from the original samples such that 5ng RNA was used for these reactions.

## RNAseq

RNA was extracted from HeLa WT or TRIM25 KO cells using Tri-Reagent as previously described. To ensure purity, RNA samples were subjected to a second round of purification using Phenol:Chloroform:Isoamyl Alcohol 25:24:1 (Sigma-Aldrich). Equal parts phenol-chloroform reagent and RNA samples were mixed and subsequently centrifuged for 5 minutes at 12,000 rcf, room temperature. The aqueous phase containing purified RNA was transferred to a fresh tube and this process was repeated two more times.

RNA purity and integrity was analysed on an Agilent 2100 Bioanalyzer to ensure that total quantity of RNA, OD260/280 ratio and 28S:18S rRNA ratios met minimum standards for RNAseq analysis. Samples were subsequently sent to BGI Tech Solutions for library preparation, sequencing and analysis. Additional analysis was performed by Shaun Webb (University of Edinburgh).

## IAV Reverse Genetics

IAV A/PR/8/34 (PR8) virions were generated using an 8 plasmid reverse genetics system as described by de Wit *et al.* <sup>223</sup>. In short, this strategy uses pDUAL plasmids encoding each of the 8 segments of the PR8 genome under both a positive sense RNA Polymerase II promoter and a negative sense RNA polymerase I promoter. This results in the transcription of positive sense mRNA encoding the viral proteins as well as negative sense vRNA. Once translated, the viral proteins and vRNA assemble into vRNPs that transcribe more mRNA and replicate vRNA. Viral proteins and vRNA can assemble into mature IAV virions that are released from cells into the supernatant and can then be harvested and used to infect Madin-Darby Canine Kidney (MDCK) cells, allowing the virus to multiply and generate a working virus stock.

250 ng of each pDUAL plasmid was transfected into HEK293T cells. To create a negative control for use in future experiments this was repeated minus the plasmid encoding segment 1, resulting in no mature virions being produced. Also, PR8 NS1 R38K41A mutant virus was generated in the same way but the plasmid encoding segment 8 of the genome was replaced with one encoding the indicated mutation. After 24 hours, media was replaced with virus growth medium (VGM, DMEM supplemented with 0.14% BSA and 1 µg/mL TPCK-treated trypsin). After a further 48 hours, P0 virus stock was harvested by removing VGM from cells and centrifuging this at 13,000 rpm for 1 minute to pellet any detached cells. P0 stock was used to infect MDCK cells in a T25 flask. MDCK cells were first washed 2 times with serum-free DMEM before addition of 1 mL VGM and 100 µL P0 stock. Cells were incubated 1 hour at 37°C before the addition of a further 5 mL VGM. After 48 hours P1 stock was harvested, media was removed from cells and cells were pelleted as before. Supernatant was then aliquoted into 100 µL portions and viral titre was calculated by plaque assay.

## Plaque Assays

MCDK cells were seeded at  $1.5 \times 10^6$  cells per well in 6-well plates in standard growth media. After 24 hours, serial 10-fold dilutions of the virus samples to be titred were made up to a dilution of  $1 \times 10^{-8}$  in serum-free DMEM. MDCK cells were washed with DMEM before addition of 800  $\mu$ L virus dilutions (from  $10^{-3}$  to  $10^{-8}$  in the same 6-well plate). Cells were incubated for 1 hour at 37°C before overlaying with Avicell overlay media (50% DMEM, 50% 2.4% Avicell, supplemented with 0.14% BSA and 1  $\mu$ g/mL TPCK-treated trypsin). Cells were incubated for 48 hours at 37°C before 1 mL 10% formaldehyde was added per well. Cells were incubated 1 hour at room temperature before media/formaldehyde were removed and 0.1% crystal violet (in methanol) was added to stain. After 30 minutes, plates were washed with water and plaques were counted to calculate titre in plaque forming units (pfu)/mL of the original virus stock.

## Infection of Cells with IAV

HEK293 cell lines were infected with PR8 WT or PR8 NS1 R38K41A at the indicated multiplicity of infection (MOI). Cells were grown such that there were  $1 \times 10^7$  cells per well before growth media was removed and 400  $\mu$ L serum-free DMEM was added. Virus stocks were diluted in DMEM such that the correct number of virus particles were present in 100  $\mu$ L for the desired MOI. 100  $\mu$ L virus dilution was added per well and cells were incubated for 1 hour at 37°C. Media was removed and 1 mL VGM was added before cells were incubated for the indicated times. Virus titre in supernatant was determined by plaque assay as previously described.



## 3p-hpRNA Assays

### *Western Blot and HEKBlue Assays*

Cells at 70% confluency were transfected with 100 ng/mL 3p-hpRNA (Invivogen) as previously described and incubated for 6 hours. Protein extracts and western blotting proceeded as previously described but supernatants from cell media were taken for analysis using the HEKBlue system. 20  $\mu$ L of the supernatant or an IFN $\alpha$ / $\beta$  standard containing indicated units of purified IFN $\alpha$  and IFN $\beta$  were added to 50,000 HEK-Blue cells (Invivogen) in a total volume of 200  $\mu$ L and incubated for 24 hours. 5  $\mu$ L of the resulting supernatant was added to 180  $\mu$ L QUANTI-Blue (Invivogen) in a 96-well plate and incubated for one hour at 37°C before absorbance was read at 680 nm.

### *Luciferase Assays*

For luciferase assays, cells were transfected with 100 ng/mL 3p-hpRNA along with a Firefly luciferase reporter under the IFN $\beta$  promoter and Renilla luciferase under a constitutive Thymidine Kinase (TK) reporter. The cells were incubated for 24 hours post-transfection before extraction with passive lysis buffer (PLB, Promega). Cells were washed twice in PBS before addition of 500  $\mu$ L of PLB and were incubated, rocking for 15 minutes at room temperature. Protein extracts were moved to fresh tubes and centrifuged for 5 minutes at 10,000 rpm, 4°C to pellet cell debris. Activity levels were measured for Firefly and Renilla luciferase using the Dual-Luciferase Reporter Assay System (Promega) according to manufacturer's instructions. In short, 50  $\mu$ L Luciferase assay buffer was added to 5  $\mu$ L protein extract and a reading was taken for Firefly luciferase activity. Subsequently, 50  $\mu$ L

Stop and Glo buffer was added and a reading taken for Renilla luciferase activity. Activity of the IFN $\beta$  promoter was calculated as the ratio of Firefly to Renilla luciferase activity.

## Minireplicon Assays

HEK293 cell lines were transfected with 250 ng each of pDUAL plasmids encoding segments 1, 2, 3 and 5 of the IAV genome (PA, PB1, PB2, NP) along with a Firefly luciferase reporter plasmid under the control of an RNA polymerase I promoter. The luciferase construct is in the negative sense and flanked by the untranslated regions of IAV segment 8. As such, it will resemble a vRNA to the vRNP and must be transcribed to positive sense mRNA to be able to be translated into luciferase protein. A negative control in which segment 5 of the IAV genome (NP) had been omitted was also performed. After incubation for 48 hours, a luciferase assay was performed as previously described but Renilla luciferase activity was not measured.

# Results

## Chapter 1 - Determining the mechanism of TRIM25 binding to RNA

### *Aims*

TRIM25 has been shown to bind to RNA previously, but little is known about the mechanism of how this occurs or any functions this activity might have. The aim of this section of the project was to determine how TRIM25 binds to RNA, as well as to design mutants of either TRIM25 or its RNA binding partners that do not bind to each other and could thus be used in experiments to uncover the function of TRIM25 RNA binding.

TRIM25 does not have a canonical RNA-binding domain (RBD) but there is evidence that removing its coiled-coil domain impairs RNA binding<sup>215</sup>. Previous work in the lab has shown that TRIM25 binding to pre-let-7a-1 can affect the stability of the RNA by recruitment of the terminal uridylyase TUT4, which adds a poly(U) chain to the 3' end of the pre-miRNA, leading to degradation by the exonuclease Dis3L2<sup>216</sup>. The mechanism of TRIM25's involvement in this process, as well as its ubiquitination target(s), are not yet known. In order to determine the effects of TRIM25 RNA binding on any of its functions it was first important to understand how TRIM25 binds to RNA. This would allow the design of mutants of TRIM25 that do not bind to RNA or RNAs that do not bind to TRIM25. These mutants could then be used in experiments to elucidate the functions of TRIM25 RNA binding by comparing them to wild-type (WT) TRIM25 or RNAs. Two strategies were used in this project to further understand the mechanisms underpinning TRIM25 RNA binding. Firstly, I attempted to identify any sequence motifs required for TRIM25 RNA binding. This would enable the deletion of these motifs to generate RNAs that cannot bind to TRIM25. It would also allow

TRIM25 binding to be induced in previously non-binding RNAs by addition of the identified motif. Secondly, identifying the amino acids of TRIM25 that are important for RNA binding would allow the design of a non-RNA binding TRIM25 mutant by mutagenizing or deleting these residues. In addition, this would provide insights into how a protein with no canonical RBD can bind to RNA, which may also apply to other non-canonical RBPs.

### *The GGAGAU motif of pre-let-7a is not necessary for TRIM25 RNA-binding*

TRIM25 has been shown to bind to RNA on multiple occasions. Previous work in this lab identified the GGAGAU motif in the terminal loop of pre-let-7a-1 as being important for TRIM25 binding to pre-let-7a-1 with a minimal terminal loop<sup>216</sup>. This was shown through RNA pull-down assays with a mutant of pre-let-7a-1 where GGAGAU of a minimal pre-let-7a-1 terminal loop has been mutated to GGAGUA<sup>216</sup>. In this experiment, the RNA with an intact GGAGAU motif in the minimal terminal loop (pre-let-7a-1@2) showed increased binding to TRIM25 compared to the GGAGUA mutant (pre-let-7a-1@3). To further determine the importance of the GGAGAU motif to TRIM25 RNA-binding activity two more mutants of pre-let-7a-1 were designed; a full-length pre-let-7a-1 with just the switch from GGAGAU to GGAGUA (pre-let-7a-1/4.2) and a mutant where the terminal loop of pre-let-7a-1 had been replaced with that of pre-miR-16 (pre-let-7a-1/16)(FIG. 6A). In addition to this a 79nt synthetic viral RNA (5'ppp-79) with unknown TRIM25 binding potential was used. This RNA had previously been shown to activate RIG-I signalling in a cell-free system<sup>116</sup>. It was hoped that modulating its ability to be bound by TRIM25 would allow it to be used to test whether TRIM25 binding to an RNA might have an effect on whether it can activate RIG-I signalling. 5'ppp-79 was mutated to introduce the pre-let-7a-1 terminal loop

with either the GGAGAU motif (5'ppp-AU) or GGAGUA (5'ppp-UA) in an effort to increase binding to TRIM25 (FIG. 6A). TRIM25 binding to these RNAs was assayed by RNA pull-down. *In vitro* transcribed and gel-purified RNAs were covalently linked to adipic acid-coated agarose beads that were subsequently incubated with HeLa whole cell extract (WCE). After washing, proteins left bound to the RNAs were analysed by western blot (FIG. 6B). 5'ppp-79, 5'ppp-AU and 5'ppp-UA all showed substantial binding to TRIM25 compared to a beads-only control with TRIM25 binding to 5'ppp-UA being slightly more efficient. Pre-let-7a-1 also showed binding to TRIM25 as expected, however both pre-let-7a-1/16 and pre-let-7a-1/4.2 also bound, although at a lower level. DHX9, a double-stranded RNA binding protein, was used as a positive control and hnRNPA1 was used as a specificity control as it should only bind to the RNAs containing the pre-let-7a-1 terminal loop<sup>224</sup>. HnRNPI was also used as a specificity control as it should not bind to pre-let-7a-1 but should to 5'ppp-79 due to its sequence specificity. This was indeed observed in the pull-down results. Taken together, these results suggest that although the GGAGAU motif may increase the efficiency of pre-let-7a-1 binding to TRIM25, it is not required for binding and does not seem to make a difference in binding efficiency when added to another, unrelated, RNA. It is possible that the GGAGAU motif in the pre-let-7a-1 terminal loop helps to stabilise the structure of the loop and it is this structure that TRIM25 is recognising, not the GGAGAU motif itself.

### *Mutating a potential TRIM25 binding site on pre-let-7a-1 does not reduce binding*

One method for determining the RNA nucleotides directly bound by a protein is through a technique called RNA foot printing<sup>225</sup>. This involves incubating purified protein of interest (in this case recombinant His-tagged TRIM25, purified from *E. coli*) with RNA radiolabelled

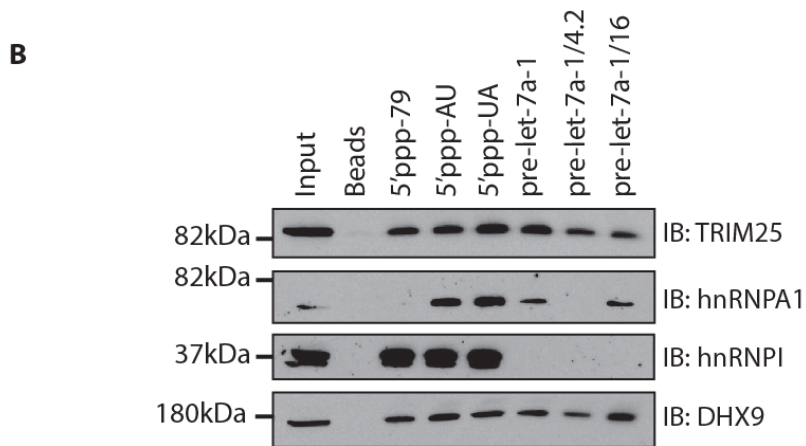
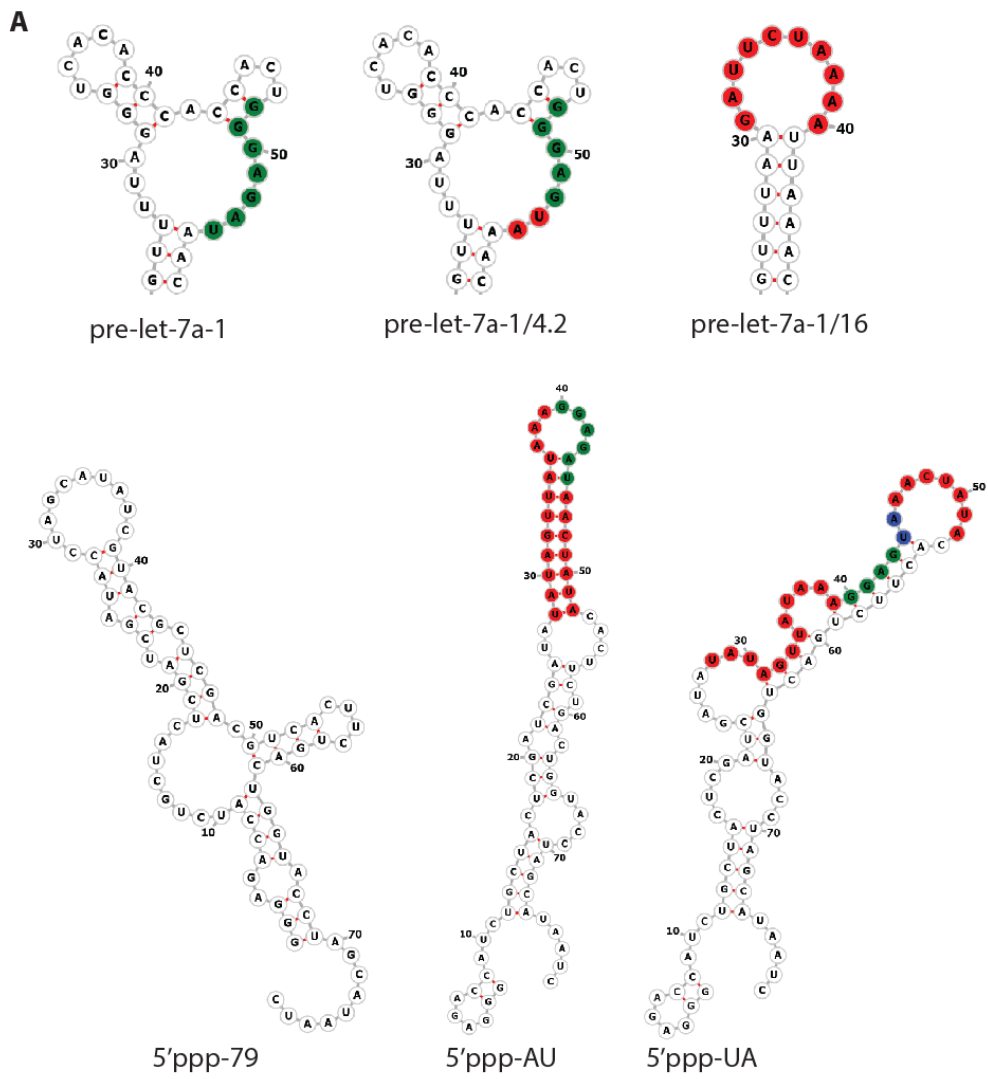


**Figure 6** - *The GGAGAU motif is not required for TRIM25 RNA binding.* (A) Secondary structures of RNAs tested for TRIM25 binding. Secondary structures are those with minimum free energy and were predicted by RNAfold (<http://rna.tbi.univie.ac.at/cgi-bin/RNAWebSuite/RNAfold.cgi>) and visualised using *forna* (<http://rna.tbi.univie.ac.at/forna>). (B) WB analysis of RNA pulldown assay of selected RNAs coupled to beads and incubated with HeLa WCE. Input lane represents 4% (40 µg) of extracts used for pulldowns.

at the 5' end (pre-let-7a-1) and subjecting the RNA to partial RNase T1 or lead ions ( $Pb^{2+}$ ) cleavage. As the purified protein binds on the RNA, it should protect the nucleotides it is bound to (and potentially some of the surrounding area) from digestion and as such this binding site can be visualised by running the RNA on a gel after digestion then developing on radioactivity-sensitive film. The protein-bound area of the RNA is identified by the absence of bands in the protein-bound sample compared to a protein free control. Purified TRIM25 used in this experiment was expressed in *E. coli* cells with a 6xHis tag at the N-terminal of the protein. It was subjected to affinity chromatography on a Nickel column (IMAC HiTrap 1 mL FF) followed by size exclusion chromatography. This experiment was performed with lead ions ( $Pb^{2+}$ ), which cleave phosphodiester bonds after any nucleotide, and T1 RNase, which cleaves after guanosine (G) nucleotides (FIG. 7A). A small sequence protected by purified TRIM25 was identified in the  $Pb^{2+}$  treated sample, corresponding to a repeated 5'-CACCCACC-3' sequence in the terminal loop of pre-let-7a-1 (nucleotides 37-44). These nucleotides were mutated to either G or U to generate the mutants pre-let-7a-1/GG and pre-let-7a-1/UU (FIG. 7B). To determine if these mutants could still bind TRIM25 with the identified binding motif removed an RNA pull-down assay was performed (FIG. 7C). Neither of the two mutants lost any binding affinity for TRIM25, suggesting that the 5'-CACCCACC-3' sequence is not the only place that TRIM25 can bind to pre-let-7a-1.

A subsequent cross-linking immunoprecipitation and sequencing (CLIP-seq) experiment performed in the lab showed that TRIM25 does not have a strong consensus sequence for RNA binding, instead showing a preference for G-rich areas<sup>219</sup>. CLIP involves cross-linking the target protein (in this case T7-TRIM25) to RNA by UV irradiation followed by immunoprecipitation of the target. RNAs cross-linked to the target protein are digested such that only the sequence in close contact with the protein of interest remains and these fragments are sequenced. Analysis of the TRIM25 CLIP-seq revealed that TRIM25 prefers



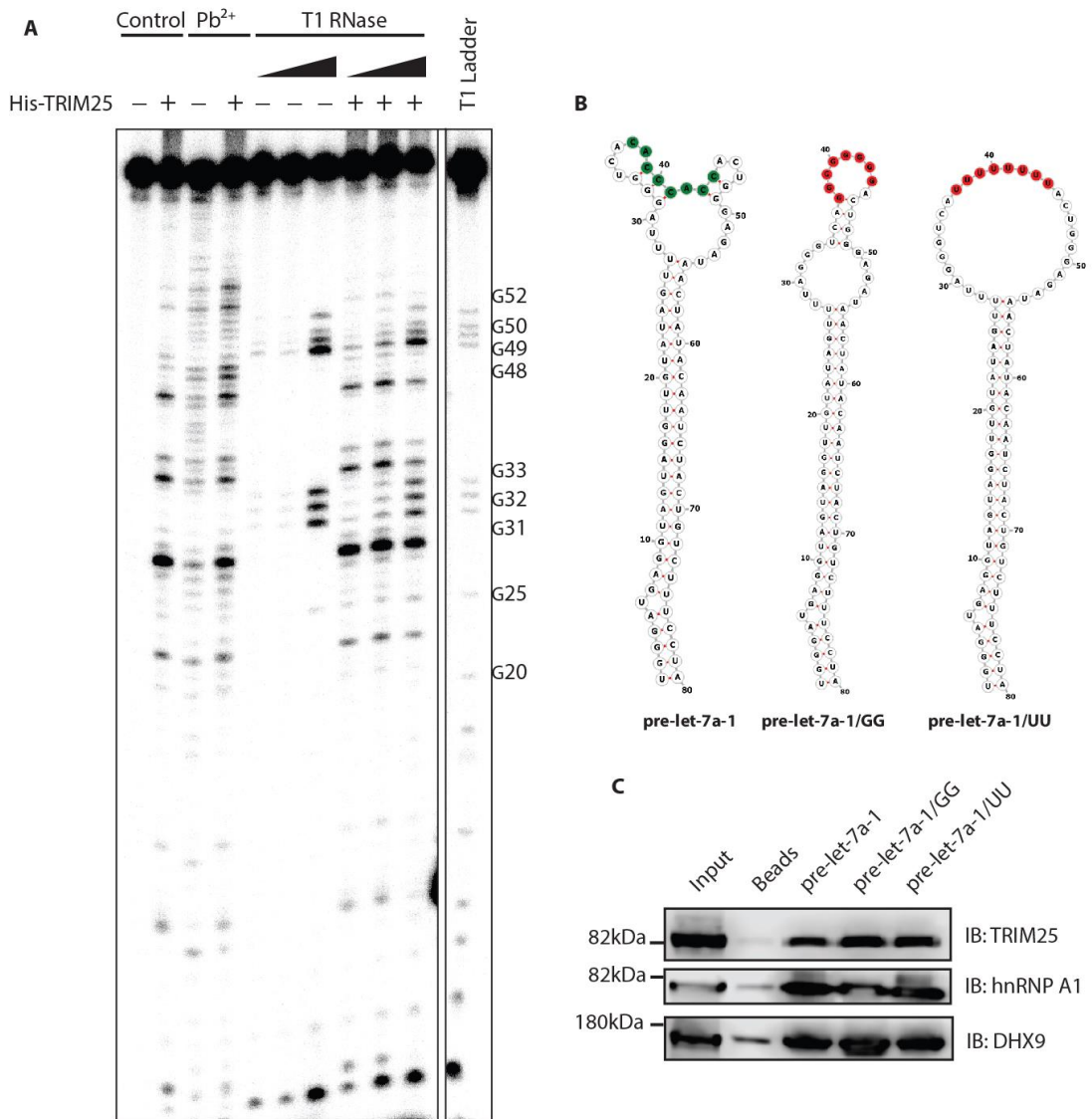


**Figure 7** – Mutagenizing *TRIM25*-binding residues on *pre-let-7a-1* does not result in less binding to *TRIM25*. (A) RNA footprinting assay. *Pre-let-7a-1* end-labelled with  $\gamma$ -ATP-32P was partially digested with T1 RNase or Pb<sup>2+</sup> in the presence or absence of 200ng purified His-TRIM25. (B) Predicted secondary structures of *pre-let-7a-1* WT, /GG and /UU. The mutated region is marked in green for *pre-let-7a-1* WT and red for *pre-let-7a-1*/GG and /UU. (C) WB analysis of RNA pull-down of *pre-let-7a-1* WT, /GG or /UU coupled beads with HeLa WCE. Input lane represents 4% (40 $\mu$ g) of extracts used for pull-downs.

G-rich sequences, with GC-rich content of RNAs also being slightly higher than would be expected if it had no preference. However, the finding that TRIM25 does not have a strong consensus motif may explain why mutagenizing the putative TRIM25-binding sequences of pre-let-7a-1 does not reduce TRIM25 binding to the RNA.

### *Amino acids 470-508 in the PRY/SPRY domain of TRIM25 contribute to RNA binding*

As it proved difficult to identify any RNA motif required for RNA binding, another strategy for elucidating how TRIM25 binds to RNA was required. Using a technique called 'mRNA interactome capture' our collaborator, Alfredo Castello (University of Oxford), identified residues which are in close contact with RNA for a number of RNA-binding proteins<sup>226</sup>. The technique involves cross-linking proteins to RNAs using UV irradiation followed by the capture of mRNAs with an oligo (dT) probe attached to beads. Proteins are subsequently cleaved by protease digestion (LysC/ArgC), leaving just the residues close to the RNA still attached by the crosslink, before another round of oligo (dT) capture. A final round of RNase digestion and protein digestion by trypsin occurs before the peptides are identified by mass spectroscopy (MS). Peptides released at the earlier digestion step are also separately treated with trypsin and identified by MS. One of the peptides identified by this screen as being in close proximity to RNA was residues 470-508 of human TRIM25, located in the PRY/SPRY domain. Peptides from the other TRIM25 domains were identified in the fraction released following the first digestion step (FIG. 8A). To test if residues 470-508 were important for RNA binding a TRIM25 mutant was generated with these residues deleted, called TRIM25 $\Delta$ RBD (delta RNA Binding Domain) (FIG. 8B). T7-tagged TRIM25 $\Delta$ RBD (T7-TRIM25 $\Delta$ RBD) and T7-TRIM25 WT were transfected into HeLa cells and tested for

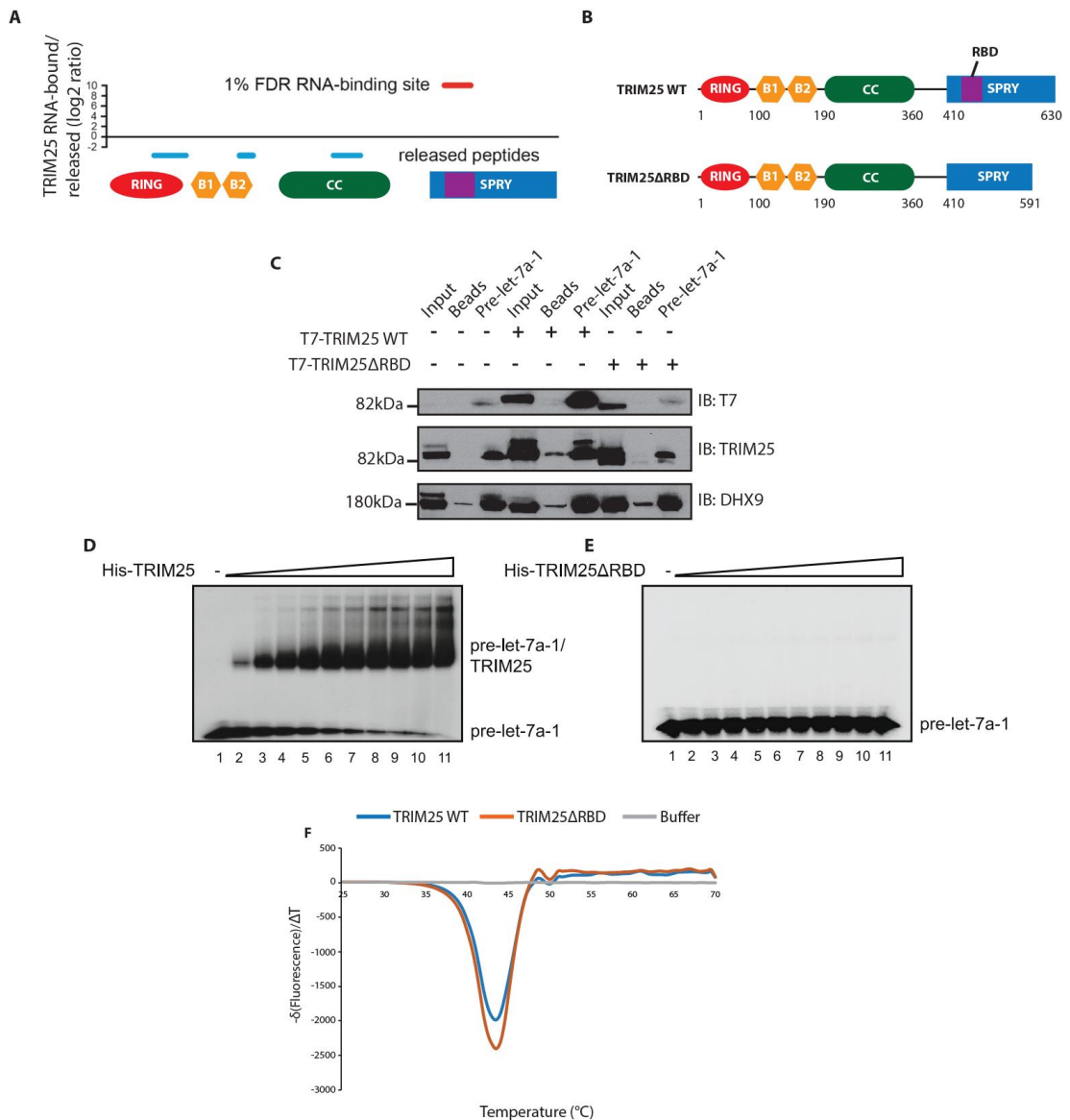


**Figure 8 – Deleting a putative RNA-binding peptide abolishes TRIM25 binding to pre-let-7a-1.** (A) mRNA capture assay result for TRIM25. Blue lines indicate peptides from TRIM25 that were identified in the fraction of peptides released after one digestion step. Red line indicates TRIM25 peptide identified in the RNA-bound fraction. (B) Schematic representation of TRIM25 WT and TRIM25ΔRBD. Residues 470-508 of TRIM25 WT were deleted to generate TRIM25ΔRBD. (C) WB analysis of RNA pulldown assay of pre-let-7a-1 with WCE of HeLa cells transfected with T7-TRIM25 WT or TRIM25ΔRBD or untransfected. Input lanes represent 4% (40 μg) of extracts used for pulldowns. Note should be taken of a non-specific band that appears in the pre-let-7a-1 pulldown lanes for untransfected extract and T7-TRIM25ΔRBD transfected extract when probed with anti-T7 antibody. (D) & (E) Electromobility shift assay (EMSA) with radiolabelled pre-let-7a-1 and purified 6His-TRIM25 WT (D) or 6His-TRIM25ΔRBD (E). Lanes 2-11 in these figures represent increasing amounts of TRIM25 protein from 200-2000 ng rising in increments of 200 ng. (F) Thermal denaturation assay of 6His-TRIM25 WT and 6His-TRIM25ΔRBD. Steps of 0.5°C between 20

and 70°C with 30 seconds at each step. Approximately 4  $\mu$ M of each protein was used. Figure A courtesy of Alfredo Castello. The experiments shown in figures D, E and F were performed by Nila Roy Choudhury, who also created these figures.

RNA-binding activity by RNA pull-down with pre-let-7a-1 (FIG. 8C). T7-TRIM25 WT showed strong binding to pre-let-7a-1 as expected, however T7-TRIM25 $\Delta$ RBD binding was substantially reduced, even though endogenous TRIM25 was present in the HeLa WCE. This is interesting as TRIM25 is known to dimerise through its coiled-coil domain, suggesting that having one copy of TRIM25 $\Delta$ RBD in the dimer is sufficient to disrupt RNA binding. Due to the presence of other proteins and RNAs in the WCE, RNA pull-down assays do not confirm if the protein is binding directly to RNA. To further confirm that TRIM25 $\Delta$ RBD cannot bind pre-let-7a-1 directly as efficiently as TRIM25 WT an electro-mobility shift assay (EMSA) was performed. This involves incubating purified protein with radiolabelled RNA and running them on a polyacrylamide gel before visualising on radioactivity-sensitive film to detect the RNA. Free RNA will run further on the gel than RNA that is bound to protein, resulting in a characteristic 'shift' in the visualised band if a complex is formed. This assay was performed with 5'-end-radiolabeled pre-let-7a-1 and purified 6His-tagged TRIM25 WT or TRIM25 $\Delta$ RBD (FIG. 8D and 8E). With TRIM25 WT a shift was seen, indicating complex formation, and at higher concentrations of TRIM25 WT almost all RNA present was bound, however with TRIM25 $\Delta$ RBD no shift was seen, even at high concentrations of protein, indicating no complex formation. This suggests that at least in these conditions TRIM25 $\Delta$ RBD cannot directly bind to pre-let-7a-1. To ensure that TRIM25 $\Delta$ RBD did not undergo large-scale changes in protein folding compared to TRIM25 WT due to the 39 amino acid deletion, it was subjected to a thermal denaturation assay (FIG. 8F). This showed that both proteins have  $T_{m,s}$  of around 43.5°C, suggesting that overall TRIM25 $\Delta$ RBD folding was not affected. This does not, however, ensure that folding of the PRY/SPRY domain alone is not affected by the deletion.

In order to test whether TRIM25 $\Delta$ RBD could bind to other RNAs apart from pre-let-7a-1 an RNA-binding protein immunoprecipitation (RIP) assay was performed. T7-TRIM25 WT or T7-

TRIM25 $\Delta$ RBD were transfected into HeLa cells and immunoprecipitated with anti-T7 antibody. Bound RNAs were subsequently analysed by quantitative real-time polymerase chain reaction (qRT-PCR). The RNAs analysed were chosen from those identified as binding to TRIM25 in the CLIP-seq experiment previously performed in the lab. All of the RNAs tested showed markedly reduced binding to T7-TRIM25 $\Delta$ RBD compared to T7-TRIM25 WT, with most having binding at the same level as the mock (no T7-tagged TRIM25 present) (FIG. 9A and 9B). For Trim25 mRNA, there was an increase in binding to T7-TRIM25 $\Delta$ RBD compared to mock, however this is likely due to the antibody picking up nascent T7-TRIM25 $\Delta$ RBD that was still associated with the ribosome. The lack of binding to T7-TRIM25 $\Delta$ RBD was seen for mRNAs and non-coding RNAs (FIG. 9A) and miRNAs (FIG. 9B). These results suggest that TRIM25 $\Delta$ RBD's lack of binding to RNA is not limited to pre-let-7a-1 and encompasses the majority of tested endogenous RNAs. It should, however be noted that this experiment does not contain a negative control as every RNA tested showed binding to TRIM25. It would be interesting to test abundant RNAs that were not identified as TRIM25 binding partners in the CLIP assay as these may provide a suitable negative control for TRIM25 RNA binding.

### *Two intact TRIM25-PRY/SPRY domains in a dimer are likely important for TRIM25 RNA binding*

As deletion of the 39 amino acid 'RBD' from the PRY/SPRY domain of TRIM25 is sufficient to disrupt TRIM25 RNA binding, knowing whether the PRY/SPRY domain alone is sufficient for RNA binding would help to elucidate the mechanism of TRIM25 RNA binding. As such, a construct encoding T7-tagged TRIM25-PRY/SPRY was generated and tested for its ability to bind pre-let-7a-1 in an RNA pull-down (FIG. 10A). T7-TRIM25-PRY/SPRY showed no binding

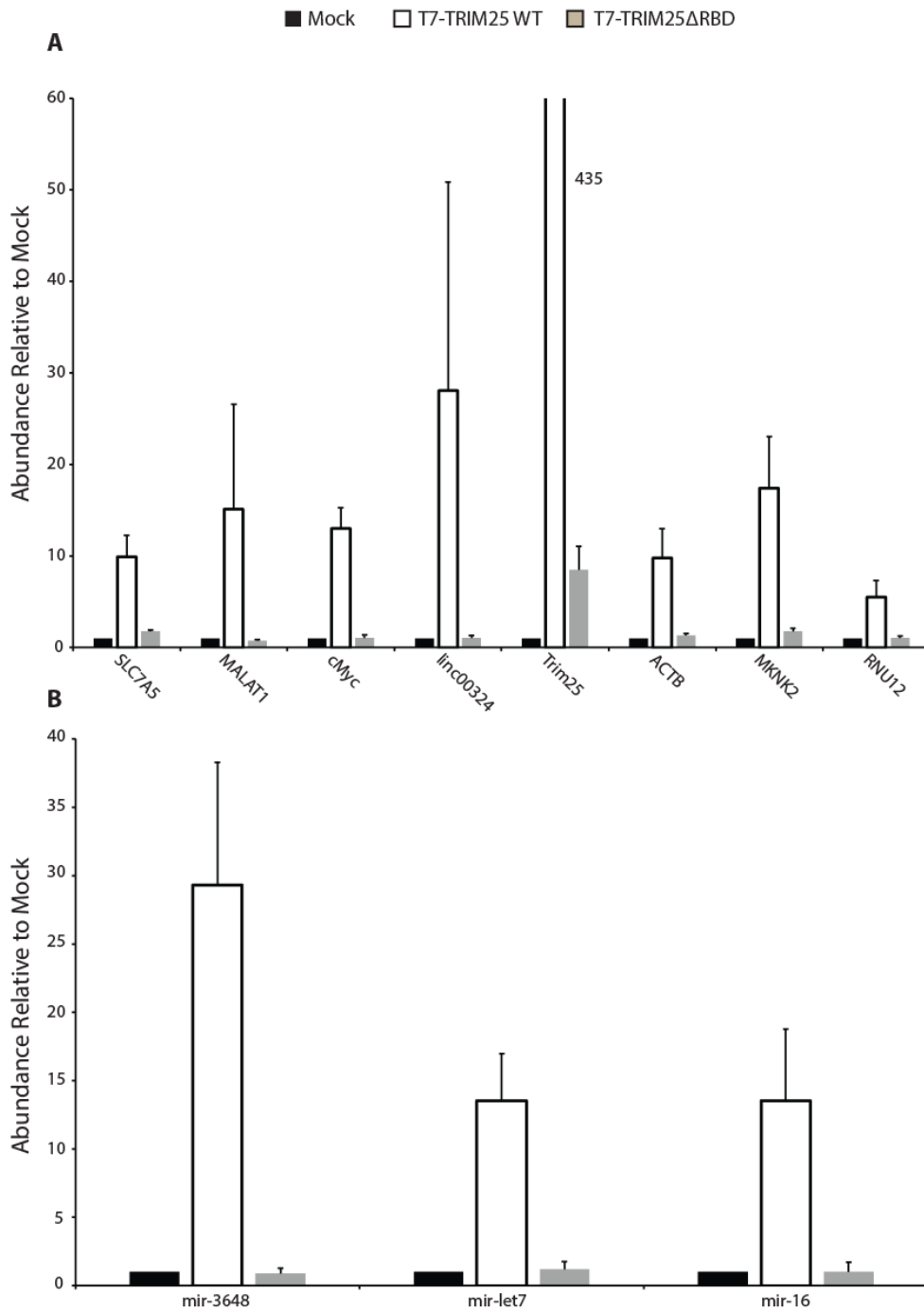


**Figure 9** – *TRIM25ΔRBD* shows reduced binding to every RNA tested in an RNA immunoprecipitation (RIP) assay. (A & B) qRT-PCR analysis of RNAs (A) or miRNAs (B) bound to TRIM25 WT or TRIM25ΔRBD in RIP assay. HeLa cells were transfected with T7-TRIM25, T7-TRIM25ΔRBD or mock transfected and extracts were subjected to immunoprecipitation with an anti-T7 antibody before bound RNAs were isolated. Values are shown relative to mock which is set at 1. Figures represent mean and standard deviation of three independent experiments. The experiments shown in this figure were performed by Nila Roy Choudhury.

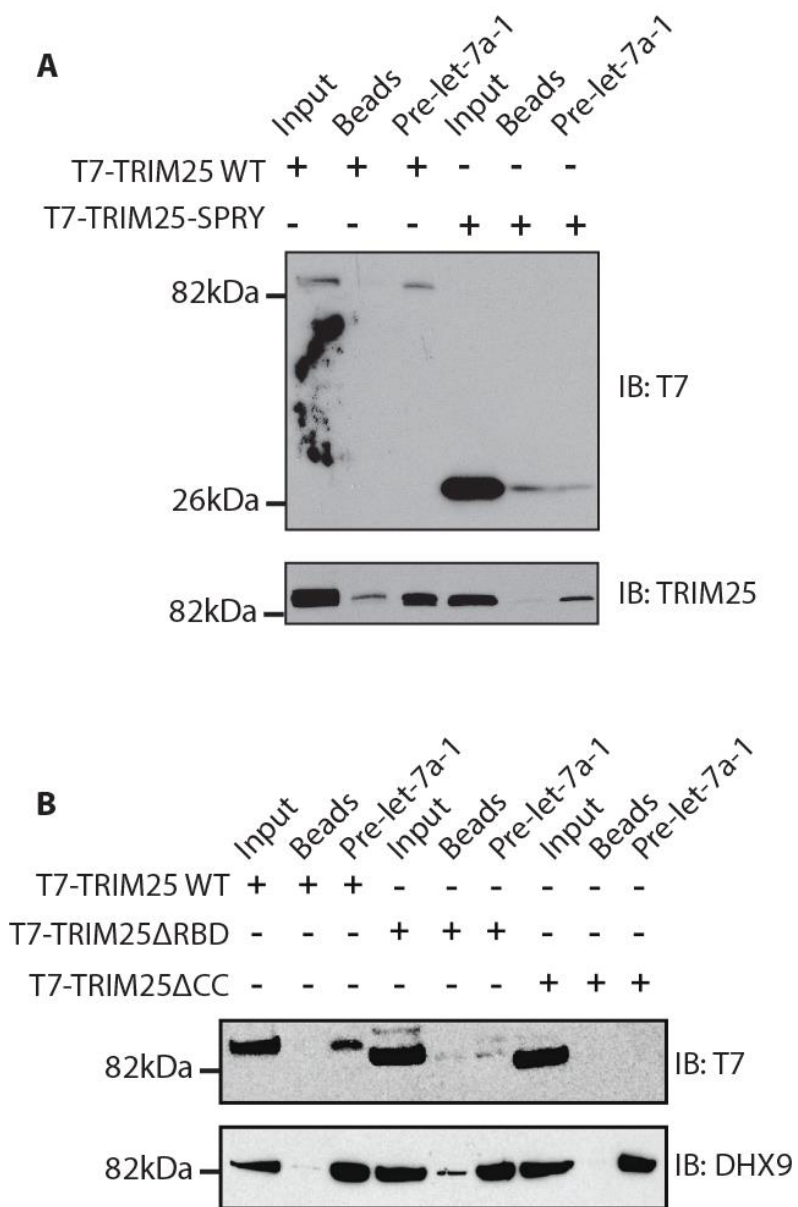


**Figure 10** – *TRIM25-SPRY* and *TRIM25 $\Delta$ CC* do not bind to *pre-let-7a-1*. (A) WB analysis of RNA pull-down of *pre-let-7a-1* with WCE of HeLa cells transfected with either T7-TRIM25 WT or T7-TRIM25-SPRY. (B) WB analysis of RNA pull-down of *pre-let-7a-1* with WCE of HeLa cells transfected with either T7-TRIM25 WT, T7-TRIM25 $\Delta$ RBD or T7-TRIM25 $\Delta$ CC.



to pre-let-7a-1 compared to a beads only control, implying that it is not sufficient for RNA binding. One reason for this could be that the PRY/SPRY domain must be part of a dimer, as it is in full-length TRIM25, to be able to bind RNA. This would also explain why TRIM25 $\Delta$ RBD does not bind RNA even in the presence of endogenous TRIM25 WT. Previous work has suggested that TRIM25 lacking the coiled-coil domain, which mediates dimerization, cannot bind to RNA<sup>215</sup>. This was tested with pre-let-7a-1 in an RNA pull-down after generating a T7-tagged TRIM25 mutant in which the coiled-coil domain had been deleted (T7-TRIM25 $\Delta$ CC) (FIG. 10B). As expected, T7-TRIM25 $\Delta$ CC did not bind to pre-let-7a-1 in the RNA pull-down. In order to ensure that TRIM25 $\Delta$ RBD was capable of dimerizing in the same way as TRIM25 WT it was subjected to analysis by Size Exclusion Chromatography followed by Multi-Angle Light Scattering (SEC-MALS). This experiment consists of separating purified proteins by size exclusion chromatography so that oligomers of the same order are grouped together followed by detecting the molecular weight and radius of the particles present by measuring the extent of light scattering by the protein sample. In short, this technique determines the molecular weight of protein complexes formed in solution, which can be used to determine if a protein exists as a monomer, dimer or higher order oligomer. SEC-MALS was performed with either purified His-TRIM25 WT or His-TRIM25 $\Delta$ RBD (FIG. 11A). TRIM25 was present with a molecular weight of  $263 \pm 5.3$  kDa and TRIM25 $\Delta$ RBD was present with a molecular weight of  $258 \pm 5$  kDa. This suggests that both purified proteins are forming tetramers in solution. This agrees with the work of others that found that TRIM25 often forms tetramers composed of two TRIM25 dimers. Overall this suggests that TRIM25 $\Delta$ RBD oligomerisation activity does not deviate from that found in TRIM25 WT. Although SEC-MALS can determine if TRIM25 $\Delta$ RBD homo-oligomerises it cannot determine whether it can heterodimerise with TRIM25 WT. It is important to know if TRIM25 $\Delta$ RBD can

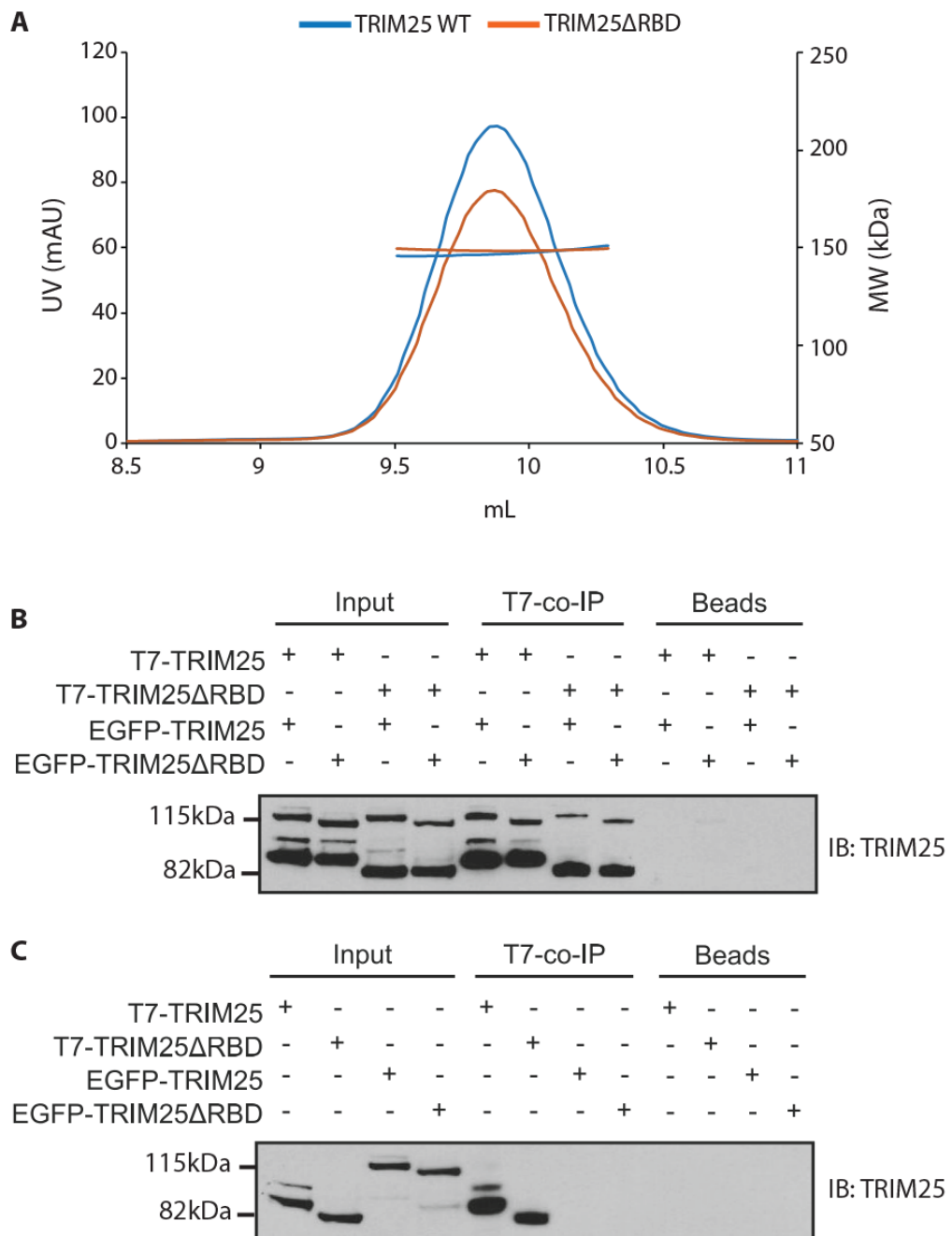


**Figure 11** – *TRIM25ΔRBD* maintains the dimerization ability of *TRIM25* WT. (A) SEC-MALS trace of *TRIM25* WT and *TRIM25ΔRBD*. Samples were run at approximately 0.75mg/mL. (B) WB analysis of T7 Co-IP of HeLa *TRIM25* KO cells transfected with T7 or eGFP-tagged *TRIM25* WT and *TRIM25ΔRBD*. Input lanes represent 10% (50 μg) of WCEs used for Co-IP. Beads lanes represent Co-IP performed with uncoupled Protein A beads. (C) WB analysis of control Co-IPs showing eGFP-tagged proteins are not pulled down in the absence of T7-tagged proteins. The experiments shown in these figures were performed by Nila Roy Choudhury, who also created these figures.

heterodimerise with TRIM25 WT as this would help elucidate whether an intact PRY/SPRY domain is needed in both copies of TRIM25 in a dimer to enable RNA binding. In order to find this out HeLa TRIM25 knockout (KO) cells (further information in chapter 2) were co-transfected with different combinations of T7 or eGFP-tagged TRIM25 WT and TRIM25 $\Delta$ RBD before co-immunoprecipitation (Co-IP) with an anti-T7 antibody (FIG. 11B). The eGFP-TRIM25 fusion proteins were used as these could be distinguished by size from T7-TRIM25 constructs. This showed that eGFP-TRIM25 $\Delta$ RBD can Co-IP with T7-TRIM25 WT and conversely eGFP-TRIM25 WT can Co-IP with T7-TRIM25 $\Delta$ RBD. In addition, eGFP-TRIM25 WT co-Co-IPs with T7-TRIM25 WT and eGFP-TRIM25 $\Delta$ RBD Co-IPs with T7-TRIM25 $\Delta$ RBD. Neither eGFP-tagged protein precipitates in the absence of a T7-tagged protein in the anti-T7 Co-IP (FIG. 11C). These results provide further confirmation that TRIM25 $\Delta$ RBD can homodimerise and suggest that TRIM25 $\Delta$ RBD can heterodimerise with TRIM25 WT. Following on from this, these data suggest that TRIM25 $\Delta$ RBD can probably heterodimerise with endogenous TRIM25 WT and the lack of RNA binding of TRIM25 $\Delta$ RBD in the presence of endogenous TRIM25 WT, coupled with TRIM25-PRY/SPRY being insufficient for RNA binding, suggests that at least two intact PRY/SPRY domains in a dimer are required for TRIM25 RNA binding.

### *TRIM25 requires RNA binding for efficient auto-ubiquitination*

TRIM25 is an E3 ubiquitin ligase and undergoes auto-ubiquitination on Lysine 117 (K117), which is present in the B-box domain of the protein<sup>152</sup>. Ubiquitination activity is dependent on the RING domain of TRIM25, as it is for all TRIM family proteins. To determine if auto-ubiquitination of TRIM25 $\Delta$ RBD is impaired compared to TRIM25 WT *in vitro* ubiquitination

assays were performed. T7-tagged TRIM25 WT or TRIM25 $\Delta$ RBD were immunoprecipitated with an anti-T7 antibody before the addition of purified ubiquitin, the E2 Ube2D3 and the E1 UBE1 which comprise all the components required for TRIM25 ubiquitination activity. The samples were incubated for an hour at 37°C with time points taken at 5, 30 and 60 minutes before being analysed by WB. Under these conditions T7-TRIM25 WT was efficiently ubiquitinated while T7-TRIM25 $\Delta$ RBD was not (FIG. 12A). A negative control where Ube2D3 was excluded abrogated auto-ubiquitination by T7-TRIM25 WT showing that the E2 conjugating enzyme did not Co-IP with T7-TRIM25 WT in this experiment. The experiment was repeated with T7-TRIM25K117R and T7-TRIM25 $\Delta$ RING, which should not be auto-ubiquitinated due to the absence of the auto-ubiquitinated residue and the RING domain, respectively. As expected, both of these proteins are not ubiquitinated efficiently after 60 minutes of incubation with the ubiquitination components (FIG. 12B). This confirms the specificity of this assay by showing that TRIM25 is not being ubiquitinated by another protein or on a different residue. To confirm that loss of RNA binding is responsible for the loss of TRIM25 $\Delta$ RBD auto-ubiquitination, the *in vitro* ubiquitination assay was repeated with T7-TRIM25 WT in the presence of RNases A and T1 (FIG. 12C). Addition of the RNases after immunoprecipitation (at the same time as the ubiquitination components) greatly reduced polyubiquitination of T7-TRIM25 WT while monoubiquitination was mostly unaffected. This could be because of direct transfer of ubiquitin between the E2 Ube2D3 and TRIM25 as monoubiquitination is abrogated in the absence of Ube2D3. Taken together, these results strongly suggest that binding to RNA greatly increases the efficiency of TRIM25 auto-ubiquitination. This could be because TRIM25 RNA binding elicits a change in the protein, for example in the protein structure, that allows efficient ubiquitination activity or because TRIM25 uses RNA as a 'scaffold' to target it to itself to the proteins it is to ubiquitinate.

Further *in vitro* ubiquitination experiments in the lab identified ZC3HAV1 (zinc-finger antiviral protein, ZAP) as another target of TRIM25 for which loss of TRIM25 RNA binding reduces ubiquitination<sup>219</sup>. This was shown by the failure of TRIM25 $\Delta$ RBD, or TRIM25 WT in the presence of RNase, to ubiquitinate ZAP while TRIM25 WT could in the absence of RNase<sup>219</sup>. This further implies the reliance of TRIM25 ubiquitination activity on RNA binding and gives an example of this occurring for a TRIM25 ubiquitination target. There are currently conflicting reports as to whether ubiquitination enhances the anti-viral role of ZAP, with reports indicating that the E3 ligase activity of TRIM25 is required for activation but ubiquitination of the ZAP protein itself may be dispensable<sup>211</sup>.

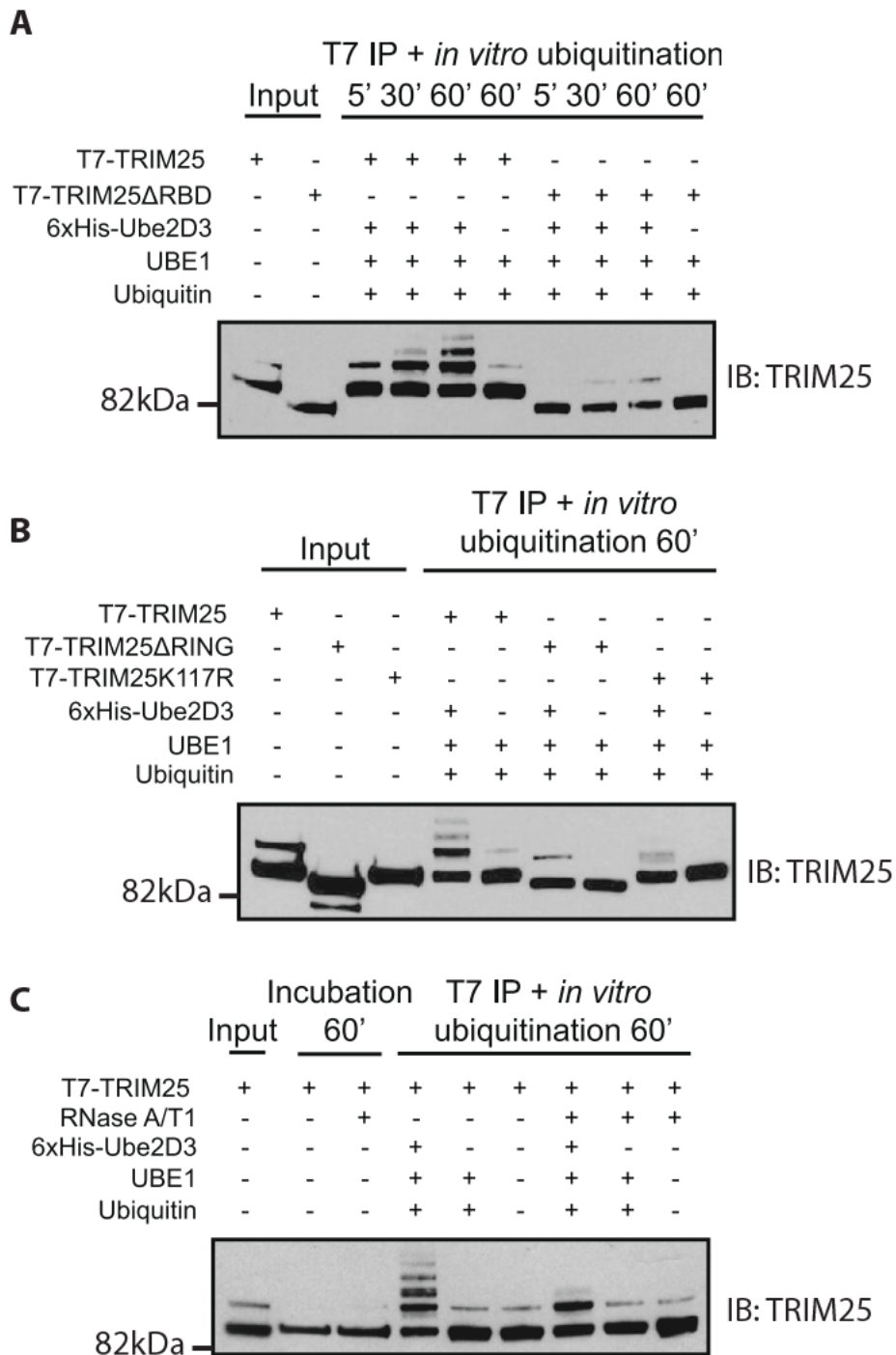


**Figure 12** – RNA binding is necessary for TRIM25 auto-ubiquitination activity. (A) *In vitro* ubiquitination of T7-TRIM25 WT and T7-TRIM25ΔRBD. T7-tagged proteins were immunoprecipitated from extracts with an anti-T7 antibody before the addition of recombinant, purified components 6His-Ube2D3, UBE1 and Ubiquitin which are required for ubiquitination. Samples were taken at 5, 30 and 60 minutes. A negative control was also performed in the absence of 6His-Ube2D3 for each protein. Input lanes contain

immunoprecipitated T7-tagged proteins prior to the addition of ubiquitination components.  
(B) *In vitro* ubiquitination of TRIM25 $\Delta$ RING and TRIM25K117R performed in the same way.  
(C) *In vitro* ubiquitination of T7-TRIM25 in the presence or absence of RNases. Purified RNases A and T1 were added subsequently to immunoprecipitation at the same time as ubiquitination components. The experiments shown in these figures were performed by Nila Roy Choudhury, who also created these figures.

## Conclusions

The data presented here, as well as other work performed in the lab, suggest that TRIM25 has a broad specificity of RNA binding, although it shows a preference for GC-rich sequences<sup>219</sup>. A mutant of TRIM25, TRIM25 $\Delta$ RBD, which shows substantially reduced binding to RNA has been designed based on deletion of a peptide in the TRIM25 PRY/SPRY domain identified by mRNA interactome capture. This helped to validate this technique as a method of identifying RNA-binding peptides and provided a non-RNA binding mutant of TRIM25 that can be used in experiments to determine the functions of TRIM25 RNA binding. TRIM25 $\Delta$ RBD was also shown to maintain the ability to dimerize with either itself or TRIM25 WT; however, its inability to bind RNA is maintained even in the presence of endogenous TRIM25 WT. This, along with the inability of TRIM25-PRY/SPRY alone or TRIM25 $\Delta$ CC to bind RNA, suggests that TRIM25 dimerization is necessary for RNA binding and at least two copies of the PRY/SPRY domain are required. However, the exact mechanism of TRIM25 RNA binding remains to be uncovered, for example the individual residues that contact RNA. The best way of determining this would be x-ray crystallography or cryogenic electron microscopy (Cryo-EM) of TRIM25 in complex with RNA, although this can be difficult and time-consuming and was beyond the scope of this project. Finally, it was shown that TRIM25 ubiquitination activity, both auto-ubiquitination and ubiquitination of one of its target proteins (ZAP), was impaired by the loss of RNA binding.

Interestingly, several other TRIM family proteins (as well as a total of around 100 human proteins) contain a PRY/SPRY, also known as a B30.2, domain and several of these proteins are also involved in innate immunity<sup>154,227</sup>. This raises the question of whether these proteins can also bind RNA and if this is important for their functions. To this end, work in the lab has replaced the TRIM25-RBD with homologous sequences from several other TRIM



family proteins (TRIM5, TRIM21, TRIM27 and TRIM65) that have a PRY/SPRY domain. Some, but not all, of these chimeric proteins were shown to bind to pre-let-7a-1 in an RNA pull-down assay and a positive correlation was shown between the pull-down efficiency and the efficiency of auto-ubiquitination of these proteins<sup>219</sup>. This suggests that other TRIM family proteins may have the ability to bind RNA and that the ubiquitination activity of TRIM25 is reliant on RNA binding, not the exact sequence of the PRY/SPRY domain. Further experiments will be needed to determine if RNA binding activity of other TRIM proteins is required for their ubiquitination activity. It is also currently not known by what mechanism TRIM25 RNA binding contributes to its enzymatic activity. One possible model is that TRIM25 uses RNA as a scaffold to bring it into close proximity to its target proteins, allowing ubiquitination. Another model is that RNA binding induces a conformational change in the protein that increases the efficiency of its E3 ligase activity. In order to determine which of these models, if either, is true, further work will be required.

## Chapter 2 – Generation of TRIM25 KO HeLa and HEK293 cells

### *Aims*

One way to determine the effects of removing the RNA binding ability of TRIM25 on its functions in the cell is to compare the ability of TRIM25 WT to TRIM25 $\Delta$ RBD to perform these functions. In cells that express TRIM25 endogenously it is almost impossible to perform these experiments as the endogenous protein would likely be sufficient to mask any difference between additional WT or mutant protein. In addition, by reducing endogenous TRIM25 expression and analysing the cells' phenotype (e.g. expression levels of TRIM25 RNA binding partners) it would be possible to discover novel functions of TRIM25.

One way to reduce endogenous expression of a protein is through the use of RNA interference (RNAi)<sup>228</sup>. Small interfering RNAs (siRNAs) are short, double stranded RNAs that can silence gene expression by specific binding to mRNA, leading to mRNA degradation or preventing translation. RNAi can be a powerful tool in some situations however there are limitations. RNAi does not silence gene expression entirely, meaning that there will always be some endogenous protein left in the cell. In the case of TRIM25, previous work in the lab has shown that it is difficult to reduce levels to less than 30-40% of endogenous levels, which may be sufficient to perform some of its functions. In addition, RNAi is transient; meaning that in experiments run over a long period of time, levels of the protein will begin to return to normal and it may be difficult to see effects that require extended perturbation from steady state expression levels.

Another option was to knock out the protein, i.e. to modify the DNA such that the gene cannot be expressed. This has the advantage of being permanent and ensuring there is no

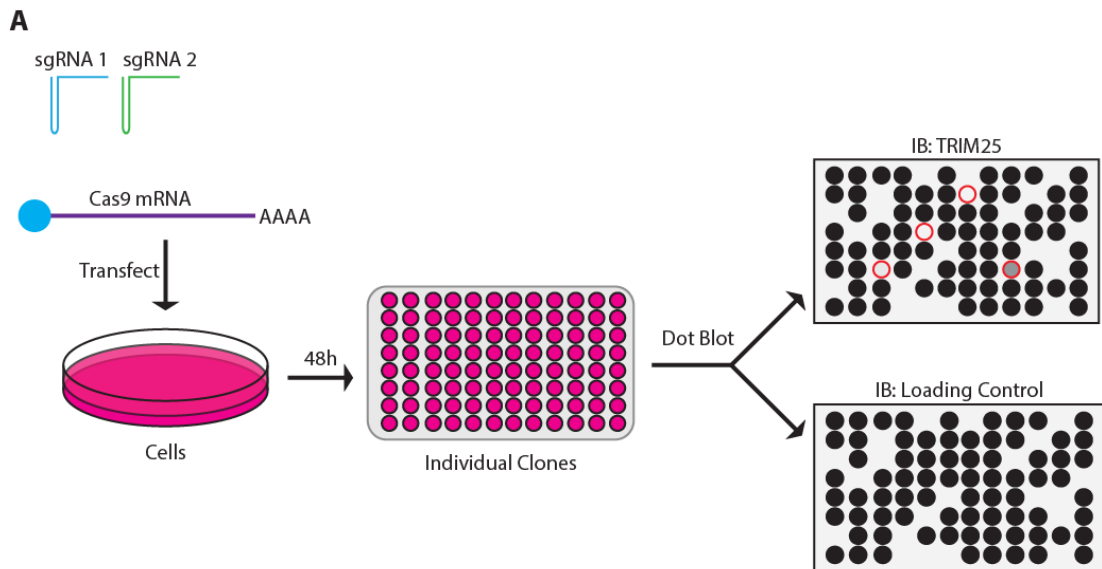
endogenous protein whatsoever which makes it easier for TRIM25 WT and TRIM25 $\Delta$ RBD to be directly compared. CRISPR/Cas9 is a recently developed method for the editing of DNA that can be used to disrupt a gene and prevent its expression or to introduce a new DNA sequence into the genome<sup>229,230</sup>. The Cas9 protein is added to cells along with a short guide RNA (sgRNA) that is targeted to the gene of interest. Cas9 cleaves the DNA in the region of the sgRNA on both strands, causing a double strand break. The DNA repair machinery then attempts to repair the break, often using non-homologous end joining, simply attaching the two broken ends of the DNA back together. This method of DNA repair is error prone and can easily introduce small deletions or insertions in the DNA sequence that will disrupt the target gene, particularly if the mutation causes a frame shift. A frameshift occurs when an insertion or deletion is of a number of nucleotides not divisible by 3, 'shifting' the open reading frame and causing transcription of an mRNA that encodes a completely different set of amino acids. It is also possible to introduce new DNA at the break point by including a DNA cassette with flanking sequences homologous to the sequences on either side of the break. This process is known as homology directed repair and can be used, for example, to add a tag to the protein of interest.

The aim for this part of the project was to generate knockout (KO) cells for TRIM25 for use in further experiments and as such it was decided to use CRISPR/Cas9 to simply disrupt the gene without introducing any new sequences. This was done in HeLa cells as these had been used for previous experiments in the project and are easy to work with. TRIM25 KO cells were also generated for HEK293 cells as HeLa cells are not very permissive to virus infection and as such were not ideal for use in future experiments in this area. Another advantage of the HEK293 cell line used was that they contained a flippase recognition target (FRT) site that allows stable integration of a gene of choice into the genome<sup>231</sup>. This meant that TRIM25 WT, TRIM25 $\Delta$ RBD and other mutants could be reintegrated into the

genome of TRIM25 KO cells to be expressed in a constitutive manner. This would be ideal for confirming whether phenotypes seen in TRIM25 KO cells were due to loss of TRIM25 (i.e. they could be rescued by reintegration of TRIM25) as opposed to any off-target effects from CRISPR/Cas9 targeting, as well as comparing the ability of mutants of TRIM25 to perform its functions compared to WT protein. The strategy used for generating the KO cells was based on one used by Estep *et al.* whereby colonies were screened for expression of the target protein by dot immunoblot, allowing easy and fast screening of many colonies at once (FIG. 13A)<sup>232</sup>.

### *HeLa TRIM25 KO cells were generated by CRISPR*

The first task of this part of the project was to design sgRNAs targeting *TRIM25* for use in the CRISPR experiment. HeLa cells have an altered karyotype and contain three copies of chromosome 17, on which the *TRIM25* gene is located, therefore all three copies must be disrupted to knock out TRIM25. Two sgRNAs were designed to target exon 1 of the *TRIM25* gene (FIG. 13B). Two sgRNAs were used to increase the chances of disrupting the gene and exon 1 was targeted as frameshift-causing mutations in this area would affect the entire protein, ensuring that it would not be expressed. The two sgRNAs were transcribed using *in vitro* transcription and subsequently gel purified. They were transfected into HeLa cells along with purified mRNA for the Cas9 nuclease. 48 hours post-transfection, cells were split into a 96-well plate such that the majority of wells had a single clonal colony growing in them. The cells were grown up before being split into two new 96-well plates, one of these being harvested for use in a dot immunoblot. Protein extracts were harvested using 30  $\mu$ L passive lysis buffer per well and 2  $\mu$ L of this extract was added directly to a nitrocellulose



**B**

sgRNA 1 ■ sgRNA 2 ■

1 ATGGCAGAGCTGTGCCCCCTGGCCGAGGAGCTGTCGTGCTCCATCTGCCTGGAGCCCTTCAA  
63 GGAGCCGGTCACCACTCCGTGCGGCCACAACCTTCTGCGGGTTCGTGCCTGAATGAGACGTGGG  
125 CAGTCCAGGGCTCGCCATACCTGTGCCCGCAGTGCCGCG CCGTCTACCGGCGACCGCAG  
187 CTGCACAA GAACACGGTGCTGTGCAACGTGGTGGAGCAGTTCCTGCAGGCCGACCTGGCCG  
249 GGAGCCACCGCCGACGTCTGGACGCCGCCGCCGCGCCTCTGCACCCAGCCGGAATGCC  
311 AGGTGGCCTGCGACCACTGCCTGAAGGAGGCCGCGTGAAGACGTGCTTGGTGTGCATGGCC  
373 TCCTTCTGTGAGGACACCTGCAGCCGCACTTCGACAGCCCCGCTTCCAGGACCACCCGCT  
435 GCAGCCGCCGTTGCGGACCTGTTGCGCCGCAATGTTCCAGCACAATCGGCTGCGGGAAT  
497 TTTTCTGCCCGAGCACAGCGAGTGCATCTGCCACATCTGCCTGGTGGAGCATAAGACCTGC  
559 TCTCCCGCGTCCCTGAGCCAGGCCAGCGCCGACCTGGAG

TRIM25 Exon 1

**Figure 13 - Knock out of *TRIM25* by CRISPR.** (A) Schematic of the strategy used for knocking out *TRIM25* by CRISPR. Cells were transfected with 2 sgRNAs targeted at exon 1 of *TRIM25* and incubated for 48 hours before being split into individual clones in a 96-well plate. Clones were grown up and tested for *TRIM25* expression by dot immunoblot to identify clone in which *TRIM25* expression was reduced compared to a loading control. (B) The target sequences for the 2 sgRNAs in exon 1 of *TRIM25*.

membrane. Clones were then screened by immunoblot for TRIM25 expression, with DHX9 as a loading control (FIG. 14A). Several clones were identified from this as potentially having reduced TRIM25 expression (red circles). These clones were transferred from the second 96-well plate to 6-well plates and were grown up before protein was extracted to validate levels of TRIM25 by western blot (FIG. 14B). Clone E10 (blue circles) was used as a positive control for TRIM25 expression. None of the clones tested showed complete loss of TRIM25 expression, however several (E8, E11, F9, G8) showed reduced expression. Of these clone E8 showed the largest reduction in TRIM25 levels, with likely two of the three copies of *TRIM25* being disrupted.

Clone E8 was subjected to a second round of CRISPR/Cas9 treatment that was performed in the same way as the first. Again, several clones from this second round were identified as potential KO clones (FIG. 15A) and TRIM25 levels were validated by western blot, with WT HeLa cells and clone E8 used as controls (FIG. 15B). Every clone tested here showed complete loss of TRIM25 expression, although of these only clone C3 showed a similar growth rate to WT HeLa cells with the others either dying or having slower growth. As such, clone C3 was selected for use in future experiments. It is possible that the reason that most clones in which TRIM25 had been deleted showed growth defects is that TRIM25 is essential for normal growth. If this is the case, it is possible that clone C3 contains mutations that compensate for the loss of TRIM25, for example the upregulation of a protein that can perform TRIM25's roles. To confirm that the *TRIM25* gene had been disrupted, genomic DNA was isolated from clone C3 and the area surrounding the sgRNA target sequences was sequenced. The target area was amplified by PCR and cloned into pJET vector before being transformed into *E. coli* cells. Bacterial cells were isolated as individual clones, grown up and the sequence-containing pJET vectors were harvested by

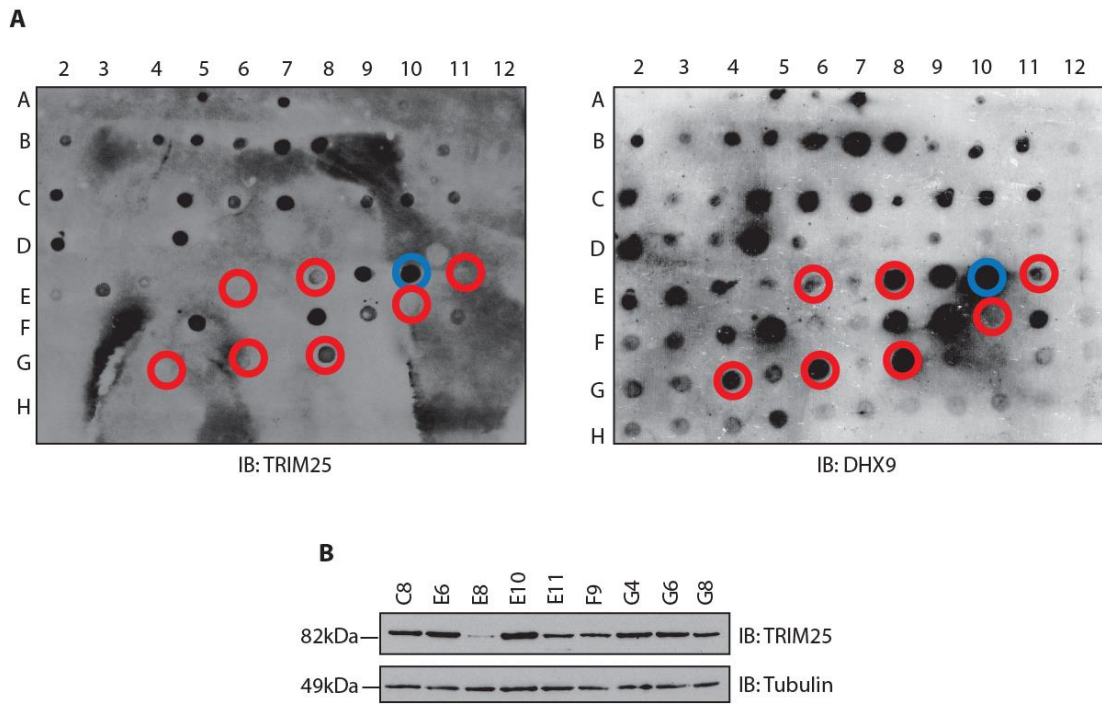


**Figure 14** – *The first round of CRISPR in HeLa cells generated a clone with substantially reduced TRIM25 expression.* (A) Dot immunoblots for HeLa clones that had undergone CRISPR. 2  $\mu$ L protein extract from clones was added directly to a nitrocellulose membrane before antibody probing. Clones that may have reduced expression of TRIM25 are marked by red circles and a positive control for TRIM25 expression is marked with a blue circle. DHX9 was used as a loading control. (B) Western blot validation of identified clones with tubulin used as a loading control. Clone E10 was used as a positive control for TRIM25 expression.

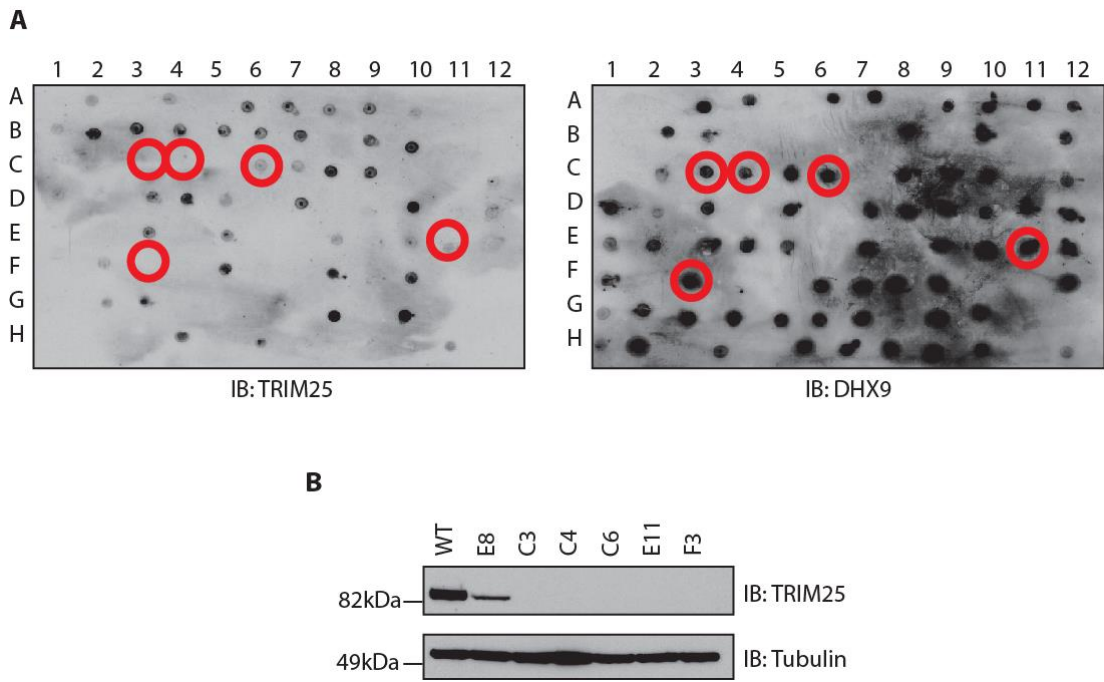


**Figure 15** – *The second round of CRISPR in HeLa E8 cells generated several TRIM25 KO clones. (A) Dot immunoblots for HeLa E8 clones that had undergone CRISPR. Potential KO clones are marked by a red circle. DHX9 was used as a loading control. (B) Western blot validation of potential TRIM25 KO clones. WT HeLa cells and HeLa E8 cells were used as positive controls for TRIM25 expression. Tubulin was used as a loading control.*



miniprep before being sequenced. This confirmed disruption of two copies of *TRIM25* with two different mutations identified; a 234-nucleotide deletion (positions 128-362 of exon 1) and a 13 nucleotide deletion (169-182, causing a frameshift). Although several clones were sequenced, only two separate mutations were identified despite the three copies of *TRIM25* in the HeLa genome. This may be due to mutations on two of the copies of *TRIM25* being identical or a failure to generate a PCR product in the target region on one of the copies of chromosome 17, for example due to a mutation in the sequence one of the primers binds to. As no TRIM25 protein was detectable, it was decided to proceed with this clone, which was called HeLa TRIM25 KO.

#### *HEK293 TRIM25 KO cells were generated by CRISPR*

After the successful generation of HeLa TRIM25 KO cells, generation of HEK293 TRIM25 KO cells was performed in the same way. In the initial screen, much fewer clones managed to grow in the 96-well plate, however a few possible KO clones were identified on the dot immunoblot (FIG. 16A). These clones were validated for TRIM25 expression by western blot (FIG. 16B). Of these, one clone, C8, showed complete knockout of TRIM25. This clone was also sequenced to confirm disruption of *TRIM25* in the same manner as HeLa TRIM25 KO.

#### *TRIM25 was reintegrated into the HEK293 TRIM25 KO genome using the Flp-In system*

The HEK293 cells that were used to generate HEK293 TRIM25 KO contain an FRT site under a constitutive CMV promoter. This allows permanent integration of a gene into the genome

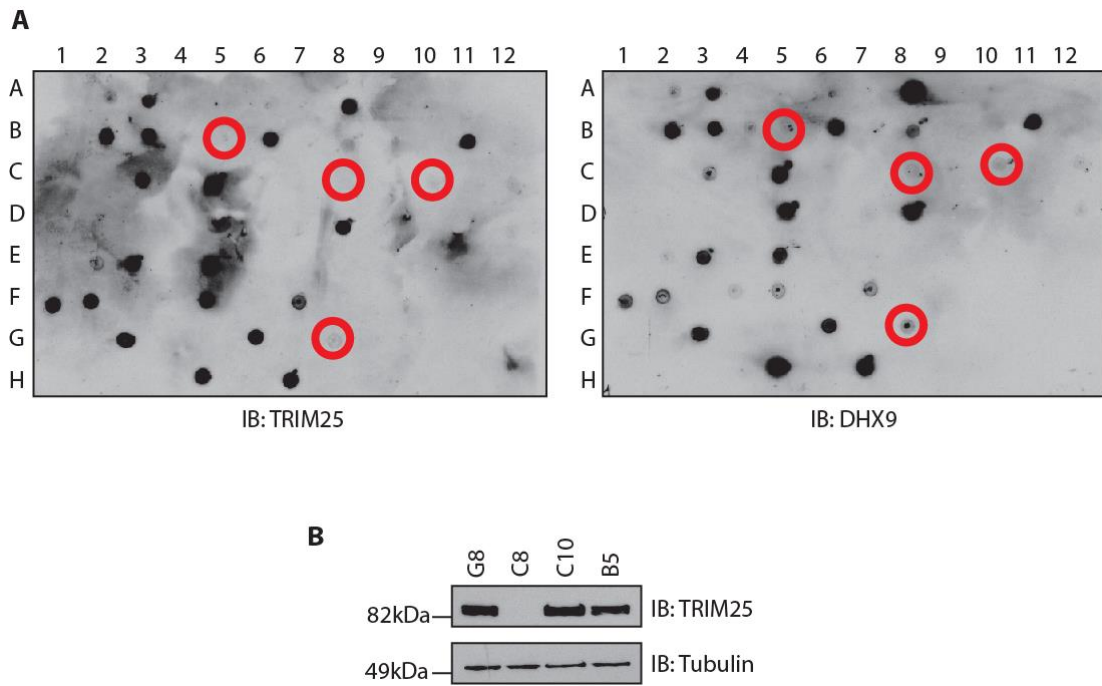


**Figure 16** – *The first round of CRISPR for HEK293 cells generated a TRIM25 KO clone.* (A) Dot immunoblots of HEK293 clones that had undergone CRISPR. Potential KO clones are marked with red circles. DHX9 was used as a loading control. (B) Western blot validation of potential TRIM25 KO clones. Tubulin was used as a loading control.

and stable, constitutive expression of the protein encoded by that gene. The genes of interest, in this case codon optimised TRIM25 WT, TRIM25 $\Delta$ RBD or TRIM25 $\Delta$ RING, were cloned into the pcDNA5/FRT expression vector, which contains FRT flanking sequences for homologous recombination with the FRT site in the genome as well as a hygromycin resistance cassette. The pcDNA5/FRT plasmid with the gene of interest was co-transfected with pOG44 (encoding the Flp recombinase) into HEK293 TRIM25 KO cells. Cells in which the genes of interest had been successfully integrated were selected for by colony growth in the presence of hygromycin. These colonies were then picked to a 24-well plate and tested for expression of TRIM25 WT, TRIM25 $\Delta$ RBD or TRIM25 $\Delta$ RING. One clone of each cell line with integrated WT or mutant TRIM25 with similar expression levels of TRIM25 and growth rate to WT HEK293 cells was selected for use in future experiments to ensure consistency (FIG. 17A). These cell lines were called HEK293 TRIM25 KO+TRIM25 WT, HEK293 TRIM25 KO+TRIM25 $\Delta$ RBD and HEK293 TRIM25 KO+TRIM25 $\Delta$ RING. Of note, it proved more difficult to re-integrate TRIM25 WT into the genome than the TRIM25 mutants, with attempts initially yielding no hygromycin-resistant colonies as opposed to many colonies for both TRIM25 $\Delta$ RBD and TRIM25 $\Delta$ RING. In order to remedy this, different amounts and ratios of the pcDNA5/FRT and pOG44 plasmids were used, with higher amounts of pcDNA5/FRT compared to pOG44 (1:5 ratio as opposed to 1:10 used initially) successfully generating a small number of hygromycin resistant clones.

It was important that TRIM25 WT and its mutants maintained their RNA-binding activity upon re-integration into the genome. As such RNA binding for these proteins was tested by RNA pull-down with pre-let-7a-1 (FIG. 17B). TRIM25 WT and TRIM25 $\Delta$ RING were both able to bind to pre-let-7a-1 while TRIM25 $\Delta$ RBD showed reduced binding, as would be expected from previous results. This indicates that the reintegrated proteins have maintained their respective RNA binding activity.

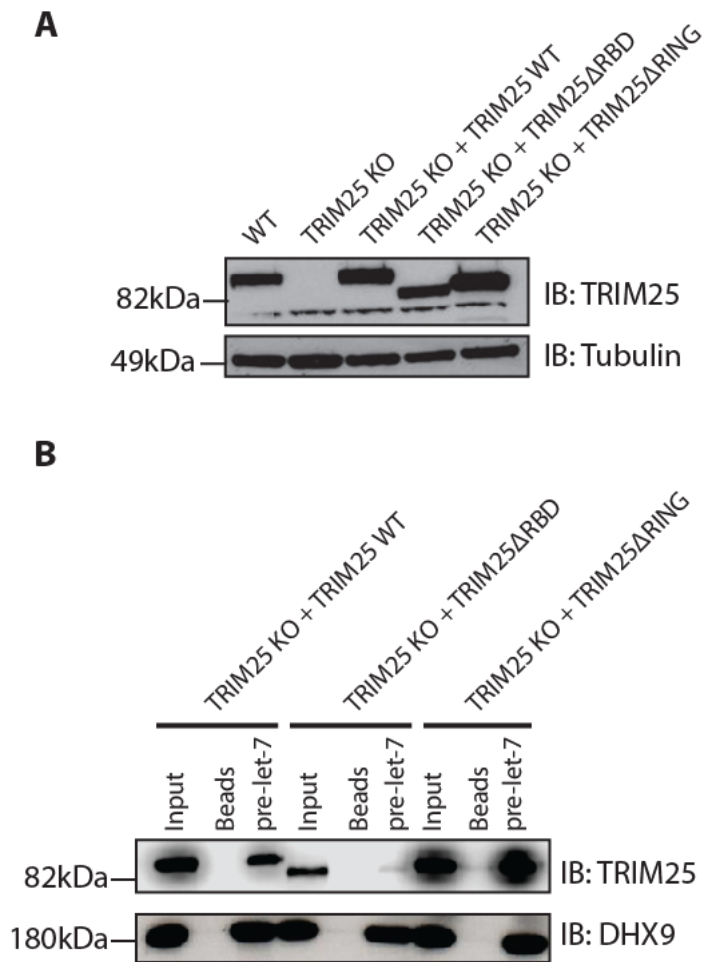


**Figure 17** – *TRIM25* WT and mutants maintained their respective RNA-binding ability upon re-integration into the HEK293 *TRIM25* KO genome. (A) Western blot validation of *TRIM25* expression levels in selected HEK293 cell lines. (B) RNA pull-down of WCE of selected HEK293 cell lines with pre-let-7a-1. Input represents 4% (40  $\mu$ g) of extracts used for pull-down. Beads represents uncoupled beads alone.

## Conclusions

TRIM25 KO cell lines were successfully generated for both HeLa and HEK293 cells. In addition to this, TRIM25 WT, TRIM25 $\Delta$ RBD and TRIM25 $\Delta$ RING were successfully reintegrated into the HEK293 TRIM25 KO genome with expression levels similar to WT cells and maintaining their respective RNA-binding capabilities.

CLIP-seq experiments performed in the lab identified thousands of TRIM25-bound RNA transcripts in HeLa cells<sup>219</sup>. Creation of HeLa TRIM25 KO cells will allow analysis of the possible effects of TRIM25 on the levels of these transcripts, as well as any effects on RNA processing or stability. They also allowed experiments concerning the ability of TRIM25 $\Delta$ RBD to function without the possible masking of any effects of loss of RNA binding by the presence of endogenous TRIM25. In addition, they enabled analysis of any proteins whose levels change upon deletion of TRIM25, for example targets of TRIM25 ubiquitination that are no longer targeted for degradation by the proteasome. It is, however, possible that clone C3 contains compensatory mutations for the loss of TRIM25, potentially masking the effects of TRIM25 deletion when assaying the cells' functions.

HEK293 TRIM25 KO and the cell lines with reintegrated TRIM25 WT, TRIM25 $\Delta$ RBD and TRIM25 $\Delta$ RING provide an ideal system for determining if the RNA binding or E3 ubiquitin ligase activity of TRIM25 are necessary for its functions. In addition to this, the HEK293 TRIM25 KO+TRIM25 WT cell line can be used to confirm that any differences seen between HEK293 WT and HEK293 TRIM25 KO are due to the loss of TRIM25. If any difference in phenotype in HEK293 TRIM25 KO compared to HEK293 WT is rescued in HEK293 TRIM25 KO+TRIM25 WT cells, this would show that the difference was due to loss of TRIM25 and not due to any off-target effects from CRISPR. HEK293 TRIM25 KO+TRIM25 $\Delta$ RBD and

HEK293 TRIM25 KO+TRIM25 $\Delta$ RING can be used in a similar way to determine if a function of TRIM25 is reliant on its RNA binding or E3 ubiquitin ligase activity respectively.

## Chapter 3 – Analysis of changes in RNA and protein levels in HeLa TRIM25 KO cells

### *Aims*

Previous work in the lab has shown that TRIM25 can bind to and affect the stability of prelet-7a-1 by acting as a co-factor for Lin28/TuT4-mediated uridylation<sup>216</sup>. As such, it would be interesting to find out if TRIM25 could influence the stability of other RNAs to which it binds. TRIM25 could affect RNA stability in several ways. Firstly, by binding RNAs, TRIM25 may exclude the binding of other RBPs or directly recruit other binding partners that can modify RNA in a way that leads to stabilisation or degradation. In addition to this, TRIM25 could use the RNA as a scaffold to ubiquitinate other proteins that are bound to the RNA, either targeting them for degradation or otherwise modulating their activity. A Co-IP experiment to identify proteins that interact with TRIM25 identified many proteins that are involved in RNA metabolism, for example ribosomal proteins, helicases and proteins involved in RNA processing, stability or splicing<sup>219</sup>. This further underlines the potential roles that TRIM25 could play in RNA biology. A CLIP-seq experiment performed in the lab identified over 2000 RNAs that associate with TRIM25 in HeLa cells, with most of these being mRNAs (56%) or long non-coding RNAs (lncRNAs, 29%)<sup>219</sup>. This indicates that there is a large pool of RNAs that TRIM25 could potentially regulate.

TRIM25 is an E3 ubiquitin ligase, meaning it can catalyse the formation of polyubiquitin chains on its target proteins. The addition of a K48-linked polyubiquitin chain to a protein targets it for degradation via the proteasome and is an essential aspect of the control of protein abundance and the targeting of damaged or improperly translated proteins for degradation. As such, it would be important to identify proteins that are stabilised by the

loss of TRIM25 as changes in protein abundance can have knock-on effects on the functions and proliferation of the cell.

The aim of this part of the project was to identify RNAs or proteins whose levels or stability are affected by the loss of TRIM25 in HeLa TRIM25 KO cells. Initially, the stability and levels of individual RNAs identified in the CLIP experiment were tested. Following this, genome-wide screening techniques were used to identify any other RNAs or proteins whose abundance is controlled by TRIM25.

### *Stability of cMyc and ZAP mRNAs is not affected by loss of TRIM25*

One possible function for TRIM25 RNA binding was regulating the stability of its target RNAs, for example through recruitment or inhibition of enzymes such as endo- or exonucleases. To this end the stability of two physiologically relevant mRNAs that were identified in the previous CLIP-seq experiment as being TRIM25 binding partners, cMyc and ZAP, were tested in HeLa TRIM25 KO cells compared to HeLa WT cells. This was done using Actinomycin D (ActD), which blocks RNA Polymerase II transcription, allowing the rate of decay of the mRNAs to be followed without the confounding effect of *de novo* transcription. Cells were treated with ActD and total RNA samples taken at different intervals before RNA abundance was measured by qRT-PCR (FIG. 18). Of note, RNA levels were normalised to 18S rRNA as this is stable over the time periods measured. However, as 18SrRNA is much more abundant than the RNAs tested, it required a 1 in 100 dilution to be measured (i.e. 5 ng RNA loaded instead of 500 ng). As such it may have been better to use a different RNA for normalisation such as Actin or GAPDH. Neither cMyc nor ZAP mRNA showed any change in rates of degradation between HeLa WT and TRIM25 KO cells.



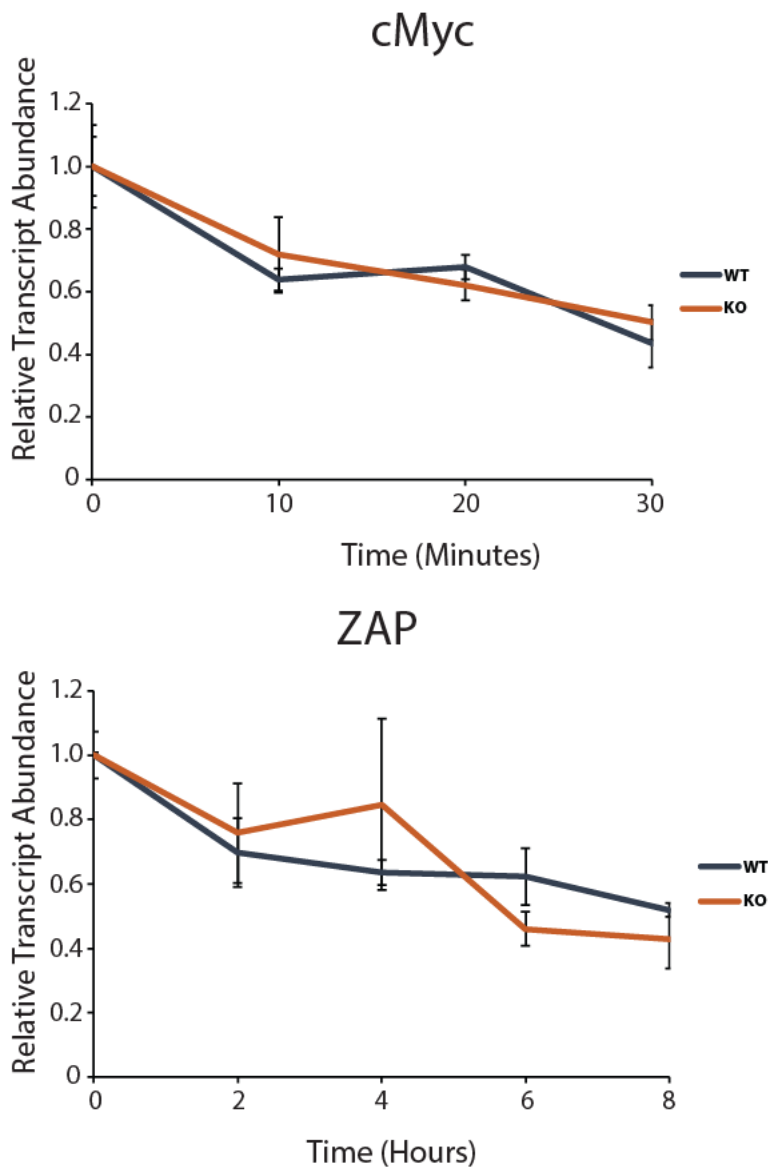


**Figure 18** – *Degradation of cMyc and ZAP mRNAs do not change upon loss of TRIM25.* HeLa WT or HeLa TRIM25 KO cells were treated with Actinomycin D and total cellular RNA samples taken at the time points indicated. Levels of cMyc and ZAP mRNA were assayed by qRT-PCR and were normalised to levels of 18S rRNA. Figures represent means and standard deviations of two independent experiments.

### *Levels of SUB1 mRNA decrease upon loss of TRIM25 in HeLa cells*

As many RNAs were identified as TRIM25 binding partners in the CLIP experiments, it would be interesting to test some of these to determine if their abundance changes upon loss of TRIM25. Total cellular RNA was isolated from HeLa WT and HeLa TRIM25 KO using TRI Reagent and quantified by nanodrop. Levels of selected mRNAs in HeLa WT or HeLa TRIM25 KO cells were determined by qRT-PCR and were normalised to levels of GAPDH (FIG. 19). Of the mRNAs tested, most showed no significant difference in expression upon deletion of TRIM25. However, one, *SUB1*, showed a modest (around 30%) but statistically significant decrease in abundance in HeLa TRIM25 KO cells. *SUB1* encodes a transcriptional coactivator that mediates interactions between upstream transcriptional activators and the transcriptional machinery. These results suggest that loss of TRIM25 does not have substantial effects on mRNAs that it binds to, however this is only a very small subset of these RNAs so more need to be tested to draw any conclusions.

### *RNAseq identifies changes in RNA levels in HeLa TRIM25 KO cells*

In order to determine the changes in mRNA abundance on a genome-wide scale, RNAseq was used. RNAseq is a technique that uses next generation sequencing (NGS) technologies to determine the presence and abundance of different mRNAs across the entire transcriptome<sup>233,234</sup>. Three samples of total cellular RNA for each of HeLa WT and HeLa TRIM25 KO were isolated at different times using TRI Reagent before further purification using phenol-chloroform extraction. Total RNA samples were sent to BGI who performed the library generation and sequencing. First RNA was tested to ensure it met the quality standards needed for the process. RNA was analysed on an Agilent 2100 Bioanalyser and

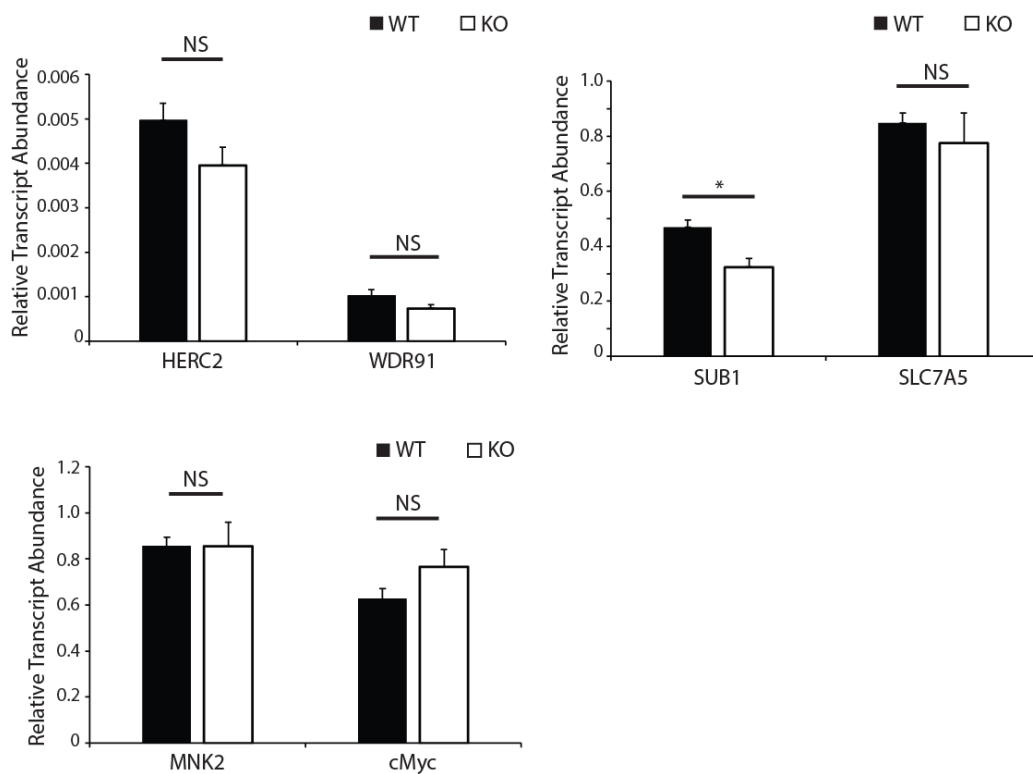


**Figure 19** – Levels of selected RNAs in HeLa WT and HeLa TRIM25 KO cells. Total cellular RNAs were assayed for levels of selected mRNAs by qRT-PCR. All RNAs were normalised to levels of GAPDH. Figures represent means and standard deviations from three independent experiments. Statistical significance calculations were performed using Welch's t-test (\* signifies  $p < 0.05$ ).

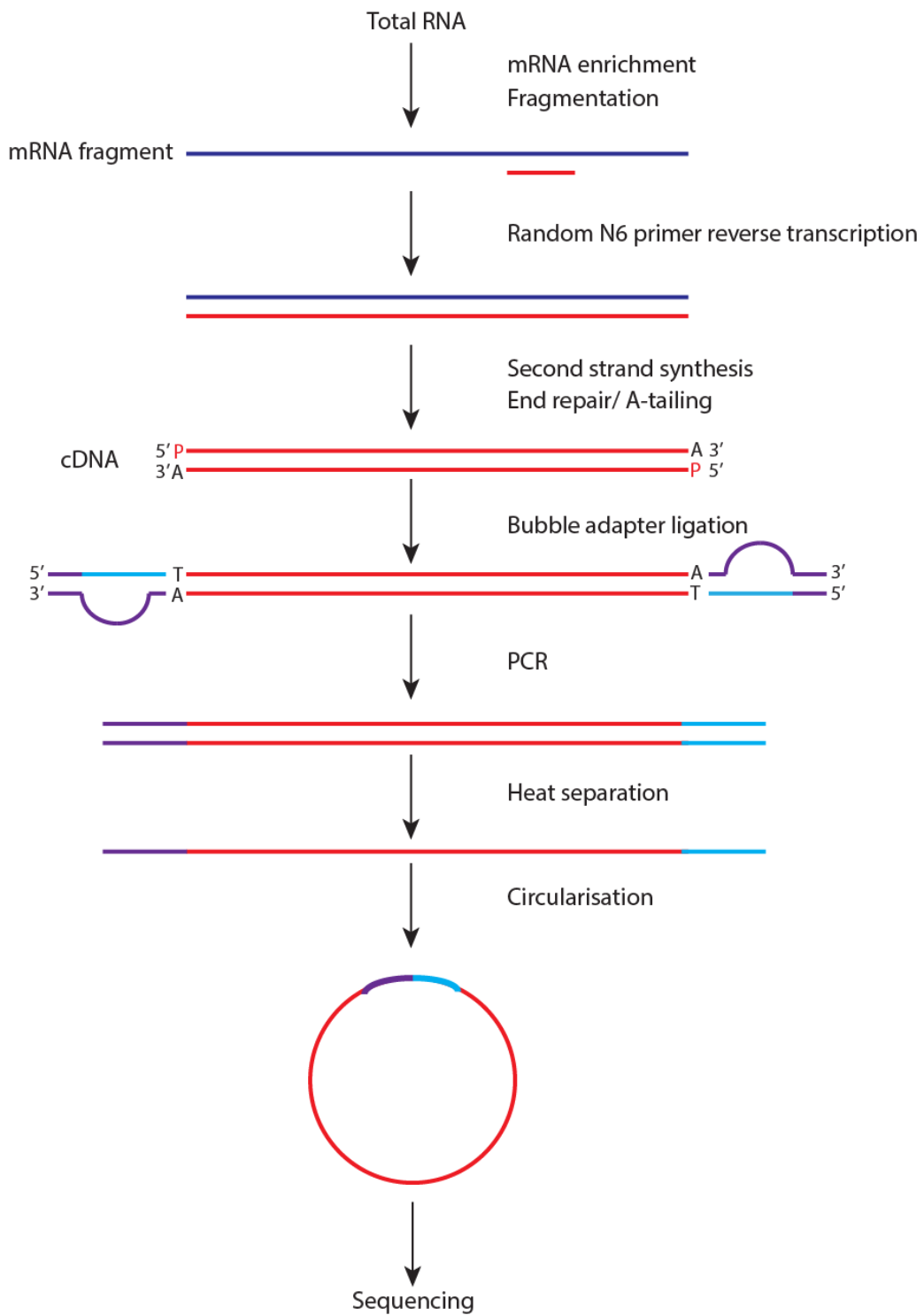
the concentration, RNA integrity number (RIN) and 28S/18S ratio were measured (Table 10). All of the samples had RNA of sufficient quality to proceed to RNAseq.

| Sample           | Concentration (ng/ $\mu$ L) | Total mass ( $\mu$ g) | RIN | 28S/18S |
|------------------|-----------------------------|-----------------------|-----|---------|
| HeLa WT 1        | 390                         | 7.8                   | 9.9 | 1.8     |
| HeLa WT 2        | 266                         | 5.32                  | 10  | 1.8     |
| HeLa WT 3        | 394                         | 7.88                  | 9.9 | 1.8     |
| HeLa TRIM25 KO 1 | 408                         | 9.38                  | 10  | 1.8     |
| HeLa TRIM25 KO 2 | 280                         | 5.6                   | 10  | 1.9     |
| HeLa TRIM25 KO 3 | 512                         | 10.24                 | 9.9 | 1.9     |

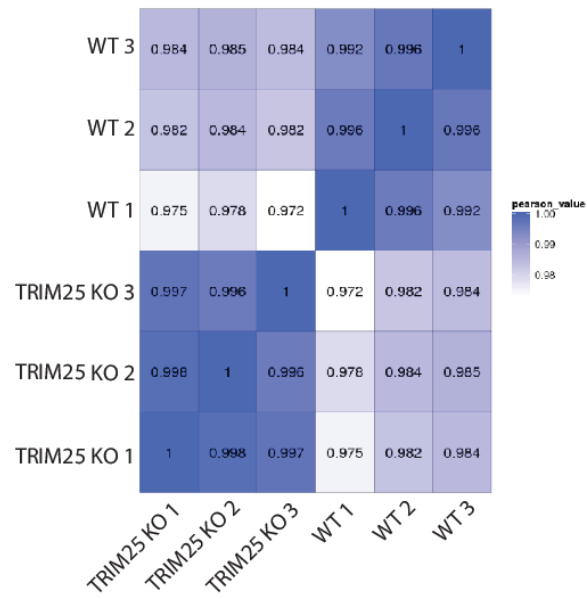
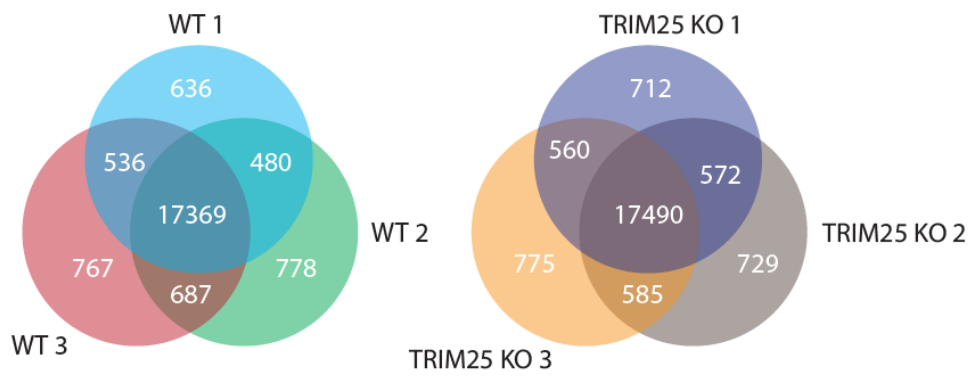
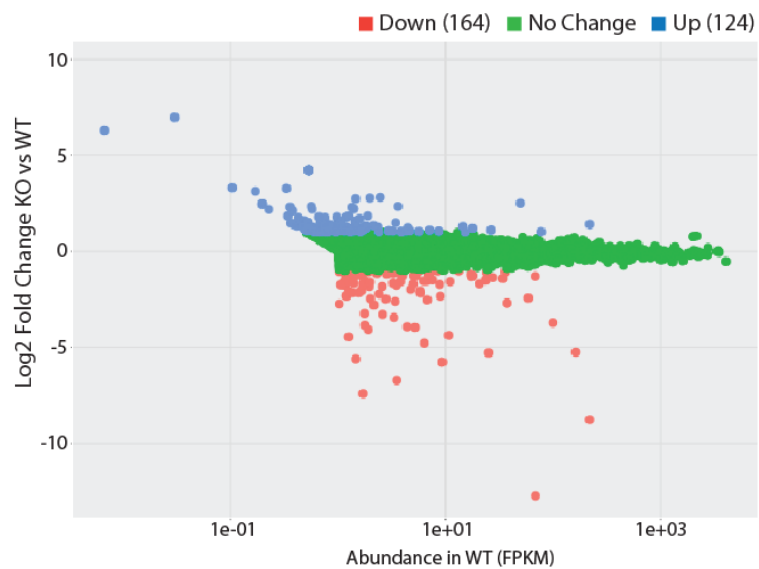
**Table 10** – Total RNA samples were of sufficient quality to proceed to RNAseq. Samples were analysed on an Agilent 2100 Bioanalyser.

A schematic of the RNAseq process is shown in FIG. 20. RNA samples were first enriched for mRNA as around 85% of the total RNA will be ribosomal RNA (rRNA). Oligo(dT) capture was used to select for mRNAs as the poly(A) tail of the mRNAs will bind to the oligo(dT) probe. Subsequently, RNAs were fragmented and reverse transcribed to generate double-stranded cDNAs. Adapters were ligated to both the 5' and 3' end of the cDNAs and primers specific to these adapters were used to amplify cDNAs by PCR. The amplified cDNAs were then circularised before the library was sequenced and analysed by aligning reads to a reference genome.

On average around  $24 \times 10^6$  reads were generated for each sample, with on average 95% of these being successfully mapped to the reference genome (Table 11). Biological replicates were highly correlated, with correlation values between samples isolated from the same cell lines at above 0.99, with a slight reduction in this for samples isolated from different cell lines, as would be expected (FIG. 21A). This suggests that the results obtained from this experiment were reliable. Around 19000 genes were identified in each sample, with 17369 identified in all three HeLa WT samples and 17490 in all three HeLa TRIM25 KO samples



**Figure 20** – Schematic of the process for RNAseq. After sequencing, sequenced reads underwent quality control to remove low quality sequences before being aligned to a reference genome. Quality control was performed at every step to improve quality and reliability of sequences.

**A****B****C**

**Figure 21** – 288 differentially expressed genes were identified in HeLa TRIM25 KO cells. (A) Correlation of gene expression values between samples. (B) Number of genes identified in HeLa WT or HeLa TRIM25 KO samples. (C) Scatter graph of genes identified in RNAseq. FPKM stands for Fragments Per Kilobase Million.

| Sample           | Total Reads | Total mapped reads (%) | Total unmapped reads (%) |
|------------------|-------------|------------------------|--------------------------|
| HeLa WT 1        | 24,104,504  | 95.68                  | 4.32                     |
| HeLa WT 2        | 24,096,601  | 95.44                  | 4.56                     |
| HeLa WT 3        | 24,101,277  | 95.43                  | 4.57                     |
| HeLa TRIM25 KO 1 | 24,098,396  | 95.36                  | 4.64                     |
| HeLa TRIM25 KO 2 | 24,094,450  | 95.55                  | 4.45                     |
| HeLa TRIM25 KO 3 | 24,103,091  | 95.74                  | 4.26                     |

**Table 11** – Number of total and mapped reads for each sample in RNAseq.

(FIG. 21B). Of these, 288 were differentially expressed by at least 2-fold in HeLa TRIM25 KO cells compared to HeLa WT, with abundance increasing for 124 and decreasing for 164 (FIG. 21C). This suggests that only a small proportion of genes were affected by knock-out of TRIM25. Interestingly only 9 mRNAs identified in the previous CLIP-seq experiment were differentially expressed in HeLa cells (Table 12). 3 of these were increased (TSPAN5, OPN3 and C14orf37) while 6 were decreased (COL5A1, PCDH11X, PPAN-P2RY11, SYBU, C16orf62 and TRIM25 itself). This indicates that TRIM25 binding to mRNAs does not generally have a substantial effect on their abundance in steady state cells.

| mRNA        | Fold Change (TRIM25 KO vs WT) |
|-------------|-------------------------------|
| TRIM25      | 0.31011                       |
| C16orf62    | 0.316872                      |
| SYBU        | 0.344156                      |
| COL5A1      | 0.402863                      |
| PPAN-P2RY11 | 0.43741                       |
| PCDH11X     | 0.456231                      |
| OPN3        | 2.079334                      |
| C14orf37    | 2.253968                      |
| TSPAN5      | 2.368421                      |

**Table 12** – mRNAs identified as binding to TRIM25 in the previous CLIP experiment that were found to be differentially expressed in HeLa TRIM25 KO cells compared to WT cells.

Differentially expressed genes were analysed in an attempt to find any commonalities between them. This could give insights into the mechanism by which these RNAs are regulated by TRIM25. Firstly, the base composition of differentially expressed genes was analysed (FIG. 22A). This showed that nucleotide content does not change between upregulated, downregulated and non-regulated genes. This was also analysed for the promoter regions of differentially expressed genes as TRIM25 has previously been shown to function as a regulator of transcription and as such may be regulating genes on the



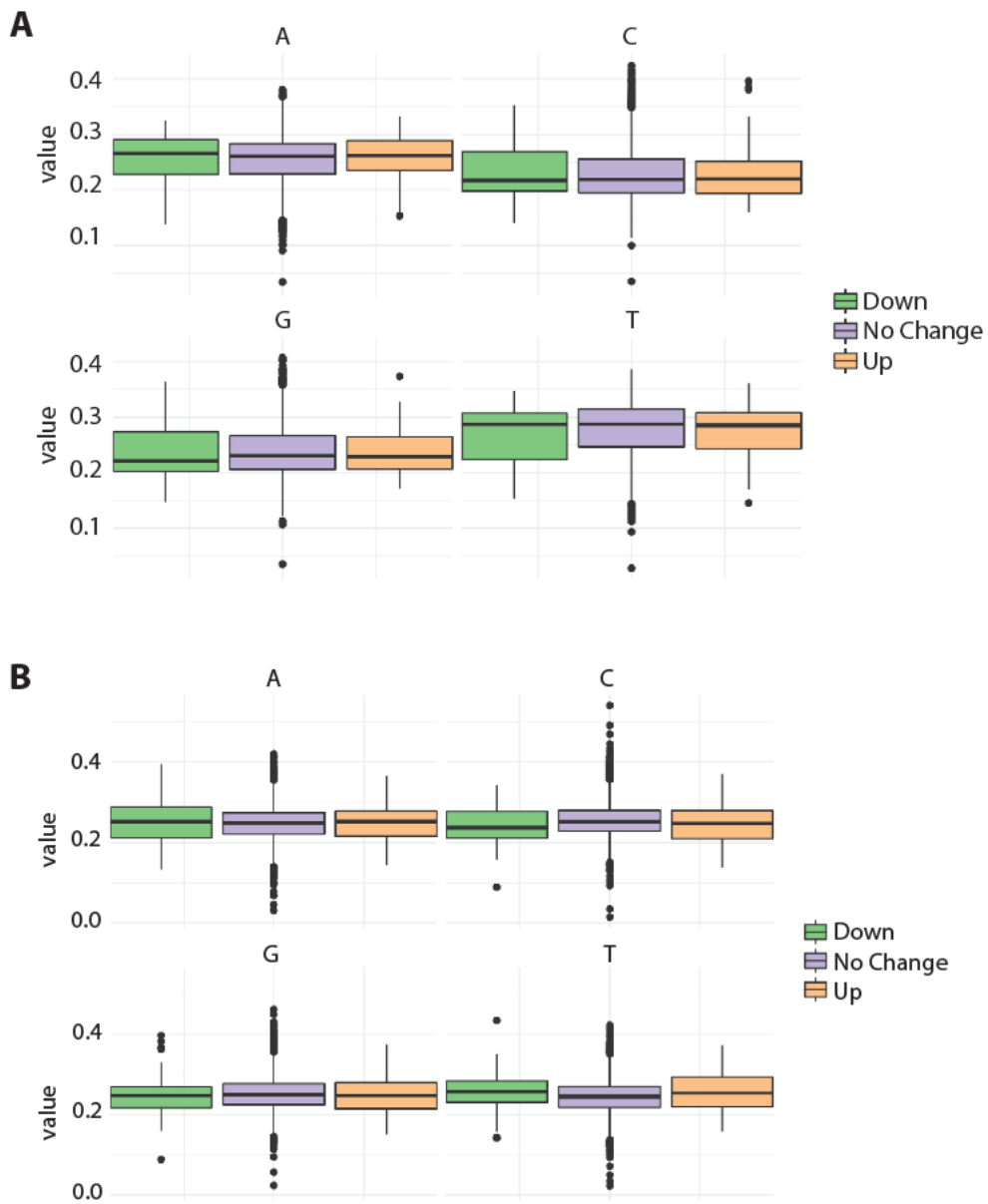


**Figure 22** - No difference in base composition for genes or promoters was seen in genes differentially expressed in HeLa TRIM25 KO cells. (A) Base composition of upregulated, downregulated and non-regulated genes identified in RNAseq. (B) Base composition of promoter sequences of upregulated, downregulated and non-regulated genes identified in RNAseq.

transcriptional level. Again no difference was seen between differentially expressed genes and genes that do not change (FIG. 22B). It was also discovered that there are no common motifs found in multiple differentially expressed genes, either in the coding sequence itself or the promoter regions. Taken together, these data suggest nucleotide content is not a common factor for genes that are differentially regulated upon TRIM25 deletion in HeLa cells.

### *Abundance of very few proteins is changed by loss of TRIM25*

TRIM25 is known to target some proteins for degradation via the proteasome by using its E3 ubiquitin ligase activity to catalyse the addition of K48-linked polyubiquitin chains to its targets<sup>202</sup>. As such it was important to determine whether loss of TRIM25 leads to changes in levels of particular proteins. In addition, this would determine whether changes in mRNA levels upon loss of TRIM25 are followed by corresponding changes in protein levels. To determine changes in protein levels at a whole proteome level, Stable Isotope Labelling with Amino acids in Cell culture (SILAC) coupled with Mass Spectrometry (MS) was used. SILAC-MS involves growing two different populations of cells in either 'heavy' media supplemented with amino acids labelled with heavy isotopes (for example arginine labelled with six <sup>13</sup>C atoms) or 'light' media with unlabelled amino acids (for example arginine incorporating regular <sup>12</sup>C atoms)<sup>235</sup>. Proteins from either cell population can be distinguished by trypsin digestion followed by MS due to the difference in mass of the resulting peptides for each labelled amino acid. Expression levels of proteins can then be compared between populations.

HeLa WT and HeLa TRIM25 KO were grown in both light and heavy media before proteins were extracted. 'Heavy' HeLa WT extract and 'light' HeLa TRIM25 KO extract were mixed

and the proteins present analysed by MS. This was also done reciprocally for ‘heavy’ HeLa TRIM25 KO extract and ‘light’ HeLa WT extract in an attempt to negate any bias for detection of particular peptides in either ‘light’ or ‘heavy’ extracts. Only 8 proteins were identified as being differentially expressed at a greater than 2-fold level in HeLa TRIM25 KO cells compared to HeLa WT cells in both experiments (Table 13). Excluding TRIM25 itself, of these, only SERPINB5 was also identified as being differentially expressed in the RNAseq experiment, indicating that it is downregulated at both the mRNA and the protein level. In addition, two genes identified in the previous CLIP experiment were also identified here, TMX2 and ERLIN1 and one protein identified as being a TRIM25 binding partner in a previous Co-IP experiment performed in the lab, ZC3HAV1, was also identified. Taken together, these results suggest that TRIM25 is not exerting an effect on the levels of a large number of proteins but may be acting on some individual proteins either through its E3 ligase activity, its RNA-binding activity or a combination of both.

| Protein  | Heavy[WT]/<br>light[TRIM25KO] | Heavy[TRIM25KO]/<br>light[WT] | CLIP     | Co-<br>IP | RNA<br>seq |
|----------|-------------------------------|-------------------------------|----------|-----------|------------|
| SERPINB5 | 5.9                           | 0.25                          |          |           | <b>X</b>   |
| TMX2     | 3.8                           | 0.68                          |          |           |            |
| ERLIN1   | 2.3                           | 0.74                          | <b>X</b> |           |            |
| EPHX1    | 2.3                           | 0.56                          | <b>X</b> |           |            |
| RCN3     | 2.1                           | 0.52                          |          |           |            |
| ZC3HAV1  | 0.84                          | 2.3                           |          | <b>X</b>  |            |
| CRABP2   | 0.70                          | 2.3                           |          |           |            |

**Table 13** – Proteins identified in SILAC-MS screen as being differentially expressed in HeLa TRIM25 KO cells compared to WT cells.

### *Expression of SERPINB5 is substantially reduced in HeLa TRIM25 KO cells*

To validate the RNAseq experiment, levels of selected mRNAs identified as being differentially expressed were measured. Initially, SERPINB5 (as it had also been identified as

being downregulated at the protein level), PCDHX11 and SYBU (as these had been identified as binding to TRIM25 in the CLIP experiment) were selected. Levels of SERPINB5, PCDHX11 and SYBU mRNA were assayed by qRT-PCR in total cellular RNA samples from HeLa WT and HeLa TRIM25 KO cells, as well as from two more TRIM25 KO HeLa cell lines (D11 and E10) that were generated in a separate CRISPR experiment in the lab (FIG. 23A). SERPINB5 was substantially downregulated in all three TRIM25 KO cell lines compared to HeLa WT cells, in agreement with the results from the RNAseq. PCDHX11 was slightly downregulated in all three cell lines, although less considerably than was suggested by RNAseq. Levels of SYBU mRNA were only slightly downregulated in the HeLa TRIM25 KO cells but were unchanged in both D11 and E10 cells, suggesting that this downregulation may just be due to off-target effects from CRISPR. As SERPINB5 was substantially downregulated in all three cell lines this was further validated by repeating the experiment (FIG. 23B). This showed a significant reduction in SERPINB5 mRNA levels in all three KO cell lines. In addition to this, levels of SERPINB5 protein in the KO cell lines were assayed by western blot (FIG. 23C). This also showed a large reduction in SERPINB5 expression upon loss of TRIM25. To determine if SERPINB5 expression could be rescued by TRIM25, T7-TRIM25 was transfected into HeLa TRIM25 KO cells and total cellular RNA harvested before levels of SERPINB5 were analysed by qRT-PCR (FIG. 23D). There was no significant difference in SERPINB5 mRNA levels after addition of T7-TRIM25, implying that transient expression of TRIM25 is not sufficient to rescue the phenotype in KO cells. These data suggest that although SERPINB5 levels are significantly reduced upon loss of TRIM25 in HeLa cells, it was not possible to rescue this by expression of exogenous TRIM25. One possibility is that the *SERPINB5* gene was disrupted as an off target effect of CRISPR. It is also possible that transient transfection of TRIM25 is not sufficient for rescue and stable re-integration is required. To this end, expression of SERPINB5 mRNA in HEK293 WT, TRIM25

KO and reintegrated cell lines was analysed by qRT-PCR and protein level by western blot. However, SERPINB5 was not detectable at either the RNA or protein level in any HEK293 cells (data not shown).

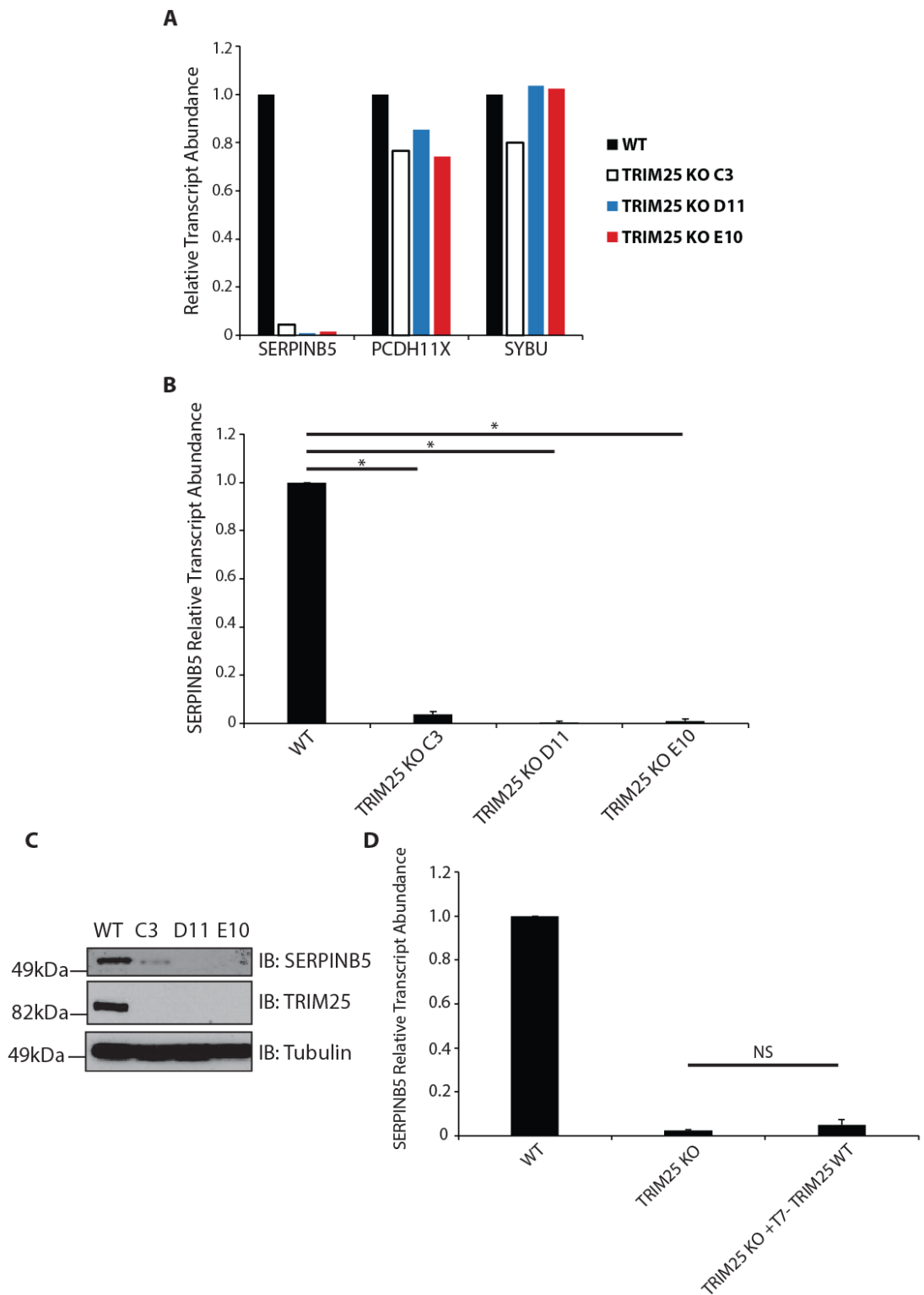


**Figure 23** – *SERPINB5* is downregulated at the mRNA and protein levels in HeLa *TRIM25* KO cells. (A) qRT-PCR showing abundance of selected mRNAs identified as being differentially expressed in HeLa *TRIM25* KO cells by RNAseq. In addition to the HeLa *TRIM25* KO cells used in RNAseq (C3), two other HeLa *TRIM25* KO cell lines were tested (D11 and E10). RNAs

were normalised to levels of GAPDH. (B) qRT-PCR of SERPINB5 in HeLa cell lines, normalised to GAPDH. Data represents means and standard deviations of three independent experiments. Statistical significance tests were performed using one-way ANOVA with post-hoc Tukey HSD (\* indicates  $p < 0.05$ ). (C) Western blot of whole cell extract from HeLa cell lines. (D) qRT-PCR of SERPINB5 RNA levels upon transient transfection of T7-TRIM25. A plasmid encoding T7-TRIM25 was transfected into cells and total cellular RNA was harvested after 48 hours. Data represents means and standard deviations of two independent experiments. Statistical significance tests were performed using Welch's t-test.

## Conclusions

The data presented here suggest that TRIM25 does not have a substantial effect on expression of the majority of the genes that it interacts with, either through mRNAs or proteins. Selected RNAs identified in the CLIP-seq experiment previously performed in the lab showed no difference in stability or abundance in HeLa TRIM25 KO cells, with the exception of SUB1 which showed a small reduction in expression. RNAseq identified several differentially expressed mRNAs in TRIM25 KO cells, however very few of these were identified in the CLIP-seq experiment as being bound by TRIM25. It should be noted, however, that CLIP cannot distinguish between RNAs that directly bind TRIM25 and those that may be associated with TRIM25-interacting proteins that are cross-linked to TRIM25 during the UV cross-linking step. It is therefore possible that the CLIP experiment over-estimated the number of TRIM25 interacting RNAs and this may be why so few are seen to change levels upon TRIM25 deletion. It may be useful to also identify proteins that are co-precipitating with TRIM25 in these experiments, for example by using MS. SILAC-MS identified just 8 proteins that were differentially expressed in TRIM25 KO cells. One gene, *SERPINB5*, was identified as being substantially downregulated in HeLa TRIM25 KO cells at both the mRNA and the protein level, although this could not be rescued by transient expression of T7-TRIM25 and as such it could not be confirmed that this was due to loss of TRIM25 and not due to off-target effects of CRISPR/Cas9.

The techniques used in this part of the project, although potentially powerful tools for detecting changes in gene expression across the whole transcriptome or proteome, were only used to look at gene expression in steady state cells. It is possible that TRIM25 can aid in the regulation of gene expression in response to particular stimuli, for example it has been previously shown to be involved in the oestrogen response<sup>198</sup>. TRIM25 binds to a large



number of RNAs in steady state cells, as shown by the CLIP experiment. It could be that TRIM25 requires the presence of other proteins that interact with or modify it in particular conditions in order for it to have a greater effect on regulation of gene expression. It would be interesting in the future to test the effect of the loss of TRIM25 in response to different stimuli.

It is also possible that the functions of TRIM25 do not extend to the regulation of gene expression and are instead more focused on the modulation of activity of its target proteins. Ubiquitination is often used for targeting proteins for degradation via the proteasome through the addition of K48-linked polyubiquitin chains. However, other types of polyubiquitin chains, for example K63-linked chains, are often used in signalling or for modifying protein function. TRIM25 may be using RNA as a scaffold to bring it into contact with its target proteins so that they can be ubiquitinated in this way. These functions are unlikely to be uncovered through the use of whole genome screening techniques. There is also a possibility that there is a level of redundancy whereby the loss of TRIM25 can be compensated for, for example by other TRIM family proteins. Further experiments on individual targets of TRIM25 ubiquitination would be required to determine if this hypothesis is true.

## Chapter 4 – The role of TRIM25 in viral infection

### *Aims*

The innate immune system provides the first line of defence for the body when fighting pathogens such as bacteria or viruses. Pathogens are detected non-specifically, as opposed to the adaptive immune system that is moderated by antibodies, resulting in the activation of a variety of anti-pathogenic factors. One of the most important components of the anti-viral innate immune system are the interferons (IFNs), a group of signalling proteins that trigger the expression of many genes, termed IFN-stimulated genes (ISGs), that perform anti-pathogenic functions, such as activation of immune cells or down-regulating protein expression. Expression of IFNs is triggered by signalling cascades that result from the recognition of pathogen-specific molecules, termed pathogen associated molecular patterns (PAMPs), by pattern recognition receptors (PRRs) in the host cell. PRRs are grouped into four main types; Toll-like receptors (TLRs), Nod-like receptors (NLRs), C-type lectin receptors (CLRs) and RIG-I-like receptors (RLRs). Of these, TRIM25 has been shown to have a role in the signalling of RIG-I, a cytoplasmic PRR that recognises 5'-triphosphate (5'ppp) moieties that are present on RNAs produced during the replication of RNA viruses such as Influenza virus or Dengue virus. Work has shown that upon binding to a 5'ppp-RNA, RIG-I undergoes a conformational change that exposes its 2 caspase recruitment domains (2CARD). TRIM25 then binds to and ubiquitinates the 2CARD, allowing RIG-I to recruit its downstream partner MAVS and triggering a signalling cascade resulting in phosphorylation of the transcription factor IRF-3, which translocates to the nucleus and activates expression of type I IFNs<sup>113</sup>. It has been suggested that the E3 ubiquitin ligases Riplet, TRIM4 and MEX3C can also perform this role, meaning that TRIM25 may be redundant in human cells<sup>125</sup>. In addition to this, recent work has suggested that TRIM25 can directly inhibit

replication of Influenza A virus (IAV) by binding to viral ribonuclear proteins (RNPs) in an RNA-dependent manner, blocking their transcription<sup>187</sup>.

The aim of this section of the project was to try to confirm the functions of TRIM25 in restricting virus replication and in the RIG-I pathway. Due to the combination of TRIM25's RNA-binding activity and its role in defence against RNA viruses, it was important to determine if these functions were dependent on RNA-binding activity. The development of HEK293 TRIM25 KO cells in which TRIM25 WT, TRIM25 $\Delta$ RBD and TRIM25 $\Delta$ RING had been reintegrated provided the perfect model in which to test the dependence of TRIM25's anti-viral function on its RNA-binding and ubiquitination activity. By infecting cells with IAV it would be possible to see which of these cell lines can restrict viral replication and therefore whether this is dependent on ubiquitination or RNA binding. In addition, TRIM25's role in the RIG-I pathway could be assayed by transfecting these cells with isolated 5'ppp-RNAs and determining levels of IRF-3 phosphorylation and type I IFN expression in response to this.

### *HEK293 TRIM25 KO cells are more permissive to an NS1 deficient IAV than HEK293 WT cells*

The NS1 protein of IAV, encoded by segment 8 of the genome, inhibits TRIM25 by binding directly to its coiled-coil domain, preventing oligomerisation and therefore enzymatic activity<sup>145,147</sup>. This would make it hard to determine the effects of deletion of TRIM25 from cells as even in WT cells TRIM25 would be antagonised by NS1. However, a mutant NS1 that cannot inhibit TRIM25 has previously been identified (NS1 R38K41A)<sup>146</sup>. This mutant is unable to bind to TRIM25, among other defects, and interestingly, unlike WT NS1, is also unable to bind to RNA<sup>236,237</sup>. IAV with NS1 R38K41A is restricted upon infection when

compared to WT IAV and it is also deficient in preventing expression of type I IFNs. As such, cells were challenged with two IAVs, a lab-adapted strain A/PR/8/34 (PR8 WT)<sup>223</sup> and a mutant of this strain encoding NS1 R38K41A (PR8 NS1 R38K41A). Viruses were produced using a reverse genetics system. Plasmids encoding all 8 segments of the PR8 genome were transfected into HEK293T cells. Both positive and negative sense RNA are produced from the plasmids, with the positive sense RNA being translated into IAV proteins that are packaged with the negative sense RNAs that form the IAV genome, resulting in complete virus particles<sup>223</sup>. These virus particles are capable of replication and were used to infect Madin-Darby Canine Kidney (MDCK) cells to propagate them and generate a virus working stock. MDCK cells are used for this as they are highly susceptible to IAV infection and generally produce high virus titres due in part to a dampened response to IFNs<sup>238</sup>. The virus titre of the working stock was assayed by plaque assay. A series of 10-fold dilutions of the virus stock were used to infect a lawn of MDCK cells, overlaid with a thixotropic medium and incubated for 48 hours. The thixotropic overlay medium prevents virus particles spreading across the media by convection, meaning that viruses must propagate from cell to cell and plaques are formed that represent the initial infection of one plaque forming unit (pfu) of virus. The cells were fixed with formalin and stained with toluidine blue to visualise plaques so that they can be counted. Virus working stocks were produced on average at a titre of  $10^8$ - $10^9$  pfu/mL.

To test HEK293 TRIM25 KO cells for their ability to restrict IAV replication compared to HEK293 WT, cells were infected with PR8 WT or PR8 NS1 R38K41A at a multiplicity of infection (MOI, the number of virus particles per cell) of 1. Virus titres post-infection for several time points were measured by plaque assay (FIG. 24). PR8 WT titres were similar at all time points and no differences were statistically significant. At 48 hours there was a large increase in virus titre in HEK293 TRIM25 KO cells in one repeat, however, to be sure

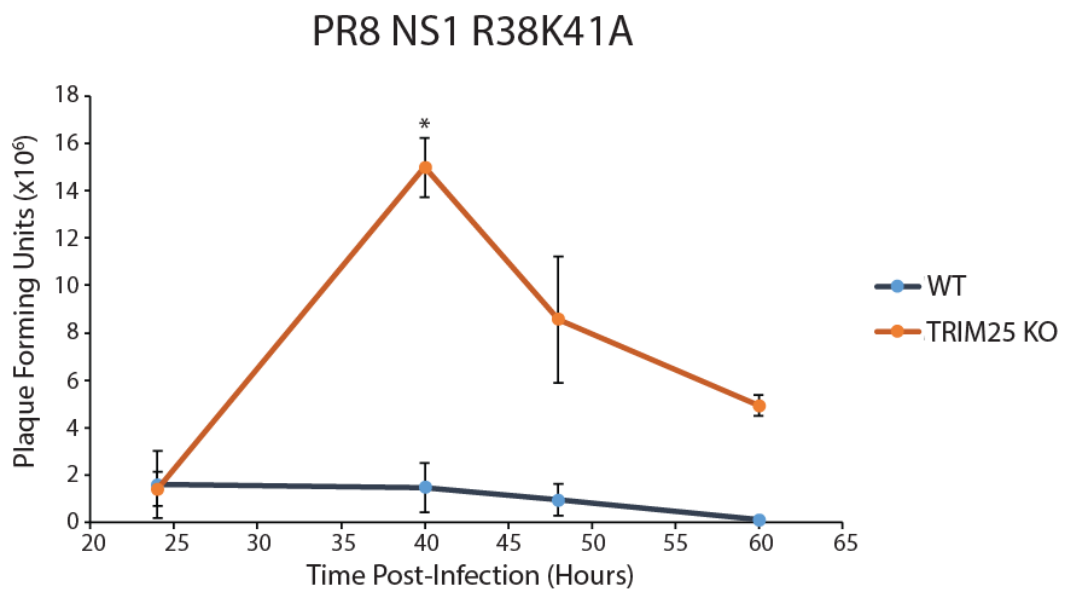
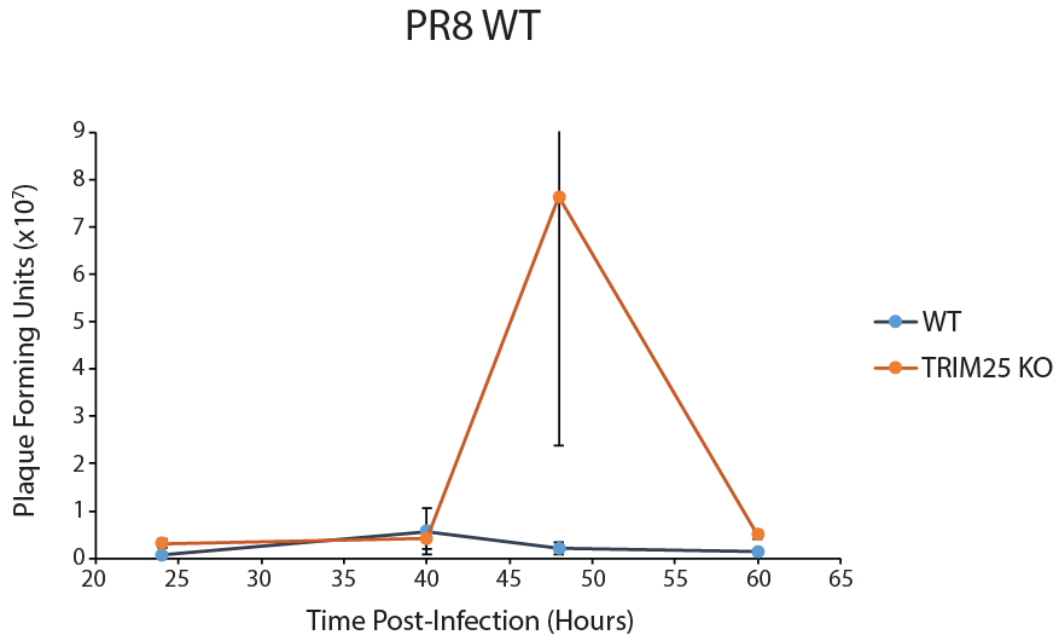


**Figure 24** – HEK293 TRIM25 KO cells are more permissive to PR8 NS1 R38K41A infection than HEK293 WT. Either HEK293 WT or TRIM25 KO cells were infected with IAV PR8 WT or PR8 NS1 R38K41A at an MOI of 1 and viral load was assessed by plaque assay at the time points indicated. Data represents the means and standard deviations of two independent experiments. Statistical significance calculations were performed using Welch’s t-test (\* signifies  $p < 0.05$ ). The experiments shown in these figures were performed by Eleanor Gaunt in the laboratory of Paul Digard (Roslin Institute, University of Edinburgh).

that this is an outlier the experiment would have to be repeated. PR8 NS1 R38K41A titres were significantly higher post-infection in HEK293 TRIM25 KO cells than HEK293 WT cells at the 40-hour time point, indicating that HEK293 TRIM25 KO cells are more permissive to PR8 and suggesting that the presence of TRIM25 restricted IAV replication in the absence of functional NS1. As this experiment was only performed twice, statistical power of the results was diminished, leading to the differences seen at 48 and 60 hours not being statistically significant. However, these results were deemed promising enough to move on to a larger scale experiment.

### *PR8 NS1 R38K41A restriction is rescued by TRIM25 WT, TRIM25 $\Delta$ RBD and TRIM25 $\Delta$ RING*

To ensure that the differences seen between HEK293 WT and HEK293 TRIM25 KO cells were due to the absence of TRIM25, not off target effects of the CRISPR process, as well as determine if this phenotype can be rescued by TRIM25 $\Delta$ RBD or TRIM25 $\Delta$ RING. HEK293 TRIM25 KO cell lines with reintegrated TRIM25 WT, TRIM25 $\Delta$ RBD or TRIM25 $\Delta$ RING were infected with IAV PR8 WT or PR8 NS1 R38K41A at an MOI of 0.001 and virus titre was assessed after 48 hours (FIG. 25A & B). Differences seen in the raw titres of IAV after infection were found not to be significant, probably due to large variations in titres seen between experiments (FIG. 25A). However, when titres of PR8 NS1 R38K41A were expressed as a proportion of those of PR8 WT from the same experiment, HEK293 TRIM25 KO cells were found to be significantly more permissive to growth of PR8 NS1 R38K41A than each of the other cell lines (FIG. 25B). HEK293 WT cells restricted growth of PR8 NS1 R38K41A in comparison to PR8 WT. As seen previously, HEK293 TRIM25 KO cells lost the ability to restrict PR8 NS1 R38K41A replication compared to PR8 WT. This confirmed our

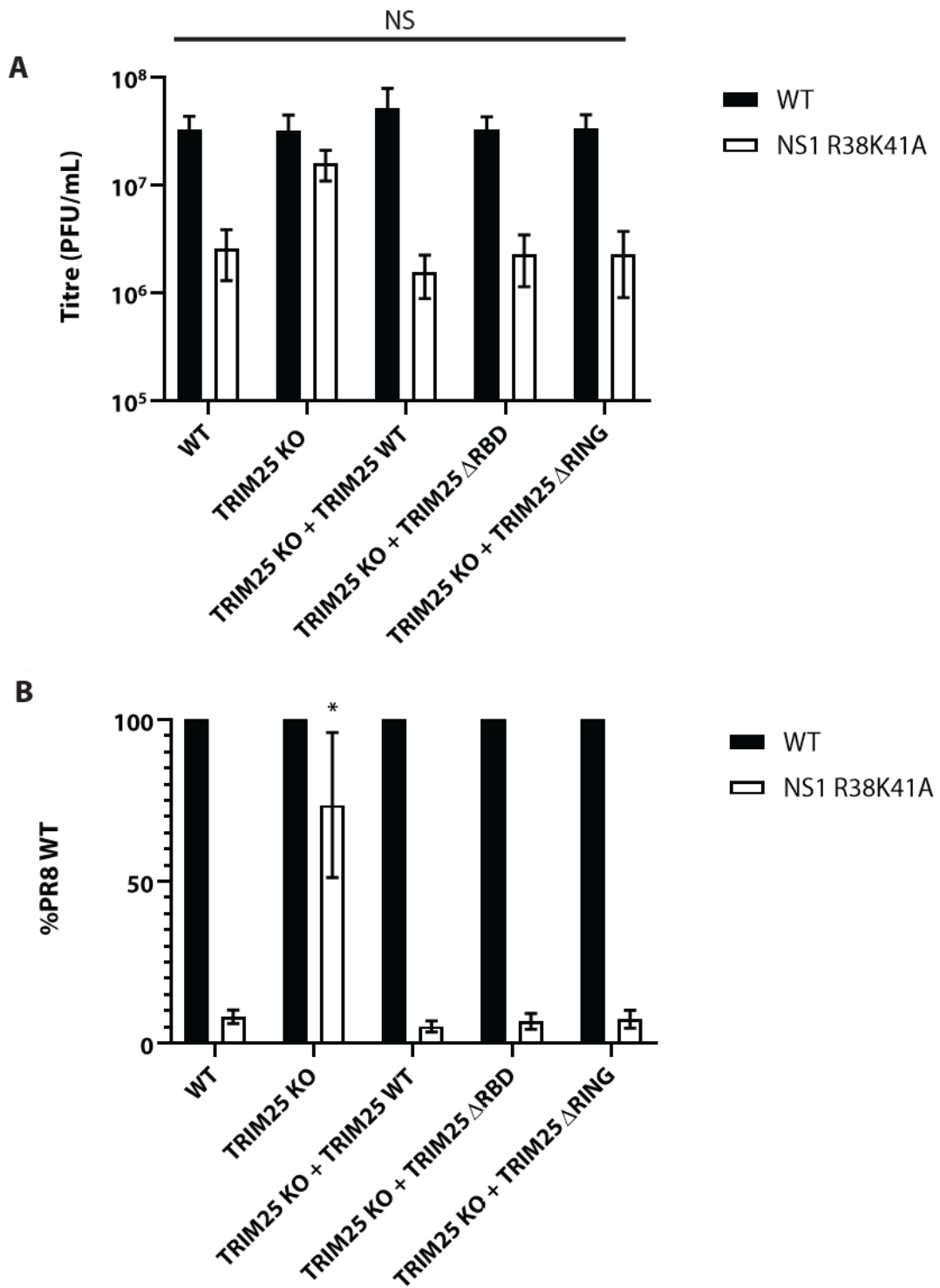


**Figure 25** – HEK293 TRIM25 KO cells restriction of IAV replication is rescued by reintegration of TRIM25 WT,  $\Delta$ RBD or  $\Delta$ RING. HEK293 cell lines were infected with IAV PR8 WT or PR8 NS1 R38K41A at an MOI of 0.001 and virus titres were assessed by plaque assay after 48 hours. (A) Raw virus titres resulting from this infection. (B) PR8 NS1 R38K41A titres as a proportion of PR8 WT titres from the same repeat of the experiment. Both graphs

represent the same experiments, n=4. Statistical significance tests performed with 2 way ANOVA with post-hoc Tukey HSD test. \* indicates  $p < 0.05$  in comparison to other cell lines infected with the same virus. The experiments shown in these figures were performed by Rute Pinto in the laboratory of Paul Digard (Roslin Institute, University of Edinburgh).



earlier results. Restriction of PR8 NS1 R38K41A was rescued by re-integration of TRIM25 WT, suggesting that the loss of restriction in HEK293 TRIM25 KO cells was due to the loss of TRIM25, not any off-target effects resulting from the CRISPR process. Surprisingly, restriction was also rescued by integration of TRIM25 $\Delta$ RBD and TRIM25 $\Delta$ RING. The ability of TRIM25 $\Delta$ RBD to rescue IAV restriction suggests that TRIM25 RNA binding activity is not required for IAV restriction. TRIM25 $\Delta$ RBD also shows a defect in ubiquitination activity, hinting that TRIM25's ubiquitination of RIG-I is not required for IAV restriction. There is a possibility, however, that TRIM25 $\Delta$ RBD could bind to vRNAs using a different mechanism, separate to that which it uses to bind to endogenous RNAs. The ability of TRIM25 $\Delta$ RING to rescue restriction confirms that the ubiquitination activity of TRIM25 is not important for its role in restricting IAV and therefore TRIM25 ubiquitination of RIG-I is not required during IAV infection in cultured HEK293 cells. Taken together, these results suggest that there may be another, as yet unknown, mechanism of IAV restriction by TRIM25 that does not require its RNA binding or ubiquitination activities. However it was first important to ensure that the deletion of TRIM25 was not affecting the RIG-I pathway or the efficiency of transcription of vRNAs, as has been shown by other groups previously.

#### *Deletion of TRIM25 does not reduce activation of RIG-I signalling upon 5'ppp-RNA transfection in HEK293 cells*

To test the ability of HEK293 TRIM25 KO to activate RIG-I signalling in response to a 5'ppp-RNA, 3p-hpRNA, a synthetic 5'ppp panhandle RNA derived from the beginning of segment 8 of the IAV genome (FIG. 26A), was transfected into the HEK293 cell lines used in the previous experiment. Cells were incubated for 6 hours post-transfection before being harvested and levels of phospho-IRF-3 were analysed by western blot (FIG. 26B). All of the

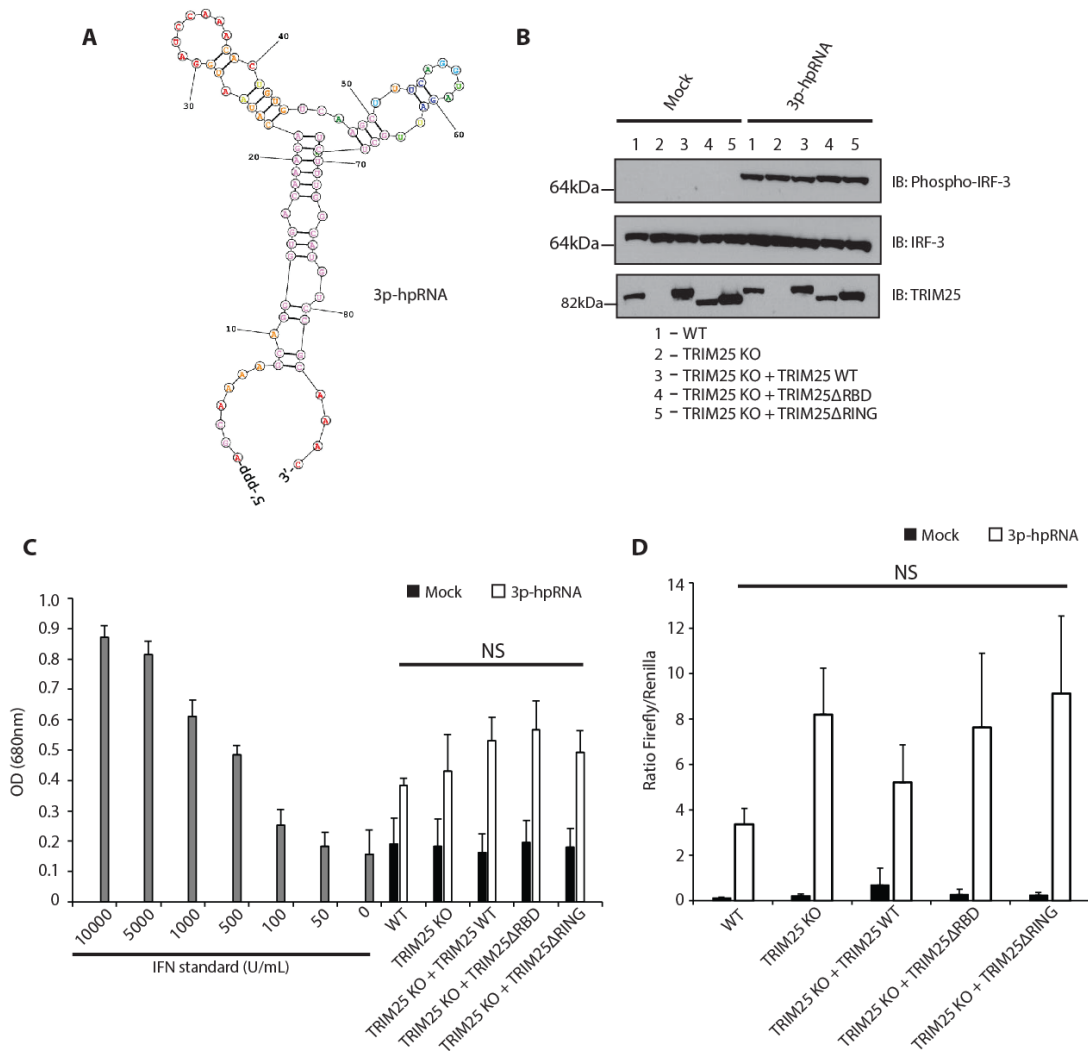


**Figure 26** – Activation of the RIG-I/IFN type I pathway is not affected by loss of TRIM25 in HEK293 cells. (A) 3p-hpRNA, a 5'ppp-RNA derived from the IAV genome. (B) HEK293 cell lines were transfected with 100 ng/mL 3p-hpRNA and levels of phospho-IRF-3 were assessed by western blot after 6 hours. (C) The same experiment was performed but this time levels of IFN $\alpha/\beta$  were assessed using the HEK-Blue assay. Data represents means and standard deviations of three independent experiments. Statistical significance calculations were performed using one-way ANOVA followed by post-hoc Tukey HSD test. (D) HEK293 cells were transfected with 100 ng/mL 3p-hpRNA along with firefly luciferase under the IFN $\beta$  promoter and a constitutively expressed renilla luciferase. Luciferase activity was assessed after 24 hours. Data represents means and standard deviations of three independent experiments. Statistical significance calculations were performed using one-way ANOVA followed by post-hoc Tukey HSD test.

cell lines tested showed similar levels of IRF-3 phosphorylation, suggesting the RIG-I pathway was fully functional even in the absence of TRIM25 and that re-integration of TRIM25 into HEK293 TRIM25 KO cells does not increase RIG-I activation. This rules out the possibility that any off-target effects from CRISPR have masked a possible drop in RIG-I activation in HEK293 TRIM25 KO cells that may have resulted from the loss of TRIM25. This was further confirmed by analysing expression of IFN $\alpha$  and IFN $\beta$  (type I IFNs) in response to transfection of 3p-hpRNA. This was done using the HEK-Blue system. As IFN $\alpha$  and IFN $\beta$  are secreted by cells, supernatant can be taken from treated cells and added directly to HEK-Blue cells. HEK-Blue cells contain a gene encoding a secreted alkaline phosphatase (SEAP) under the control of the IFN $\alpha$ / $\beta$ -responsive ISG54 promoter, meaning the more IFN $\alpha$ / $\beta$  they are treated with, the more SEAP will be secreted. Supernatant from HEK-Blue cells is added to the QUANTI-Blue substrate, in which SEAP catalyses a colour change from pink to blue that can be measured by absorbance at 680 nm. HEK293 cell lines were transfected with 3p-hpRNA and 6 hours post-transfection the HEK-Blue assay was performed (FIG. 26C). As with IRF-3 phosphorylation, there were no significant differences between the HEK293 cell lines. Finally, RIG-I activation in response to 3p-hpRNA was measured using a dual-luciferase assay. Cells were transfected with a plasmid encoding firefly luciferase under the IFN $\beta$  promoter, in addition to 3p-hpRNA with renilla luciferase under a constitutive promoter (thymidine kinase, TK) as a loading/transfection control. The higher the level of RIG-I activation in response to 3p-hpRNA, the higher the expression of firefly luciferase and therefore the higher the ratio of firefly/renilla. Cells were incubated for 24 hours and luciferase activity was measured (FIG. 26D). Cell lines containing WT TRIM25 (HEK293 WT and TRIM25 KO + TRIM25 WT) had slightly lower expression of firefly luciferase than the other cell lines but these differences were not statistically significant. Taken together these data indicate that 3p-hpRNA-induced activation of the RIG-I pathway is not compromised in

HEK293 cells in the absence of TRIM25 and provide further evidence that loss of PR8 NS1 R38K41A restriction in HEK293 TRIM25 KO cells is not due to a defect in RIG-I signalling. The lack of defect in RIG-I signalling could be due to redundancy in the system, with other E3 ubiquitin ligases (e.g. Riplet, MEX3C) previously having been shown to be able to perform the function of TRIM25 by ubiquitinating the RIG-I 2CARD.

*TRIM25 deletion compromises RIG-I activity in response to 5'pppRNA transfection in MEF, but not HeLa, cells*

To determine if the RIG-I pathway can still function in the absence of TRIM25 in other cell lines apart from HEK293, HeLa WT and TRIM25 KO cells were transfected with 3p-hpRNA and levels of phospho-IRF-3 were determined by western blot 6 hours post-transfection (FIG. 27A). Phosphorylation of IRF-3 was in fact marginally more pronounced in HeLa TRIM25 KO than WT cells, again indicating that loss of TRIM25 did not compromise RIG-I activation. Response to 3p-hpRNA in HeLa WT and HeLa TRIM25 KO was also tested by HEK-Blue assay in HeLa WT and TRIM25 KO cells (FIG. 27B). Both HeLa WT and HeLa TRIM25 KO cells did not show a significant response to 3p-hpRNA compared to mock transfected cells.

To determine if RIG-I signalling was affected by loss of TRIM25 in an organism other than humans, mouse embryonic fibroblast (MEF) WT and TRIM25 KO cells were used. MEF WT and TRIM25 KO cells were treated with 3p-hpRNA and phospho-IRF-3 levels were analysed 6 hours post-transfection by western blot (FIG. 27C). In these cells loss of TRIM25 lead to lower levels of phospho-IRF-3 upon 3p-hpRNA transfection, although IRF-3 phosphorylation was not completely abolished. This indicates that RIG-I signalling had been compromised and suggests that TRIM25 is important for RIG-I signalling in mouse cells but is not completely essential. This could be due to a lack of redundancy in the system, with other

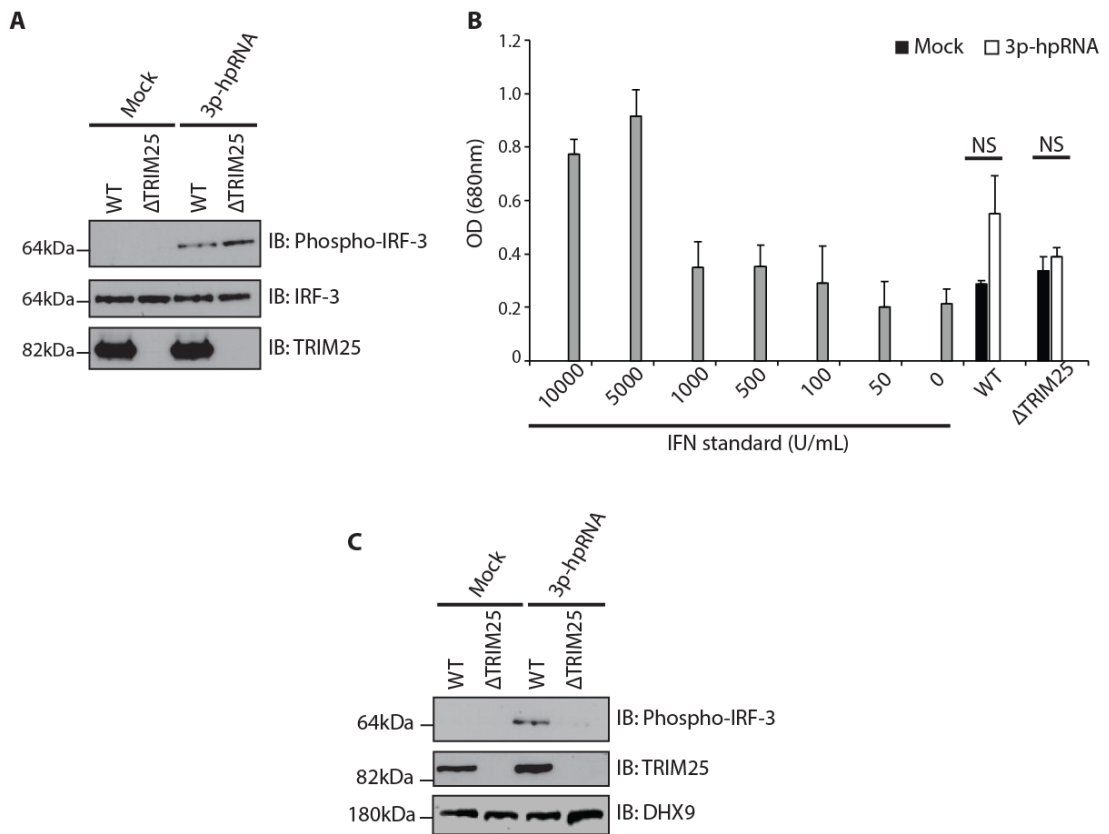


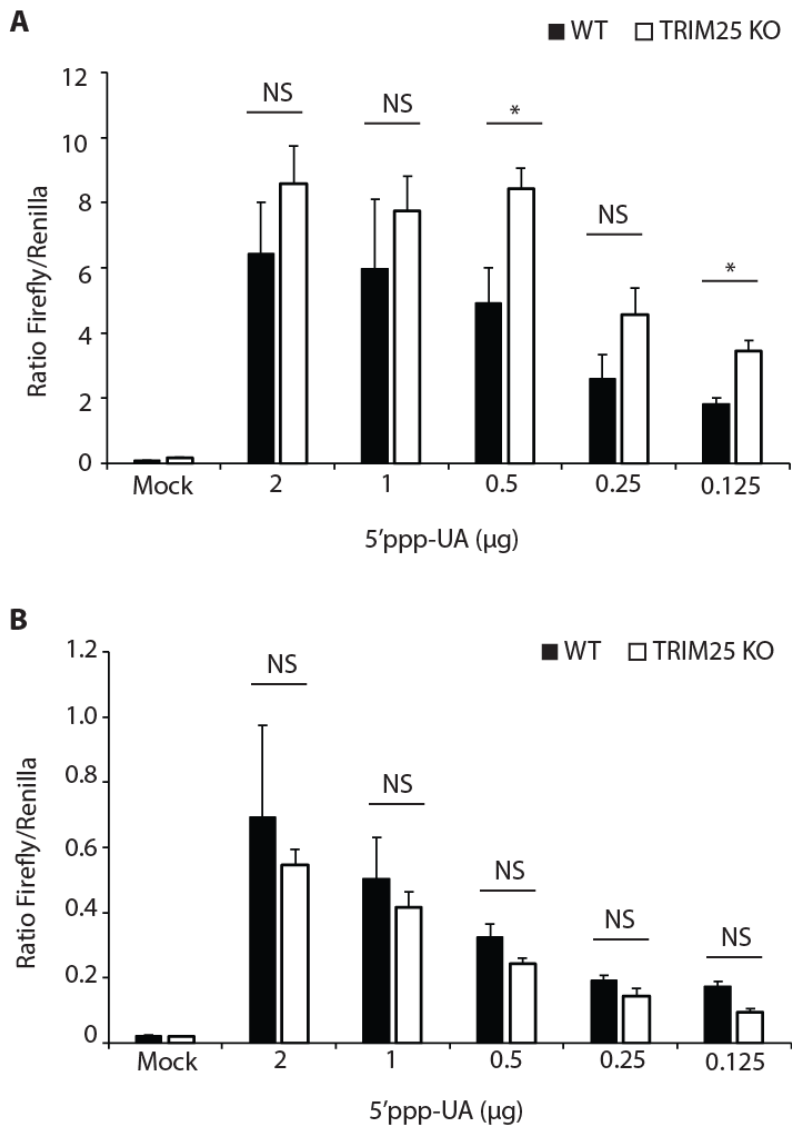
**Figure 27** – Activation of the RIG-I pathway is attenuated in MEF, but not HeLa, cells upon loss of TRIM25. (A) HeLa cell lines were transfected with 100 ng/mL 3p-hpRNA and levels of phospho-IRF-3 were assessed by western blot after 6 hours. (B) The same experiment was performed but this time levels of IFN $\alpha/\beta$  were assessed using the HEK-Blue assay. Data represents means and standard deviations of three independent experiments. Statistical significance calculations were performed using Welch's t-test. (C) MEF cell lines were transfected with 100 ng/mL 3p-hpRNA and levels of phospho-IRF-3 were assessed by western blot after 6 hours. DHX9 was used as a loading control as the total IRF-3 antibody did not cross-react with mouse IRF-3.

proteins being unable to ubiquitinate RIG-I or inefficient in this process. Taken together, these results confirm RIG-I/IFN type I activation dependence on TRIM25 in mouse cells, but provide further evidence that TRIM25 is dispensable for RIG-I/IFN type I activation in selected human cultured cell lines. Due to the variation in the presence of proteins and other factors, there is likely to be variation in the RIG-I/IFN type I response between cell lines. As such, more cell lines from both species, as well as different 5'ppp-RNAs, must be tested to draw further conclusions about the role of TRIM25 in RIG-I/IFN type I activation in both humans and mice.

To ensure that the previous results were not confined to 3p-hpRNA, another 5'ppp-RNA was tested in HEK293 and HeLa WT and TRIM25 KO cells. Various amounts of 5'ppp-UA (see FIG. 6A) was transfected into cells along with Firefly luciferase under the IFN $\beta$  promoter and Renilla luciferase under the TK promoter. Cells were incubated for 24 hours and luciferase activity was assayed in HEK293 (FIG. 28A) and HeLa (FIG. 28B) cells. Levels of RIG-I activation were slightly higher in HEK293 TRIM25 KO cells at all amounts of 5'ppp-UA, although these differences were only statistically significant for 0.5  $\mu$ g and 0.125  $\mu$ g of RNA. In HeLa cells, RIG-I activation showed no significant differences between WT and TRIM25 KO cells for any amount of 5'ppp-UA. These data provide further evidence that RIG-I/IFN type I activation is not dependent on TRIM25 in HeLa or HEK293 cells.

### *TRIM25 does not inhibit IAV RNA polymerase in HEK293 cells*

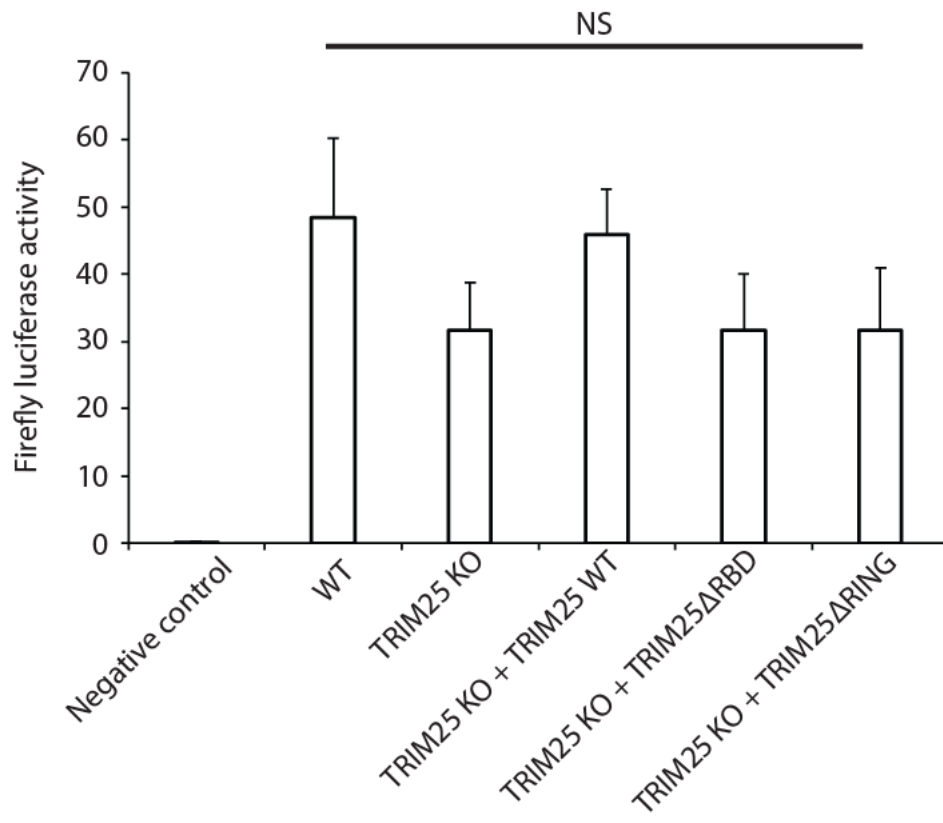
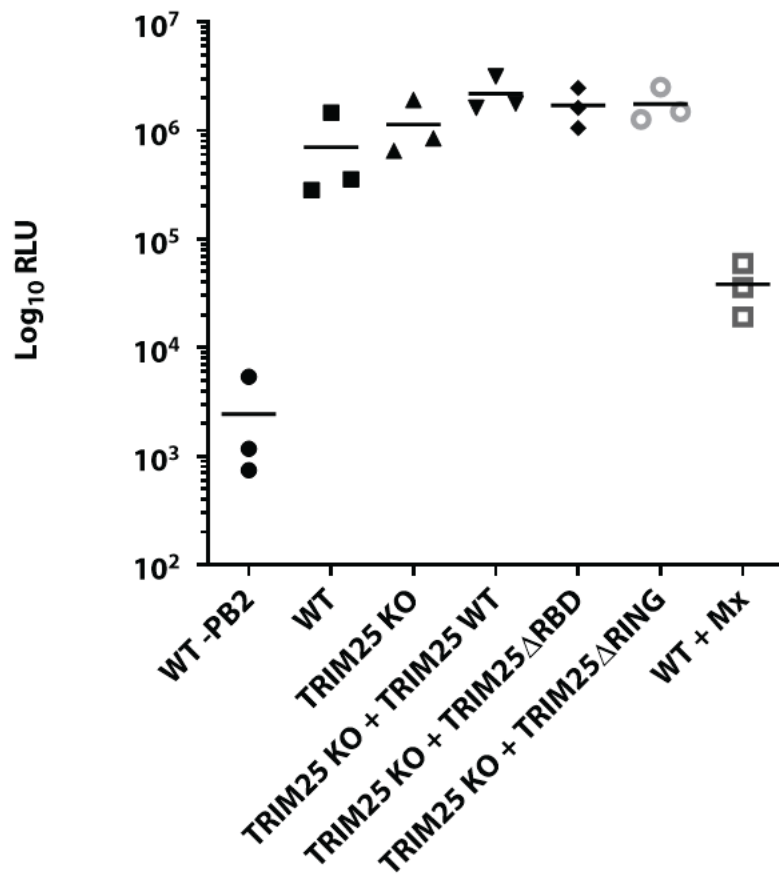
Previous work has shown that TRIM25 may inhibit transcription of IAV RNAs by direct binding to vRNPs in an RNA-dependent manner. To test whether this occurs in these cells, a viral minireplicon assay was performed. This involved transfecting plasmids encoding the



**Figure 28** – Activation of the RIG-I/IFN type I pathway is not attenuated in HEK293 or HeLa cells in response to 5'ppp-UA transfection upon loss of TRIM25. (A) HEK293 WT or TRIM25 KO cells and (B) HeLa WT and TRIM25 KO cells were transfected with the indicated amounts of 5'ppp-UA (see Chapter 1, FIG. 1A) along with firefly luciferase under the IFN $\beta$  promoter and a constitutively expressed renilla luciferase. Luciferase activity was assessed after 24 hours. Data represents means and standard deviations of three independent experiments. Statistical significance calculations were performed using Welch's t-test (\* signifies  $p < 0.05$ ).

components required for IAV to transcribe negative sense RNA (found in the IAV genome) into positive sense mRNA (required for translation by the host cell), along with a reporter to determine how efficient this transcription is. Plasmids encoding the components of the IAV RNA polymerase (PA, PB1, PB2) along with NP (required for formation of vRNPs) were transfected into HEK293 cell lines in addition to a firefly luciferase reporter. The firefly luciferase reporter is transcribed as a negative sense RNA with flanking regions resembling those found in IAV RNAs. It requires IAV RNA polymerase activity to be transcribed to positive sense mRNA so that it can be translated into luciferase protein by the host cell. As such any inhibition of IAV RNA polymerase activity by TRIM25 can be measured. A negative control was performed in exactly the same way but lacking the plasmid encoding NP (segment 5), preventing transcription by the IAV RNA polymerase. Cells were incubated for 48 hours before luciferase activity was measured (FIG. 29A). There were no significant differences in luciferase activity between cell lines. This experiment was repeated by our collaborator Nikki Smith in the lab of Paul Digard (University of Edinburgh), showing similar results (FIG. 29B). This experiment was also performed in the presence of the IAV inhibitor protein Mx as a positive control for inhibition of IAV. No differences were seen between cell lines, however there was significant inhibition of luciferase expression in the presence of Mx. These results imply that in this case TRIM25 is not inhibiting IAV RNA polymerase activity. However, as luciferase is not part of the IAV genome, it does not reflect exactly what is happening during IAV infection, therefore this experiment needs to be repeated using IAV genome segments as reporters.



**A****B**

**Figure 29** – *Activity of the IAV RNA polymerase is not inhibited in the presence of TRIM25 in HEK293 cells.* (A) Segments 1, 2, 3 and 5 of the IAV genome (encoding the components of the IAV RNA polymerase) were transfected into HEK293 cell lines along with a firefly luciferase reporter plasmid that requires the action of the IAV RNA polymerase for luciferase protein to be expressed. After 48 hours, luciferase activity was assessed. Negative control was performed in the absence of segment 5 of the IAV genome, preventing polymerase activity. Data represents means and standard deviations of three independent experiments. Statistical significance calculations were performed using one-way ANOVA followed by post-hoc Tukey HSD test. (B) This experiment was repeated by our collaborator Nikki Smith in the lab of Paul Digard, University of Edinburgh. Negative controls were performed in the absence of Segment 1, encoding PB2 and positive controls for IAV inhibition were performed in the presence of overexpressed Mx protein, an IAV inhibitor.

## Conclusions

Taken together, the data presented here suggest that TRIM25 can efficiently restrict IAV replication in the absence of fully functional NS1 but this restriction is not due to its role in RIG-I signalling or due to direct inhibition of IAV RNA polymerase. Restriction of IAV PR8 NS1 R38K41A is lost in HEK293 cells upon deletion of TRIM25 and this restriction is efficiently rescued by re-integration of TRIM25 WT, TRIM25 $\Delta$ RBD or TRIM25 $\Delta$ RING. Rescue by TRIM25 $\Delta$ RBD implies that TRIM25 RNA binding is not required for IAV restriction, however it is possible that TRIM25 $\Delta$ RBD can bind to vRNAs by a different mechanism than that by which it binds to endogenous RNAs. Rescue by TRIM25 $\Delta$ RING implies that TRIM25 ubiquitination activity, for example the ubiquitination of RIG-I, is not required for IAV restriction. It is possible that there is redundancy in this pathway, with other E3 ubiquitin ligases able to perform the role of TRIM25.

In both HEK293 and HeLa cells, but not MEF cells, deletion of TRIM25 did not lead to lower activation of the RIG-I pathway upon transfection of 5'ppp-RNAs. This further suggests that there may be redundancy in this pathway, with other E3 ubiquitin ligases able to fulfil the function of TRIM25 in humans but not in mice. Further work will be required to uncover the proteins performing this role but previous work has identified E3 ligases such as Riplet and MEX3C as candidates<sup>103,121</sup>. Further to this, recent work has shown that deletion of TRIM25 from HEK293 or MEF cells does not decrease IFN $\beta$  expression in response to 5'ppp-RNA while deletion of Riplet abrogates IFN $\beta$  expression<sup>123</sup>. Knocking down these proteins by RNAi or knocking them out with CRISPR in HEK293 TRIM25 KO cells could uncover whether having one of these proteins is essential for RIG-I signalling activation.

Viral minireplicon assays performed here have shown that TRIM25 does not block the transcription of firefly luciferase negative sense RNA by the IAV RNA polymerase. However, as viral minireplicon assays were only performed with a luciferase reporter, it would be worthwhile to repeat this experiment using the segments of the IAV genome as reporters (for example by measuring their transcription by qRT-PCR) to uncover any possible inhibition of transcription that is specific to any particular segment.

Recent work in the lab of our collaborator Alfredo Castello (University of Oxford) using the HEK293 WT and TRIM25 KO cells generated in this project has shown that Sindbis virus (SINV) replication is restricted in the presence of TRIM25<sup>239</sup>. Cells were infected with mCherry-tagged SINV and fluorescence was measured over the course of 24 hours. More mCherry was produced in HEK293 TRIM25 KO than WT cells, indicating faster growth of SINV in the absence of TRIM25. It will be interesting to determine if this can also be rescued by re-integration of TRIM25 WT, TRIM25 $\Delta$ RBD or TRIM25 $\Delta$ RING to see if this is confined to IAV or if it can apply more broadly to RNA viruses.

## Discussion

### *The PRY/SPRY domain is the main determinant of TRIM25 RNA binding*

The data presented here show that the PRY/SPRY domain of TRIM25, specifically amino acids 470-508 of human TRIM25, is required for binding to RNA. TRIM25 $\Delta$ RBD, in which these amino acids were deleted, was unable to bind to pre-let-7a-1 in an RNA pulldown or EMSA and exhibited loss of binding to target mRNAs and miRNAs in RIP experiments. Interestingly, TRIM25 $\Delta$ RBD was capable of associating with TRIM25 WT, suggesting that dimerization with two intact PRY/SPRY domains is necessary for RNA binding. Aligning amino acids 470-508 with the crystal structure of the PRY/SPRY domain from mouse Trim25 (the composition of which is highly similar to humans) shows that this region comprises  $\beta$  sheet 1, 2 and 3 as well as loops 2, 3 and 4 of the PRY/SPRY domain<sup>195</sup>.

The requirement for the PRY/SPRY domain was confirmed by a recent study by Sanchez *et al.* that found a TRIM25 construct consisting of only the RING, B-box and CCD did not co-purify with nucleic acids, while full-length TRIM25 did<sup>240</sup>. These constructs contradict the earlier finding by Kwon *et al.* that TRIM25 without the PRY/SPRY domain precipitated with RNA<sup>215</sup>. It is worth noting that the latter construct did include the CCD-PRY/SPRY 'linker', while the former did not. Sanchez *et al.* also identified a motif containing 7 lysine residues (amino acids 381-392, 5'-KKVSKEEKSKK-3', termed 7K) in the linker region that seemingly contributed to RNA binding<sup>240</sup>. Mutating all the lysines in 7K led to a significant decrease, although not a complete abolition, of RNA binding in EMSA experiments. A CCD-7K construct was not sufficient for RNA binding whereas a CCD-SPRY construct was (with an even higher affinity for RNA than full-length TRIM25) underlining the requirement for the PRY/SPRY domain<sup>240</sup>. In contrast with our RNA pulldown experiments, PRY/SPRY alone was found to be sufficient for RNA binding in these EMSA experiments, however the binding

affinity was reduced around 20-30-fold (similarly to the construct with 7K mutated) compared to the CCD-SPRY construct<sup>240</sup>.

Taken together, these results indicate that the PRY/SPRY domain is essential for TRIM25's RNA binding and that binding is enhanced by the 7K motif in the CCD-PRY/SPRY linker and by CCD-mediated dimerization. It remains unclear exactly which amino acids are involved in direct contact with the RNA. Lysine 469 and glutamate 483 (aspartate in mouse) are positively charged and well conserved between vertebrate species so would make intriguing candidates for amino acids that contribute to RNA binding. It may, however, be difficult to elucidate the contribution of individual residues to TRIM25 RNA binding if multiple amino acids make contacts with RNA as deletion or mutation of these residues may not abolish or significantly weaken RNA binding. It is also unclear if the 7K motif makes contacts with RNA or if it enhances RNA binding by affecting the positioning or conformation of the PRY/SPRY domain. In addition, it is possible that deletion of amino acids 470-508 as in TRIM25 $\Delta$ RBD has implications on the overall structure of the PRY/SPRY domain and if this potential change in structure could be what is causing the loss of RNA binding. Likewise, the mechanism of the contribution of TRIM25 dimerization to RNA binding is also unknown. It is possible that both PRY/SPRY domains in a dimer contact the RNA in a 'pincer'-type manner or that the PRY/SPRY domains themselves dimerise and this is required for RNA binding, for example by causing a conformational change. In order to fully elucidate the mechanism of TRIM25 RNA binding, the best method would be to perform x-ray crystallography on TRIM25 or a CCD-PRY/SPRY construct bound to RNA. This would allow visualisation of the amino acids in contact with RNA and comparison with unbound TRIM25 could uncover any structural or conformational changes that occur upon RNA binding. Alternatively, the mutagenesis of one or multiple amino acids in the PRY/SPRY domain that may contribute to RNA binding would help to narrow down exactly which

amino acids are contacting RNA and would give further insights into the mechanism of TRIM25 RNA binding.

### *Other PRY/SPRY containing proteins could bind to RNA*

The PRY/SPRY domain is found in many TRIM family proteins as well as some other proteins that are not members of the TRIM family with many more containing a SPRY domain alone preceded by a domain with a structure similar to that of the PRY domain<sup>227,241</sup>. The PRY/SPRY is by far the most common C-terminal domain of TRIM family proteins, with 39 TRIMs and 6 TRIM-like proteins having this domain<sup>157,167</sup>. These include TRIM5 $\alpha$ , involved in restriction of HIV, TRIM4, ubiquitination of the RIG-I 2CARD and other TRIMs involved in innate immunity including TRIM11 and TRIM22. In addition to this, non-TRIM family proteins that contain a PRY/SPRY include Riplet which is essential for RIG-I-mediated innate immune signalling<sup>102</sup>. It is possible that the PRY/SPRY domains of these proteins also contribute to RNA binding. The overall structure of PRY/SPRY domains is very well conserved between proteins for which crystal structures are available although the sequences are not as well conserved<sup>195</sup>. Loop 3 of the TRIM25 PRY/SPRY is part of the 470-508 region and some of the residues found to contribute to RNA binding by Sanchez *et al.* also cluster in this area<sup>242</sup>. This loop corresponds to a region of PRY/SPRY domains that is particularly variable in sequence, indicating that RNA binding may not be a general characteristic of PRY/SPRY domains although this variation could also be involved in determining RNA binding specificity in different PRY/SPRY-containing proteins. Further studies into this would potentially open up a new family of RNA-binding proteins, along with an array of associated functions. This is particularly important due to the roles of PRY/SPRY-containing TRIM proteins in innate immunity. To begin to address this, work

done in this lab replaced the identified region required for RNA binding in TRIM25 (amino acids 470-508) with the equivalent sequences from other selected TRIM proteins<sup>219</sup>. When the 470-508 region was replaced with the equivalent from TRIM21 or TRIM27 the construct maintained efficient binding to pre-let-7a-1 in an RNA pulldown, however when replaced with sequences from TRIM65 and TRIM5 $\alpha$  binding was reduced compared to WT TRIM25. Replacement of 470-508 with a random sequence of amino acids of equal length resulted in complete loss of pre-let-7a-1 binding, showing the specificity of this interaction<sup>219</sup>. Further work still needs to be done to identify PRY/SPRY containing proteins that bind to RNA and this data suggests that TRIM21 and TRIM27 would be good candidates.

### *TRIM25 requires RNA binding for its E3 ubiquitin ligase activity*

Our data suggests that TRIM25 requires RNA binding to be able to auto-ubiquitinate and ubiquitinate ZAP, one of its targets. This was shown by the inability of TRIM25 $\Delta$ RBD to ubiquitinate itself or ZAP in an *in vitro* ubiquitination experiment as well as the loss of ubiquitination activity of TRIM25 upon the addition of RNase in a similar experiment. These results are similar to those obtained by Sanchez *et al.* who found that TRIM25-mediated ubiquitination of the RIG-I 2CARD was severely reduced in the TRIM25 7K mutant compared to TRIM25 WT<sup>240</sup>. Overexpression of GST-2CARD in HEK293T cells resulted in robust ubiquitination of the 2CARD and induction of IFN $\beta$  promoter activity in cells expressing WT TRIM25 but not in cells expressing the 7K mutant<sup>240</sup>. These data support the hypothesis that TRIM25 requires RNA binding to ubiquitinate its target proteins and further suggest that this is a general property of TRIM25 activity that is not restricted to a single target protein. Another recent report has also suggested that TRIM25 RNA binding is important for its ubiquitination of RIG-I 2 CARD. TRIM25 binding to the lncRNA Lnczc3h7a was shown to



enhance its interaction with and ubiquitination of RIG-I upon VSV infection and the presence of Lnczc3h7a increased the type I IFN response to RNA virus infection<sup>243</sup>. In addition to this, both RIG-I and TRIM25 co-purified with Lnczc3h7a from cells that had been infected with VSV and Lnczc3h7a interacted with the RIG-I helicase domain and TRIM25 in RNA pulldowns. The authors of this study proposed a model whereby Lnczc3h7a acts as a scaffold, binding to both RIG-I and TRIM25 in order to bring them closer together. However, it is unlikely that this would be sufficient to explain the differences in type I IFN induction seen due to the apparent redundancy of TRIM25 in RIG-I signalling with other E3 ubiquitin ligases such as Riplet, TRIM4 and MEX3C<sup>125</sup>. It is possible, for example, that the action of Lnczc3h7a is not restricted to TRIM25 and it promotes the association of RIG-I with the other E3 ligases as well.

The mechanism by which TRIM25 RNA binding facilitates its ubiquitination activity is unknown. It is known that the RING domain of TRIM25 is active as a dimer and it is likely that this requires higher order oligomerisation of TRIM25 dimers. It is therefore possible that RNA binding is important for this higher order organisation, for example by clustering the PRY/SPRY domains from separate dimers together to facilitate formation of a 'tetramer'-like structure as described in FIG. 4. This is rendered less likely by our data showing that purified His-TRIM25 $\Delta$ RBD and His-TRIM25 WT both form tetramers *in vitro*, although it remains possible that the proteins behave differently *in vivo*. It is also possible that binding to RNA causes TRIM25 to undergo a conformational change that allows ubiquitin ligase activity. Again, the ideal method for determining the effect of RNA binding would be x-ray crystallography although crystallising full-length TRIM25 (to determine any effect on the RING domain) may prove difficult.

## *TRIM25 binding to mRNAs at steady state does not have a general effect on RNA or protein stability*

According to CLIPseq experiments performed in the lab, TRIM25 binds to a large number of mRNAs in HeLa cells and can bind in the coding sequence and both the 5' and 3' untranslated regions (UTRs)<sup>219</sup>. However, as previously noted, the CLIPseq experiments performed may be overestimating the number of RNAs that TRIM25 interacts with due to the confounding effects of other proteins that may co-precipitate with TRIM25. RNAseq of WT and TRIM25 KO HeLa cells showed that few of the mRNAs identified as associating with TRIM25 were differentially expressed upon loss of TRIM25. This would suggest that TRIM25 is not part of a general mechanism governing the stability of mRNAs in steady state cells. However, this does not discount the possibility that TRIM25 may affect stability of RNAs in response to certain stimuli. An example of this can be found in breast cancer cell lines, where knockdown of TRIM25 by RNAi led to changes in the levels of many RNAs that associated with TRIM25 in a RIPseq experiment<sup>204</sup>. This study also found that TRIM25 could act at the transcriptional level and that elevation of TRIM25 levels was strongly associated with tumour metastasis and poor prognosis, exemplifying the potential importance of TRIM25 in cancers<sup>204</sup>. It would be interesting to identify TRIM25 RNA binding partners and any post-transcriptional regulation it may exert in other cancer types in which it has been shown to be associated with tumour growth or metastasis such as endometrial and gastric cancers<sup>209,244</sup>. As RNA binding seems to be tied to TRIM25's catalytic activity, it is plausible that the primary function of TRIM25 binding to RNAs is to use them as a scaffold to aid interaction with its target proteins, leading to their ubiquitination and either degradation or changes in activity.

Similarly to its effects on RNA levels, loss of TRIM25 in HeLa cells seemingly has very little effect on protein levels as seen by SILAC-MS. Again, this data only provides a snapshot of

steady state cells and as such does not take into account any stimuli that could change TRIM25 activity. It has already been established that TRIM25 is an integral component of the oestrogen response and that it ubiquitinates ER $\alpha$  in the presence of oestrogen<sup>199</sup>. This underlines how certain stimuli can affect protein function and it is possible that the functions that TRIM25 may have in regulating protein levels may not be detectable in steady state cells. It is also likely that TRIM25 can exert different effects on protein and RNA levels depending on cell types as there may be co-factors or inhibitors integral to TRIM25 function that are expressed at different levels in different cells.

### *TRIM25 is not required for RIG-I signalling in HEK293 cells*

The data obtained in this project shows that TRIM25 is not necessary for RIG-I signalling in HEK293 cells as upon TRIM25 deletion there is no defect in RIG-I signalling in response to transfection of a 5'ppp-RNA, with similar results seen in HeLa TRIM25 KO cells. This goes against previous work that has posited that TRIM25 is essential for efficient RIG-I mediated innate immune signalling<sup>113,115,145,245</sup>. However, some recent studies have suggested that Riplet, not TRIM25, is the essential E3 ubiquitin ligase for RIG-I signalling<sup>122,123,125</sup>. In particular, recent work by Cadena *et al.* has shown that deletion of TRIM25 from HEK293T and MEF cells results in an increase, not a reduction in RIG-I activation in response to 5'ppp-RNA. In contrast, deletion of Riplet from the same cell line results in complete abolition of RIG-I signalling, to the same level as deletion of RIG-I itself<sup>123</sup>. The same was found to be true for expression of IFN $\beta$  mRNA in response to infection with Sendai virus, with deletion of TRIM25 in this case resulting in a significant increase in IFN $\beta$  expression<sup>123</sup>. This supports our conclusion that TRIM25 is dispensable for RIG-I signalling in HEK293 cells and further shows that this is not limited to our cultured cells. Interestingly this study also found that

TRIM25 was not capable of ubiquitinating RIG-I *in vitro*, even in the presence of 5'ppp-dsRNA. This goes against previous work which has shown TRIM25 to be capable of ubiquitinating the RIG-I 2CARD *in vitro*, although these studies used purified 2CARD and not full-length RIG-I<sup>117,240</sup>. It is possible that TRIM25 is not capable of ubiquitinating full-length RIG-I, although it is not certain as there may be other factors in the cell that are required for this activity that are not present *in vitro*. It was also shown that deletion of TRIM25 did result in lower RIG-I signalling activity in response to transfection of GST-tagged 2CARD alone, suggesting that there may be different mechanisms of activation for isolated 2CARD and 2CARD in the context of full-length RIG-I. This study also further explored the interaction between Riplet and RIG-I. It found that Riplet only binds to RIG-I in the presence of RNA and that it can bind to full-length RIG-I or a mutant in which the 2CARD has been deleted but not to the isolated 2CARD<sup>123</sup>. Interestingly, the Riplet PRY/SPRY domain was required for its interaction with RIG-I and Riplet dimerization was also required for this interaction. This bears striking similarities to the requirements for TRIM25 binding to RNA, which also requires dimerization and the PRY/SPRY domain. Due to the similar domain structures of TRIM25 and Riplet, and the RNA-dependence of the Riplet-RIG-I interaction, this raises the question of whether Riplet is binding directly to RNA in this instance and, if it is, whether this RNA binding is necessary for the interaction with RIG-I. It was also demonstrated that Riplet was capable of 'cross-bridging' dsRNA-RIG-I filaments, resulting in the formation of aggregates that were visible by electron microscopy and this activity was independent of the RING domain of Riplet and the 2CARD of RIG-I<sup>123</sup>. Finally it was shown that this cross-bridging activity was sufficient to induce MAVS oligomerisation and RIG-I signalling in the absence of ubiquitination of RIG-I. This is likely because the clustering of RIG-I induced by Riplet cross-bridging allows the formation of RIG-I 2CARD tetramers. However, Riplet $\Delta$ RING was not as efficient at rescuing RIG-I signalling in Riplet KO HEK293T

cells, suggesting that ubiquitination is required for optimal 2CARD tetramer formation and RIG-I signalling<sup>123</sup>.

On balance, taking into account our data and that of others, it is likely that TRIM25 is dispensable for RIG-I activation in human cells while Riplet is essential. It is, however, still possible that requirements for different E3 ligases vary between different cell and tissue types as expression levels may be different and there could be other differences in the environments of different cells. As such it would be prudent to perform a large-scale screen of Riplet and TRIM25 (as well as TRIM4 and MEX3C) knock outs of many different cell types. The idea that TRIM25 was the key E3 ligase for RIG-I activation was mainly based off experiments in which the RIG-I 2CARD was overexpressed in cells or *in vitro* experiments using the 2CARD. The experiments performed with full length RIG-I exemplify the fact that full-length proteins may function differently to their domains in isolation and this can lead to confusion about how biological processes work.

### *TRIM25 and direct restriction of IAV*

Previous work by Meyerson *et al.* showed that TRIM25 can associate with IAV vRNPs in an RNA-dependent manner and suggested that this blocked the initiation of transcription by the IAV RNA polymerase<sup>220</sup>. Similarly to this work, our data showed that deletion of TRIM25 in HEK293 cells resulted in higher replication of a mutant IAV strain with NS1 that cannot inhibit TRIM25 (PR8 NS1 R38K41A). In addition, we found that restriction of PR8 NS1 R38K41A was rescued by stable expression of TRIM25 WT, TRIM25 $\Delta$ RBD or TRIM25 $\Delta$ RING. However, unlike Meyerson *et al.* we found that a minireplicon assay using the IAV RNA polymerase and a luciferase reporter resulted in no significant differences in luciferase expression between WT and TRIM25 KO cells. This would suggest that TRIM25 was not

inhibiting IAV RNA polymerase-mediated transcription in our cells, in contrast to the Meyerson *et al.* study that found that overexpressing human or gibbon TRIM25 in HEK293T cells restricted luciferase expression. It is possible that the overexpression of TRIM25 beyond endogenous levels in the Meyerson *et al.* study is enough to inhibit transcription but the endogenous or near-endogenous levels used in our experiments are not sufficient. It is likely that there are more copies of the RNA polymerase proteins and the negative sense RNA than would be found in the initial stages of infection of a cell with IAV. This could explain the discrepancy between the  $\Delta$ RING-independent restriction of IAV by TRIM25 and the seeming lack of inhibition of IAV transcription in our experiments.

Preliminary data from CLIPseq experiments conducted in our lab on cells infected with either IAV or Sindbis virus have indicated that TRIM25 $\Delta$ RBD may be capable of binding to viral RNAs upon infection, as well as to endogenous snoRNAs. Interestingly, TRIM25 $\Delta$ RBD seems to bind only some RNAs that are bound by WT TRIM25 while losing binding to others. This suggests the possibility that TRIM25 $\Delta$ RBD does not lose its ability to bind to all RNAs and of a second mechanism of TRIM25 binding to viral RNAs. It is possible, for example, that the 7K motif in the CCD-PRY-SPRY linker region identified by Sanchez *et al.* is sufficient for binding to some RNAs but not to others. It is also possible, however, that the CLIP is identifying RNAs that are not bound directly to TRIM25 $\Delta$ RBD and are interacting via the interaction of TRIM25 $\Delta$ RBD with other proteins. Further experiments are needed to determine the mechanisms underlying this. Further CLIPseq experiments and optimisation of these experiments are required to ensure that these results are repeatable and physiologically relevant. If this is achieved, comparing the sequences of RNAs bound or not bound by TRIM25 $\Delta$ RBD could uncover RNA motifs that can be bound in the absence of the 470-508 region and these could be used as the basis for further experiments to uncover how TRIM25 $\Delta$ RBD is able to bind to these RNAs. In addition, mutation of the viral RNAs that

TRIM25 binds to could help elucidate whether TRIM25 binding to these RNAs is important for TRIM25's restriction of viral replication.

### *Concluding Remarks*

This project aimed to elucidate the mechanism and functions of TRIM25 RNA binding. We have uncovered a region of the TRIM25 PRY/SPRY domain that is important for RNA binding and showed that RNA binding is necessary for TRIM25's ubiquitination activity. In addition to this we have showed that TRIM25 does not seem to play a role in RNA stability in unperturbed cells and is not necessary for activation of the RIG-I pathway in innate immunity despite being required for efficient restriction of IAV infection.

As TRIM25 is part of the larger TRIM family of proteins, many of which also contain a PRY/SPRY domain, our results raise the question of whether other PRY/SPRY-containing TRIMs can bind to RNA and whether this is important for their functions. Many TRIMs function in innate immunity and carcinogenesis and as such the new lines of research opened up by this project could aid understanding of these important and complex processes, possibly leading to the development of novel therapeutics in the future. For example, many vaccines contain adjuvants to help promote a stronger immune response. For example, an oil-in-water emulsion of squalene oil (MF59) is commonly used as an adjuvant in Influenza vaccines and works by inducing expression of pro-inflammatory cytokines<sup>246</sup>. It is conceivable that an adjuvant could be developed that would help prevent Influenza virus inhibition of innate immunity in vaccines using live attenuated Influenza strains, leading to a stronger innate immune response and a greater priming of the adaptive immune system.





## References

1. Johnson, N. P. A. S. & Mueller, J. Updating the Accounts: Global Mortality of the 1918-1920 'Spanish' Influenza Pandemic. *Bull. Hist. Med.* **76**, 105–115 (2002).
2. Gayle, H. D. & Hill, G. L. Global Impact of Human Immunodeficiency Virus and AIDS. *Clin. Microbiol. Rev.* **14**, 327–335 (2001).
3. Kaner, J. & Schaack, S. Understanding Ebola: the 2014 epidemic. *Global. Health* **12**, (2016).
4. Baltimore, D. Expression of animal virus genomes. *Bacteriol. Rev.* **35**, 235–41 (1971).
5. Simmonds, P. *et al.* Consensus statement: Virus taxonomy in the age of metagenomics. *Nat. Rev. Microbiol.* **15**, 161–168 (2017).
6. Detjen, B. M., Angelo, C. S. T., Katze, M. G. & Krug, R. M. The Three Influenza Virus Polymerase (P) Proteins Not Associated with Viral Nucleocapsids in the Infected Cell Are in the Form of a Complex. *J. Virol.* **61**, 16–22 (1987).
7. Portela, A. & Digard, P. The influenza virus nucleoprotein: a multifunctional RNA-binding protein pivotal to virus replication. *J. Gen. Virol.* **83**, 723–734 (2002).
8. Skehel, J. J. & Wiley, D. C. Receptor Binding and Membrane Fusion in Virus Entry: The Influenza Hemagglutinin. *Annu. Rev. Biochem.* **69**, 531–569 (2000).
9. Shtyrya, Y. A., Mochalova, L. V & Bovin, N. V. Influenza Virus Neuraminidase: Structure and Function. *Acta Naturae* **2**, 26–32 (2009).
10. Martin, K. & Helenius, A. Nuclear Transport of Influenza Virus Ribonucleoproteins : The Viral Matrix Protein (M1) Promotes Export and Inhibits Import. *Cell* **67**, 117–130 (1991).
11. Pinto, L. H. & Lamb, R. A. The M2 Proton Channels of Influenza A and B Viruses. *J. Biol. Chem.* **281**, 8997–9000 (2006).
12. Chien, C. *et al.* A novel RNA-binding motif in influenza A virus non-structural protein 1. *Nat. Struct. Mol. Biol.* **4**, 891–895 (1997).
13. Neill, R. E. O., Talon, J. & Palese, P. The influenza virus NEP (NS2 protein) mediates the nuclear export of viral ribonucleoproteins. *EMBO J.* **17**, 288–296 (1998).
14. Boulo, S., Akarsu, H., Ruigrok, R. W. H. & Baudin, F. Nuclear traffic of influenza virus proteins and ribonucleoprotein complexes. *Virus Res.* **124**, 12–21 (2007).
15. Bouloy, M., Plotch, S. J. & Krug, R. M. Globin mRNAs are primers for the transcription of influenza viral RNA in vitro. *Proc. Natl. Acad. Sci. U. S. A.* **75**, 4886–4890 (1978).
16. Krug, R. M. & Broni, B. A. Are the 5' Ends of Influenza Viral mRNAs Synthesized in Vivo Donated by Host mRNAs? *Cell* **18**, 329–334 (1979).
17. Shapiro, G. I., Gurney, T. & Krug, R. M. Influenza Virus Gene Expression: Control Mechanisms at Early and Late Times of Infection and Nuclear-Cytoplasmic Transport of Virus-Specific RNAs. *J. Virol.* **61**, 764–773 (1987).
18. Fujii, Y., Goto, H., Watanabe, T., Yoshida, T. & Kawaoka, Y. Selective incorporation of influenza virus RNA segments into virions. *Proc. Natl. Acad. Sci.* **100**, 2002–2007

(2003).

19. Nayak, D. P., Balogun, R. A., Yamada, H., Zhou, Z. H. & Barman, S. Influenza virus morphogenesis and budding. *Virus Res.* **143**, 147–161 (2009).
20. Palese, P., Tobita, K. & Ueda, M. Characterization of Temperature Sensitive Influenza Virus Mutants Defective in Neuraminidase. *Virology* 397–410 (1974).
21. Krammer, F. *et al.* Influenza. *Nat. Rev. Dis. Prim.* **4**, (2018).
22. Iuliano, A. D. *et al.* Estimates of global seasonal influenza-associated respiratory mortality: a modelling study. *Lancet* **391**, 1285–1300 (2018).
23. World Health Organisation. World Health Organisation. Influenza (seasonal) factsheet. (2018). Available at: [https://www.who.int/en/news-room/factsheets/detail/influenza-\(seasonal\)](https://www.who.int/en/news-room/factsheets/detail/influenza-(seasonal)).
24. Webster, R. G., Bean, W. J., Gorman, O. T. & Chambers, T. M. Evolution and Ecology of Influenza A Viruses. *Microbiol. Rev.* **56**, 152–179 (1992).
25. Smith, G. J. D. *et al.* Origins and evolutionary genomics of the 2009 swine-origin H1N1 influenza A epidemic. *Nature* **459**, 1122–1125 (2009).
26. Sellers, S. A., Hagan, R. S., Hayden, F. G. & Fischer, W. A. The hidden burden of influenza: A review of the extra-pulmonary complications of influenza infection. *Influenza Other Respi. Viruses* **11**, 372–393 (2017).
27. Krammer, F. & Palese, P. Advances in the development of influenza virus vaccines. *Nat. Rev. Drug Discov.* **14**, 167–182 (2015).
28. Centers for Disease Control and Prevention. Influenza Antiviral Medications: Summary for Clinicians. (2018). Available at: <https://www.cdc.gov/flu/professionals/antivirals/summary-clinicians.htm>.
29. Deyde, V. M. *et al.* Surveillance of Resistance to Adamantanes among Influenza A (H3N2) and A (H1N1) Viruses Isolated Worldwide. *J. Infect. Dis.* **196**, 249–257 (2007).
30. Chaplin, D. D. Overview of the immune response. *J. Allergy Clin. Immunol.* **125**, S3–S23 (2010).
31. Schroeder Jr, H. W. & Cavacini, L. Structure and Function of Immunoglobulins. *J. Allergy Clin. Immunol.* **125**, (2010).
32. Davis, M. M. & Bjorkmant, P. J. T-cell antigen receptor genes and T-cell recognition. *Nature* **334**, 395–402 (1988).
33. Bassing, C. H., Swat, W. & Alt, F. W. The Mechanism and Regulation of Chromosomal V(D)J Recombination. *Cell* **109**, 45–55 (2002).
34. Sun, J. C., Ugolini, S. & Vivier, E. Immunological memory within the innate immune system. **33**, 1295–1303 (2014).
35. Mogensen, T. H. Pathogen Recognition and Inflammatory Signaling in Innate Immune Defenses. *Clin. Microbiol. Rev.* **22**, 240–273 (2009).
36. Mogensen, T. H. & Paludan, S. R. Reading the viral signature by Toll-like receptors and other pattern recognition receptors. *J. Mol. Med.* **83**, 180–192 (2005).

37. Yoshimura, A., Lien, E., Ingalls, R. R., Dziarski, R. & Golenbock, D. Cutting Edge: Recognition of Gram-Positive Bacterial Cell Wall Components by the Innate Immune System Occurs Via Toll-Like Receptor 2. *J. Imm* **163**, 1–5 (1999).
38. Schwandner, R., Dziarski, R., Wesche, H., Rothe, M. & Kirschning, C. J. Peptidoglycan- and Lipoteichoic Acid-induced Cell Activation Is Mediated by Toll-like Receptor 2. *J. Biol. Chemistry* **274**, 17406–17409 (1999).
39. Hemmi, H. *et al.* A Toll-like receptor recognizes bacterial DNA. *Nature* **408**, 740–745 (2000).
40. Alexander, C. & Rietschel, E. T. Bacterial lipopolysaccharides and innate immunity. *J. Endotoxin Res.* **7**, (2001).
41. Hayashi, F. *et al.* The innate immune response to bacterial flagellin is mediated by Toll-like receptor 5. *Nature* **410**, 1099–1103 (2001).
42. Jouault, T. *et al.* *Candida albicans* Phospholipomannan Is Sensed through Toll-Like Receptors. *J. Infect. Dis.* **188**, 165–172 (2003).
43. Lebron, F., Vassallo, R., Puri, V. & Limper, A. H. *Pneumocystis carinii* Cell Wall  $\beta$ -Glucans Initiate Macrophage Inflammatory Responses through NF- $\kappa$ B Activation. *J. Biol. Chem.* **278**, 25001–25008 (2003).
44. Kawasaki, T. & Kawai, T. Toll-like receptor signaling pathways. *Front. Immunol.* **5**, (2014).
45. Liu, L. *et al.* Structural Basis of Toll-Like Receptor 3 Signaling with Double-Stranded RNA. *Science (80-. )*. **320**, 379–382 (2008).
46. Heil, F. *et al.* Species-Specific Recognition of Single-Stranded RNA via Toll-like Receptor 7 and 8. *Science (80-. )*. **303**, 1526–1530 (2004).
47. Takeshita, F. *et al.* Cutting Edge: Role of Toll-Like Receptor 9 in CpG DNA-Induced Activation of Human Cells. *J. Immunol.* **167**, 3555–3558 (2001).
48. Regan, T. *et al.* Identification of TLR10 as a Key Mediator of the Inflammatory Response to *Listeria monocytogenes* in Intestinal Epithelial Cells and Macrophages. *J. Immunol.* **191**, 6084–6092 (2013).
49. Lee, S. M. Y. *et al.* Toll-like receptor 10 is involved in induction of innate immune responses to influenza virus infection. *Proc. Natl. Acad. Sci.* **111**, 3793–3798 (2014).
50. Hoving, J. C., Wilson, G. J., Brown, G. D., Town, C. & Africa, S. Signalling C-Type lectin receptors, microbial recognition and immunity. *Cell. Microbiol.* **16**, 185–194 (2014).
51. Hardison, S. E. & Brown, G. D. C-type Lectin Receptors Orchestrate Anti-Fungal Immunity. *Nat. Immunol.* **13**, 817–822 (2013).
52. Girardin, S. E. *et al.* Nod1 Detects a Unique Muropeptide from Gram-Negative Bacterial Peptidoglycan. *Science (80-. )*. **300**, 1584–1588 (2003).
53. Girardin, S. E., Boneca, I. G., Thomas, G., Philpott, D. J. & Sansonetti, P. J. Nod2 Is a General Sensor of Peptidoglycan through Muramyl Dipeptide (MDP) Detection. *J. Biol. Chemistry* **278**, 8869–8873 (2003).

54. Satoh, T. *et al.* LGP2 is a positive regulator of RIG-I – and MDA5-mediated antiviral responses. *Proc. Natl. Acad. Sci.* **107**, 1512–1517 (2009).
55. Rothenfusser, S. *et al.* The RNA Helicase LGP2 Inhibits Sensing of Viral Replication by Retinoic Acid-Inducible Gene-I. *J. Immunol.* **175**, 5260–5268 (2005).
56. Hardy, M. P., Owczarek, C. M., Jermiin, L. S., Ejdebäck, M. & Hertzog, P. J. Characterization of the type I interferon locus and identification of novel genes. *Genomics* **84**, 331–345 (2004).
57. Novick, D., Cohen, B. & Rubinstein, M. The Human Interferon  $\alpha/\beta$  Receptor : Characterization and Molecular Cloning. *Cell* **77**, 391–400 (1994).
58. Lim, J., Xiong, J., Carrasco, N. & Langer, J. A. Intrinsic ligand binding properties of the human and bovine  $\alpha$ -interferon receptors. *FEBS Lett.* **350**, 281–286 (1994).
59. Lavoie, T. B. *et al.* Binding and activity of all human alpha interferon subtypes. *Cytokine* **56**, 282–289 (2011).
60. Cohen, B., Novick, D., Barak, S. & Rubinstein, M. Ligand-Induced Association of the Type I Interferon Receptor Components. *Mol. Cell. Biol.* **15**, 4208–4214 (1995).
61. Stark, G. R. & Darnell, J. E. The JAK-STAT Pathway at Twenty. *Immunity* **36**, 503–514 (2012).
62. Rusinova, I. *et al.* INTERFEROME v2.0: an updated database of annotated interferon-regulated genes. *Nucleic Acids Res.* **41**, 1040–1046 (2013).
63. Silverman, R. H. Viral Encounters with 2',5'-Oligoadenylate Synthetase and RNase L during the Interferon Antiviral Response □. *J. Virol.* **81**, 12720–12729 (2007).
64. Dauber, B. & Wolff, T. Activation of the Antiviral Kinase PKR and Viral Countermeasures. *Viruses* **1**, 523–544 (2009).
65. Fensterl, V. & Sen, G. C. Interferon-Induced Ifit Proteins: Their Role in Viral Pathogenesis. *J. Virol.* **89**, 2462–2468 (2015).
66. Bishop, K. N. *et al.* Cytidine Deamination of Retroviral DNA by Diverse APOBEC Proteins. *Curr. Biol.* **14**, 1392–1396 (2004).
67. Verhelst, J., Parthoens, E., Schepens, B., Fiers, W. & Saelens, X. Interferon-Inducible Protein Mx1 Inhibits Influenza Virus by Interfering with Functional Viral Ribonucleoprotein Complex. *J. Virol.* **86**, 13445–13455 (2012).
68. Le Bon, A. *et al.* Cross-priming of CD8 + T cells stimulated by virus-induced type I interferon. *Nat. Immunol.* **4**, 1009–1015 (2003).
69. Montoya, M. *et al.* Type I interferons produced by dendritic cells promote their phenotypic and functional activation. *Blood* **99**, 3263–3272 (2002).
70. Liu, T., Zhang, L., Joo, D. & Sun, S. NF- $\kappa$ B signaling in inflammation. *Signal Transduct. Target. Ther.* **2**, (2017).
71. Oeckinghaus, A. & Ghosh, S. The NF- $\kappa$ B Family of Transcription Factors and Its Regulation. *Cold Spring Harb. Perspect. Biol.* **1**, (2009).
72. Yoneyama, M., Onomoto, K., Jogi, M., Akaboshi, T. & Fujita, T. Viral RNA detection

- by RIG-I-like receptors. *Curr. Opin. Immunol.* **32**, 48–53 (2015).
73. Yoneyama, M. *et al.* The RNA helicase RIG-I has an essential function in double-stranded RNA-induced innate antiviral responses. *Nat. Immunol.* **5**, 730–737 (2004).
  74. Goubau, D. *et al.* Antiviral immunity via RIG-I-mediated recognition of RNA bearing 5'-diphosphates. *Nature* **514**, 372–375 (2014).
  75. Yoneyama, M. *et al.* Shared and Unique Functions of the DExD/H-Box Helicases RIG-I, MDA5, and LGP2 in Antiviral Innate Immunity. *J. Immunol.* **175**, 2851–2858 (2005).
  76. Hornung, V. *et al.* 5'-Triphosphate RNA is the ligand for RIG-I. *Science* **314**, 994–997 (2006).
  77. Kato, H. *et al.* Length-dependent recognition of double-stranded ribonucleic acids by retinoic acid-inducible gene-I and melanoma differentiation-associated gene 5. *J. Exp. Med.* **205**, 1601–1610 (2008).
  78. Venkataraman, T. *et al.* Loss of DExD/H Box RNA Helicase LGP2 Manifests Disparate Antiviral Responses. *J. Immunol.* **178**, 6444–6455 (2007).
  79. Bruns, A. M., Leser, G. P., Lamb, R. A. & Horvath, C. M. The Innate Immune Sensor LGP2 Activates Antiviral Signaling by Regulating MDA5-RNA Interaction and Filament Assembly. *Mol. Cell* **55**, 771–781 (2014).
  80. Schlee, M. Master sensors of pathogenic RNA – RIG-I like receptors. *Immunobiology* **218**, 1322–1335 (2013).
  81. Andrejeva, J. *et al.* The V proteins of paramyxoviruses bind the IFN-inducible RNA helicase, mda-5, and inhibit its activation of the IFN- $\lambda$  promoter. *Proc. Natl. Acad. Sci.* **101**, 17264–17269 (2004).
  82. Kato, H. *et al.* Cell Type-Specific Involvement of RIG-I in Antiviral Response. *Immunity* **23**, 19–28 (2005).
  83. Loo, Y. *et al.* Distinct RIG-I and MDA5 Signaling by RNA Viruses in Innate Immunity. *J. Virol.* **82**, 335–345 (2008).
  84. Kato, H. *et al.* Differential roles of MDA5 and RIG-I helicases in the recognition of RNA viruses. *Nature* **441**, 101–105 (2006).
  85. Feng, Q. *et al.* MDA5 Detects the Double-Stranded RNA Replicative Form in Picornavirus-Infected Cells. *Cell Rep.* **2**, 1187–1196 (2012).
  86. Cárdenas, W. B. *et al.* Ebola virus VP35 protein binds double-stranded RNA and inhibits alpha/beta interferon production induced by RIG-I signaling. *J. Virol.* **80**, 5168–5178 (2006).
  87. Habjan, M. *et al.* Processing of Genome 5' Termini as a Strategy of Negative-Strand RNA Viruses to Avoid RIG-I-Dependent Interferon Induction. *PLoS One* **3**, (2008).
  88. Rehwinkel, J. *et al.* RIG-I Detects Viral Genomic RNA during Negative-Strand RNA Virus Infection. *Cell* **140**, 397–408 (2010).
  89. Pichlmair, A. *et al.* RIG-I-Mediated Antiviral Responses to Single-Stranded RNA Bearing 5'-Phosphates. *Science* (80-. ). **314**, 997–1002 (2006).

90. Weber, M. *et al.* Incoming RNA Virus Nucleocapsids Contain Activate RIG-I and Antiviral Signaling. *Cell Host Microbe* **13**, 336–346 (2013).
91. Schlee, M. *et al.* Recognition of 5' Triphosphate by RIG-I Helicase Requires Short Blunt Double-Stranded RNA as Contained in Panhandle of Negative-Strand Virus. *Immunity* **31**, 25–34 (2009).
92. Schmidt, A. *et al.* 5'-triphosphate RNA requires base-paired structures to activate antiviral signaling via RIG-I. *Proc. Natl. Acad. Sci.* **106**, 12067–12072 (2009).
93. Wang, Y. *et al.* Structural and functional insights into 5' -ppp RNA pattern recognition by the innate immune receptor RIG-I. *Nat. Struct. Mol. Biol.* **17**, (2010).
94. Wu, B. *et al.* Structural Basis for dsRNA Recognition, Filament Formation, and Antiviral Signal Activation by MDA5. *Cell* **152**, 276–289 (2013).
95. Takahashi, K. *et al.* Solution Structures of Cytosolic RNA Sensor MDA5 and LGP2 C-terminal Domains. *J. Biol. Chem.* **284**, 17465–17474 (2009).
96. Jiang, F. *et al.* Structural basis of RNA recognition and activation by innate immune receptor RIG-I. *Nature* **479**, 423–427 (2011).
97. Kowalinski, E. *et al.* Structural Basis for the Activation of Innate Immune Pattern-Recognition Receptor RIG-I by Viral RNA. *Cell* **147**, 423–435 (2011).
98. Kageyama, M., Takahashi, K., Narita, R., Hirai, R. & Yoneyama, M. 55 Amino acid linker between helicase and carboxyl terminal domains of RIG-I functions as a critical repression domain and determines inter-domain conformation. *Biochem. Biophys. Res. Commun.* **415**, 75–81 (2011).
99. Maharaj, N. P., Wies, E., Stoll, A. & Gack, M. U. Conventional Protein Kinase C- $\alpha$  (PKC- $\alpha$ ) and PKC- $\beta$  Negatively Regulate RIG-I Antiviral Signal Transduction. *J. Virol.* **86**, 1358–1371 (2011).
100. Wies, E. *et al.* Dephosphorylation of the RNA Sensors RIG-I and MDA5 by the Phosphatase PP1 Is Essential for Innate Immune Signaling. *Immunity* **38**, 437–449 (2013).
101. Civril, F. *et al.* The RIG-I ATPase domain structure reveals insights into ATP-dependent antiviral signalling. *EMBO Rep.* **12**, 1128–1135 (2011).
102. Oshiumi, H., Miyashita, M., Matsumoto, M. & Seya, T. A Distinct Role of Riplet-Mediated K63-Linked Polyubiquitination of the RIG-I Repressor Domain in Human Antiviral Innate Immune Responses. *PLoS Pathog.* **9**, (2013).
103. Oshiumi, H., Matsumoto, M., Hatakeyama, S. & Seya, T. Riplet/RNF135, a RING finger protein, ubiquitinates RIG-I to promote interferon- $\beta$  induction during the early phase of viral infection. *J. Biol. Chem.* **284**, 807–817 (2009).
104. Myong, S. *et al.* Cytosolic Viral Sensor RIG-I Is a 5'-Triphosphate-Dependent Translocase on. *Science (80-. )*. **323**, 1070–1074 (2009).
105. Peisley, A., Wu, B., Yao, H., Walz, T. & Hur, S. RIG-I Forms Signaling-Competent Filaments in an ATP-dependent, Ubiquitin-Independent Manner. *Mol. Cell* **51**, 573–583 (2013).

106. Patel, J. R. *et al.* ATPase-driven oligomerization of RIG-I on RNA allows optimal activation of type-I interferon. *EMBO Rep.* **14**, 1–8 (2013).
107. Wu, B. *et al.* Molecular Imprinting as a Signal-Activation Mechanism of the Viral RNA Sensor RIG-I. *Mol. Cell* **55**, 511–523 (2014).
108. Peisley, A., Wu, B., Xu, H., Chen, Z. J. & Hur, S. Structural basis for ubiquitin-mediated antiviral signal activation by RIG-I. *Nature* **509**, 110–4 (2014).
109. Hou, F. *et al.* MAVS Forms Functional Prion-like Aggregates to Activate and Propagate Antiviral Innate Immune Response. *Cell* **146**, 448–461 (2011).
110. Tang, E. D. & Wang, C. Y. TRAF5 is a downstream target of MAVS in antiviral innate immune signaling. *PLoS One* **5**, (2010).
111. Takamatsu, S. *et al.* Functional Characterization of Domains of IPS-1 Using an Inducible Oligomerization System. *PLoS One* **8**, (2013).
112. Seth, R. B., Sun, L., Ea, C. & Chen, Z. J. Identification and Characterization of MAVS, a Mitochondrial Antiviral Signaling Protein that Activates NF- $\kappa$ B and IRF3. *Cell* **122**, 669–682 (2005).
113. Gack, M. U. *et al.* TRIM25 RING-finger E3 ubiquitin ligase is essential for RIG-I-mediated antiviral activity. *Nature* **446**, 916–920 (2007).
114. Shigemoto, T. *et al.* Identification of Loss of Function Mutations in Human Genes Encoding RIG-I and MDA5. *J. Biol. Chem.* **284**, 13348–13354 (2009).
115. Gack, M. U. *et al.* Roles of RIG-I N-terminal tandem CARD and splice variant in TRIM25-mediated antiviral signal transduction. *Proc. Natl. Acad. Sci. U. S. A.* **105**, 16743–16748 (2008).
116. Zeng, W. *et al.* Reconstitution of the RIG-I pathway reveals a signaling role of unanchored polyubiquitin chains in innate immunity. *Cell* **141**, 315–330 (2010).
117. Sanchez, J. G. *et al.* Mechanism of TRIM25 Catalytic Activation in the Antiviral RIG-I Pathway. *Cell Rep.* **16**, 1–11 (2016).
118. Gao, D. *et al.* REUL Is a Novel E3 Ubiquitin Ligase and Stimulator of Retinoic-Acid-Inducible Gene-1. *PLoS One* **4**, (2009).
119. Yan, J., Li, Q., Mao, A., Hu, M. & Shu, H. TRIM4 modulates type I interferon induction and cellular antiviral response by targeting RIG-I for K 63 -linked ubiquitination. *J. Mol. Cell Biol.* **6**, 154–163 (2014).
120. Sun, X. *et al.* A Hierarchical Mechanism of RIG-I Ubiquitination Provides Sensitivity, Robustness and Synergy in Antiviral Immune Responses. *Sci. Rep.* **6**, 1–15 (2016).
121. Kuniyoshi, K. *et al.* Pivotal role of RNA-binding E3 ubiquitin ligase MEX3C in RIG-I-mediated antiviral innate immunity. *Proc. Natl. Acad. Sci. U. S. A.* **111**, 5646–51 (2014).
122. Shi, Y. *et al.* Ube2D3 and Ube2N are essential for RIG-I-mediated MAVS aggregation in antiviral innate immunity. *Nat. Commun.* **8**, 1–14 (2017).
123. Cadena, C. *et al.* Ubiquitin-Dependent and -Independent Roles of E3 Ligase RIPLET in

- Innate Immunity. *Cell* **177**, 1–14 (2019).
124. Hayman, T. J. *et al.* RIPLET, and not TRIM25, is required for endogenous RIG-I-dependent antiviral responses. *Immunol. Cell Biol.* 1–13 (2019). doi:10.1111/imcb.12284
  125. Okamoto, M., Kouwaki, T., Fukushima, Y. & Oshiumi, H. Regulation of RIG-I Activation by K63-Linked Polyubiquitination. *Frontiers in Immunology* **8**, 6–11 (2018).
  126. Anchisi, S., Guerra, J. & Garcin, D. RIG-I ATPase Activity and Discrimination of Self-RNA versus Non-Self-RNA. *MBio* **6**, 1–12 (2015).
  127. Lässig, C. *et al.* ATP hydrolysis by the viral RNA sensor RIG-I prevents unintentional recognition of self-RNA. *Elife* **4**, e10859 (2015).
  128. Devarkar, S. C. *et al.* Structural basis for m7G recognition and 2'-O-methyl discrimination in capped RNAs by the innate immune receptor RIG-I. *Proc. Natl. Acad. Sci.* **113**, 596–601 (2016).
  129. Marq, J. B., Kolakofsky, D. & Garcin, D. Unpaired 5' ppp-nucleotides, as found in arenavirus double-stranded RNA panhandles, are not recognized by RIG-I. *J. Biol. Chem.* **285**, 18208–18216 (2010).
  130. Leung, D. W. *et al.* Structural basis for dsRNA recognition and interferon antagonism by Ebola VP35. *Nat. Struct. Mol. Biol.* **17**, 165–172 (2010).
  131. Bale, S. *et al.* Marburg Virus VP35 Can Both Fully Coat the Backbone and Cap the Ends of dsRNA for Interferon Antagonism. *PLoS Pathog.* **8**, 1–12 (2012).
  132. Donelan, N. R., Basler, C. F. & García-sastre, A. A Recombinant Influenza A Virus Expressing an RNA-Binding-Defective NS1 Protein Induces High Levels of Beta Interferon and Is Attenuated in Mice A Recombinant Influenza A Virus Expressing an RNA-Binding-Defective NS1 Protein Induces High Levels of Beta In. *J. Virol.* **77**, 13257–13266 (2003).
  133. Yang, Y. *et al.* Disruption of innate immunity due to mitochondrial targeting of a picornaviral protease precursor. *Proc. Natl. Acad. Sci.* **104**, 7253–7258 (2007).
  134. Wei, C. *et al.* The Hepatitis B Virus X Protein Disrupts Innate Immunity by Downregulating Mitochondrial Antiviral Signaling Protein. *J. Immunol.* **185**, 1158–1168 (2010).
  135. Papon, L. *et al.* The viral RNA recognition sensor RIG-I is degraded during encephalomyocarditis virus (EMCV) infection. *Virology* **393**, 311–318 (2009).
  136. Goswami, R. *et al.* Viral degradasome hijacks mitochondria to suppress innate immunity. *Cell Res.* **23**, 1025–1042 (2013).
  137. Lifland, A. W. *et al.* Human Respiratory Syncytial Virus Nucleoprotein and Inclusion Bodies Antagonize the Innate Immune Response Mediated by MDA5 and MAVS. *J. Virol.* **86**, 8245–8258 (2012).
  138. Dalrymple, N. a, Cimica, V. & Mackow, E. R. Dengue Virus NS Proteins Inhibit RIG-I / MAVS Signaling by Blocking TBK1 / IRF3 Phosphorylation : Dengue Virus Serotype 1 NS4A Is a Unique Interferon-Regulating Virulence Determinant. *MBio* **6**, 1–12 (2015).



139. Chen, X. *et al.* SARS coronavirus papain-like protease inhibits the type I interferon signaling pathway through interaction with the STING-TRAF3-TBK1 complex. *Protein Cell* **5**, 369–381 (2014).
140. Wang, S., Wang, K., Lin, R. & Zheng, C. Herpes Simplex Virus 1 Serine/Threonine Kinase US3 Hyperphosphorylates IRF3 and Inhibits Beta Interferon Production. *J. Virol.* **87**, 12814–12827 (2013).
141. van Kasteren, P. B. *et al.* Arterivirus and Nairovirus Ovarian Tumor Domain-Containing Deubiquitinases Target Activated RIG-I To Control Innate Immune Signaling. *J. Virol.* **86**, 773–785 (2011).
142. Liu, Y., Olagnier, D. & Lin, R. Host and viral modulation of RIG-I-mediated antiviral immunity. *Front. Immunol.* **7**, 1–12 (2017).
143. Gupta, S. *et al.* Herpesvirus deconjugases inhibit the IFN response by promoting TRIM25 autoubiquitination and functional inactivation of the RIG-I signalosome. *PLoS Pathog.* **14**, 1–24 (2018).
144. Mibayashi, M. *et al.* Inhibition of Retinoic Acid-Inducible Gene I-Mediated Induction of Beta Interferon by the NS1 Protein of Influenza A Virus. *J. Virol.* **81**, 514–524 (2007).
145. Gack, M. U. *et al.* Influenza A Virus NS1 Targets the Ubiquitin Ligase TRIM25 to Evade Recognition by the Host Viral RNA Sensor RIG-I. *Cell Host Microbe* **5**, 439–449 (2009).
146. Rajsbaum, R. *et al.* Species-Specific Inhibition of RIG-I Ubiquitination and IFN Induction by the Influenza A Virus NS1 Protein. *PLoS Pathog.* **8**, (2012).
147. Koliopoulos, M. G. *et al.* Molecular mechanism of influenza A NS1-mediated TRIM25 recognition and inhibition. *Nat. Commun.* **9**, (2018).
148. Sánchez-Aparicio, M. T., Feinman, L. J., García-Sastre, A. & Shaw, M. L. Paramyxovirus V Proteins Interact with the RIG-I/TRIM25 Regulatory Complex and Inhibit RIG-I Signaling. *J. Virol.* **92**, 1–21 (2018).
149. Lee, N.-R. *et al.* Human Respiratory Syncytial Virus NS1 Targets TRIM25 to Suppress RIG-I Ubiquitination and Subsequent RIG-I-Mediated Antiviral Signaling. *Viruses* **10**, 716 (2018).
150. Hu, Y. *et al.* The Severe Acute Respiratory Syndrome Coronavirus Nucleocapsid Inhibits Type I Interferon Production by Interfering with TRIM25-Mediated RIG-I Ubiquitination. *J. Virol.* **91**, 1–15 (2017).
151. Manokaran, G., Finol, E., Wang, C. & Gunaratne, J. Dengue subgenomic RNA binds TRIM25 to inhibit interferon expression for epidemiological fitness. *Science (80-. ).* **350**, 217–222 (2015).
152. Inn, K. S. *et al.* Linear Ubiquitin Assembly Complex Negatively Regulates RIG-I- and TRIM25-Mediated Type I Interferon Induction. *Mol. Cell* **41**, 354–365 (2011).
153. van Tol, S., Hage, A., Giraldo, M. I., Bharaj, P. & Rajsbaum, R. The TRIMendous Role of TRIMs in Virus – Host Interactions. *Vaccines* **5**, 1–38 (2017).
154. van Gent, M., Sparrer, K. M. J. & Gack, M. U. TRIM Proteins and Their Roles in

- Antiviral Host Defenses. *Annu. Rev. Virol.* **5**, 385–405 (2018).
155. Esposito, D., Koliopoulos, M. G. & Rittinger, K. Structural determinants of TRIM protein function. *Biochem. Soc. Trans.* **45**, 183–191 (2017).
  156. Short, K. M. & Cox, T. C. Subclassification of the RBCC/TRIM superfamily reveals a novel motif necessary for microtubule binding. *J. Biol. Chem.* **281**, 8970–8980 (2006).
  157. Ozato, K., Shin, D.-M., Chang, T.-H. & Morse, H. C. TRIM family proteins and their emerging roles in innate immunity. *Nat. Rev. Immunol.* **8**, 849–860 (2008).
  158. Kerscher, O., Felberbaum, R. & Hochstrasser, M. Modification of Proteins by Ubiquitin and Ubiquitin-Like Proteins. *Annu. Rev. Cell Dev. Biol.* **22**, 159–180 (2006).
  159. Baker, R. T. & Board, P. G. The human ubiquitin gene family: structure of a gene and pseudogenes from the Ub B subfamily. *Nucleic Acids Res.* **15**, 443–463 (1987).
  160. Iwai, K., Fujita, H. & Sasaki, Y. Linear ubiquitin chains: NF- $\kappa$ B signalling, cell death and beyond. *Nat. Rev. Mol. Cell Biol.* **15**, 503–508 (2014).
  161. Ye, Y. & Rape, M. Building ubiquitin chains: E2 enzymes at work. *Nat. Rev. Mol. Cell Biol.* **10**, 755–764 (2009).
  162. Komander, D. & Rape, M. The Ubiquitin Code. *Annu. Rev. Biochem.* **81**, 203–229 (2012).
  163. Sloper-Mould, K. E., Jemc, J. C., Pickart, C. M. & Hicke, L. Distinct Functional Surface Regions on Ubiquitin. *J. Biol. Chem.* **276**, 30483–30489 (2001).
  164. Winston, J. T. *et al.* The SCF $\beta$ -TRCP-ubiquitin ligase complex associates specifically with phosphorylated destruction motifs in I $\kappa$ B $\alpha$  and  $\beta$ -catenin and stimulates I $\kappa$ B $\alpha$  ubiquitination in vitro. *Genes Dev.* **13**, 270–283 (2008).
  165. Carthagena, L. *et al.* Human TRIM Gene Expression in Response to Interferons. *PLoS One* **4**, (2009).
  166. Rajsbaum, R., Stoye, J. P. & Garra, A. O. Type I interferon-dependent and -independent expression of tripartite motif proteins in immune cells. *Eur. J. Immunol.* **38**, 619–630 (2008).
  167. Versteeg, G. a. *et al.* The E3-Ligase TRIM Family of Proteins Regulates Signaling Pathways Triggered by Innate Immune Pattern-Recognition Receptors. *Immunity* **38**, 384–398 (2013).
  168. Hu, M. M., Liao, C. Y., Yang, Q., Xie, X. Q. & Shu, H. B. Innate immunity to RNA virus is regulated by temporal and reversible sumoylation of RIG-I and MDA5. *J. Exp. Med.* **214**, 973–989 (2017).
  169. Zhao, C. *et al.* The E3 Ubiquitin Ligase TRIM40 Attenuates Antiviral Immune Responses by Targeting MDA5 and RIG-I. *Cell Rep.* **21**, 1613–1623 (2017).
  170. Tan, P. *et al.* Assembly of the WHIP-TRIM14-PPP6C Mitochondrial Complex Promotes RIG-I-Mediated Antiviral Article Assembly of the WHIP-TRIM14-PPP6C Mitochondrial Complex Promotes RIG-I-Mediated Antiviral Signaling. *Mol. Cell* **68**,

293–307 (2017).

171. Zhou, Z. *et al.* TRIM14 is a mitochondrial adaptor that facilitates retinoic acid-inducible gene-I – like receptor-mediated innate immune response. *Proc* 245–254 (2013). doi:10.1073/pnas.1316941111
172. Liu, B. *et al.* The ubiquitin E3 ligase TRIM31 promotes aggregation and activation of the signaling adaptor MAVS through Lys63-linked polyubiquitination. *Nat. Immunol.* **18**, (2017).
173. Yang, B., Wang, J., Wang, Y. & Zhou, H. Novel Function of Trim44 Promotes an Antiviral Response by Stabilizing VISA. *J. Immunol.* **190**, 3613–3619 (2013).
174. Qin, Y. *et al.* TRIM9 short isoform preferentially promotes DNA and RNA virus-induced production of type I interferon by recruiting GSK3  $\beta$  to TBK1. *Cell Res.* **26**, 613–628 (2016).
175. Ran, Y. *et al.* Autoubiquitination of TRIM26 links TBK 1 to NEMO in RLR-mediated innate antiviral immune response. *J. Mol. Cell Biol.* **8**, 31–43 (2016).
176. Arimoto, K. *et al.* Polyubiquitin conjugation to NEMO by tripartite motif protein 23 (TRIM23) is critical in antiviral defense. *Proc. Natl. Acad. Sci.* **107**, 15856–15861 (2010).
177. Lee, Y., Song, B., Park, C. & Kwon, K. TRIM11 Negatively Regulates IFN $\beta$  Production and Antiviral Activity by Targeting TBK1. *PLoS One* **8**, (2013).
178. Yap, M. W., Nisole, S., Lynch, C. & Stoye, J. P. Trim5 $\alpha$  protein restricts both HIV-1 and murine leukemia virus. *Proc. Natl. Acad. Sci.* **101**, 10786–10791 (2004).
179. Stremlau, M., Owens, C. M. & Perron, M. J. The cytoplasmic body component TRIM5 $\alpha$  restricts HIV-1 infection in Old World monkeys. *Nature* **427**, 848–853 (2004).
180. Wu, X., Anderson, J. L., Campbell, E. M., Joseph, A. M. & Hope, T. J. Proteasome inhibitors uncouple rhesus TRIM5 $\alpha$  restriction of HIV-1 reverse transcription and infection. *Proc. Natl. Acad. Sci.* **103**, 7465–7470 (2006).
181. Javanbakht, H. *et al.* Characterization of TRIM5 $\alpha$  trimerization and its contribution to human immunodeficiency virus capsid binding. *Virology* **353**, 234–246 (2006).
182. Yuan, T., Yao, W., Tokunaga, K., Yang, R. & Sun, B. An HIV-1 capsid binding protein TRIM11 accelerates viral uncoating. *Retrovirology* 1–14 (2016). doi:10.1186/s12977-016-0306-5
183. Yuan, T., Yao, W., Huang, F., Sun, B. & Yang, R. The Human Antiviral Factor TRIM11 Is under the Regulation of HIV-1 Vpr. *PLoS One* **9**, (2014).
184. Pflug, A., Guilligay, D., Reich, S. & Cusack, S. Structure of influenza A polymerase bound to the viral RNA promoter. *Nature* **516**, 355–360 (2014).
185. Fu, B. *et al.* TRIM32 Senses and Restricts Influenza A Virus by Ubiquitination of PB1 Polymerase. *PLoS Pathog.* **11**, 1–23 (2015).
186. Liu, B., Li, N. L., Shen, Y. & Bao, X. The C-Terminal Tail of TRIM56 Dictates Antiviral Restriction of Influenza A and B Viruses by Impeding Viral RNA Synthesis. *J. Virol.* **90**, 4369–4382 (2016).

187. Meyerson, N. R. *et al.* Nuclear TRIM25 Specifically Targets Influenza Virus Ribonucleoproteins to Block the Onset of RNA Chain Elongation. *Cell Host Microbe* **22**, 627-638.e7 (2017).
188. Fagerberg, L. *et al.* Analysis of the Human Tissue-specific Expression by Genome-wide Integration of Transcriptomics and Antibody-based Proteomics. *Mol. Cell. Proteomics* **13**, 397–406 (2013).
189. Yang, Y., Huang, Y., Yu, Y., Yang, M. & Zhou, S. RING domain is essential for the antiviral activity of TRIM25 from orange spotted grouper. *Fish Shellfish Immunol.* **55**, 304–314 (2016).
190. Feng, Z. Q. *et al.* Molecular characterization, tissue distribution and expression analysis of TRIM25 in Gallus gallus domesticus. *Gene* **561**, 138–147 (2015).
191. Wei, Y. *et al.* TRIM25 identification in the Chinese goose: Gene structure, tissue expression profiles, and antiviral immune responses in vivo and in vitro. *Biomed Res. Int.* **2016**, (2016).
192. Orimo, A., Inoue, S., Ikeda, K., Noji, S. & Muramatsu, M. Molecular Cloning, Structure, and Expression of Mouse Estrogen-responsive Finger Protein Efp. *J. Biol. Chem.* **270**, 24406–24413 (1995).
193. Sanchez, J. G., Okreglicka, K., Chandrasekaran, V., Welker, J. M. & Sundquist, W. I. The tripartite motif coiled-coil is an elongated antiparallel hairpin dimer. *Proc. Natl. Acad. Sci. U. S. A.* **111**, (2014).
194. Koliopoulos, M. G., Esposito, D., Christodoulou, E., Taylor, I. A. & Rittinger, K. Functional role of TRIM E3 ligase oligomerization and regulation of catalytic activity. *EMBO J.* 1–15 (2016). doi:10.15252/embj.201593741
195. D’Cruz, A. A. *et al.* Crystal structure of the TRIM25 B30.2 (PRYSPRY) domain: a key component of antiviral signalling. *Biochem. J.* **456**, 231–240 (2013).
196. Cruz, A. A. D. *et al.* Identification of a second binding site on the TRIM25 B30.2 domain. *Biochem. J.* **475**, 429–440 (2018).
197. Inoue, S. *et al.* Genomic binding-site cloning reveals an estrogen-responsive gene that encodes a RING finger protein. *Proc. Natl. Acad. Sci. U. S. A.* **90**, 11117–11121 (1993).
198. Orimo, A. *et al.* Underdeveloped uterus and reduced estrogen responsiveness in mice with disruption of the estrogen-responsive finger protein gene, which is a direct target of estrogen receptor alpha. *Proc. Natl. Acad. Sci. U. S. A.* **96**, 12027–12032 (1999).
199. Nakajima, A. *et al.* Ligand-dependent transcription of estrogen receptor  $\alpha$  is mediated by the ubiquitin ligase EFP. *Biochem. Biophys. Res. Commun.* **357**, 245–251 (2007).
200. Dong, X.-Y. *et al.* Oestrogen causes ATBF1 protein degradation through the oestrogen-responsive E3 ubiquitin ligase EFP. *Biochem. J.* **444**, 581–90 (2012).
201. Zhao, K.-W. *et al.* Oestrogen causes degradation of KLF5 by inducing the E3 ubiquitin

- ligase Efp in ER-positive breast cancer cells. *Biochem. J.* **437**, 323–33 (2011).
202. Urano, T. *et al.* Efp targets 14-3-3 sigma for proteolysis and promotes breast tumour growth. *Nature* **417**, 871–875 (2002).
  203. Ueyama, K. *et al.* Knockdown of Efp by DNA-modified small interfering RNA inhibits breast cancer cell proliferation and in vivo tumor growth. *Cancer Gene Ther.* **17**, 624–632 (2010).
  204. Walsh, L. A. *et al.* An Integrated Systems Biology Approach Identifies TRIM25 as a Key Determinant of Breast Cancer Metastasis. *Cell Rep.* **20**, 1623–1640 (2017).
  205. Kasthuber, E. R. & Lowe, S. W. Putting p53 in Context. *Cell* **170**, 1062–1078 (2017).
  206. Qin, Y., Cui, H. & Zhang, H. Overexpression of TRIM25 in Lung Cancer Regulates Tumor Cell Progression. *Technol. Cancer Res. Treat.* 1–9 (2015).  
doi:10.1177/1533034615595903
  207. Zhang, P. *et al.* TRIM25 has a dual function in the p53/Mdm2 circuit. *Oncogene* **34**, 1–10 (2015).
  208. Takayama, K. I. *et al.* TRIM25 enhances cell growth and cell survival by modulating p53 signals via interaction with G3BP2 in prostate cancer. *Oncogene* **37**, 2165–2180 (2018).
  209. Zhu, Z. *et al.* TRIM25 blockade by RNA interference inhibited migration and invasion of gastric cancer cells through TGF- $\beta$  signaling. *Sci. Rep.* 1–8 (2016).  
doi:10.1038/srep19070
  210. Dai, T., Xue, Y., Li, X., Zheng, N. & Sun, N. Tripartite motif containing 25 promotes proliferation and invasion of colorectal cancer cells through TGF- $\beta$  signaling. *Biosci. Rep.* **37**, BSR20170805 (2017).
  211. Wang, Q. *et al.* TRIM25 Is Required for the Antiviral Activity of Zinc Finger Antiviral Protein. *J. Virol.* **91**, 1–16 (2017).
  212. Li, M. M. H. *et al.* TRIM25 Enhances the Antiviral Action of Zinc-Finger Antiviral Protein (ZAP). *PLoS Pathog.* **13**, 1–25 (2017).
  213. Nguyen, N. T. H., Now, H., Kim, W.-J., Kim, N. & Yoo, J.-Y. Ubiquitin-like modifier FAT10 attenuates RIG-I mediated antiviral signaling by segregating activated RIG-I from its signaling platform. *Sci. Rep.* **6**, 23377 (2016).
  214. Castello, A. *et al.* Insights into RNA Biology from an Atlas of Mammalian mRNA-Binding Proteins. *Cell* **149**, 1393–1406 (2012).
  215. Kwon, S. C. *et al.* The RNA-binding protein repertoire of embryonic stem cells. *Nat. Struct. Mol. Biol.* **20**, 1122–30 (2013).
  216. Choudhury, N. R. *et al.* Trim25 Is an RNA-Specific Activator of Lin28a/TuT4-Mediated Uridylation. *Cell Rep.* **9**, 1265–1272 (2014).
  217. Chang, H., Triboulet, R., Thornton, J. E. & Gregory, R. I. A role for the Perlman syndrome exonuclease Dis3l2 in the Lin28-let-7 pathway. *Nature* **497**, 244–248 (2013).

218. Choudhury, N. R. & Michlewski, G. Quantitative identification of proteins that influence miRNA biogenesis by RNA pull-down – SILAC mass spectrometry (RP–SMS). *Methods* **152**, 12–17 (2019).
219. Choudhury, N. R. *et al.* RNA-binding activity of TRIM25 is mediated by its PRY / SPRY domain and is required for ubiquitination. *BMC Biol.* 1–20 (2017). doi:10.1186/s12915-017-0444-9
220. Meyerson, N. R. *et al.* Nuclear TRIM25 Specifically Targets Influenza Virus Ribonucleoproteins to Block the Onset of RNA Chain Elongation. *Cell Host Microbe* **22**, 627–638.e7 (2017).
221. Hegarat, N., Francois, J.-C. & Praseuth, D. Modern tools for identification of nucleic acid-binding proteins. *Biochimie* **90**, (2008).
222. Langland, J., Pettiford, S. & Jacobs, B. Nucleic Acid Affinity Chromatography: Preparation and Characterization of Double-Stranded RNA Agarose. *Protein Expr. Purif.* **6**, (1995).
223. Wit, E. De *et al.* Efficient generation and growth of influenza virus A / PR / 8 / 34 from eight cDNA fragments. *Virus Res.* **103**, 155–161 (2004).
224. Michlewski, G. & Cáceres, J. F. Antagonistic role of hnRNP A1 and KSRP in the regulation of let-7a biogenesis. *Nat. Struct. Mol. Biol.* **17**, 1011–1018 (2010).
225. Fourmy, D. & Yoshizawa, S. Protein – RNA footprinting: an evolving tool. *WIREs RNA* **3**, 557–566 (2012).
226. Castello, A. *et al.* Comprehensive Identification of RNA-Binding Domains in Human Cells. *Mol. Cell* 1–15 (2016). doi:10.1016/j.molcel.2016.06.029
227. Cruz, A. A. D., Babon, J. J., Norton, R. S., Nicola, N. A. & Nicholson, S. E. Structure and function of the SPRY/B30.2 domain proteins involved in innate immunity. *Protein Sci.* **22**, 1–10 (2013).
228. Kim, D. H. & Rossi, J. J. RNAi mechanisms and applications. *Biotechniques* **44**, 613–616 (2008).
229. O’Connell, M. R. *et al.* Programmable RNA recognition and cleavage by CRISPR/Cas9. *Nature* **516**, 263–266 (2014).
230. Adli, M. The CRISPR tool kit for genome editing and beyond. *Nat. Commun.* **9**, (2018).
231. Schlake, T. & Bode, J. Use of Mutated FLP Recognition Target (FRT) Sites for the Exchange of Expression Cassettes at Defined Chromosomal Loci. *Biochemistry* **33**, 12746–12751 (1994).
232. Estep, J. A., Sternburg, E. L., Sanchez, G. A. & Karginov, F. V. Immunoblot screening of CRISPR/Cas9-mediated gene knockouts without selection. *BMC Mol. Biol.* **17**, 1–7 (2016).
233. Wang, Z., Gerstein, M. & Snyder, M. RNA-Seq: a revolutionary tool for transcriptomics. *Nat. Rev. Genet.* **10**, 57–63 (2009).
234. McGettigan, P. A. Transcriptomics in the RNA-seq era. *Current Opinion in Chemical*

- Biology* **17**, 4–11 (2013).
235. Mann, M. Functional and quantitative proteomics using SILAC. *Nat. Rev. Mol. Cell Biol.* **7**, 952–958 (2006).
  236. Donelan, N. R., Basler, C. F. & García-sastre, A. A Recombinant Influenza A Virus Expressing an RNA-Binding-Defective NS1 Protein Induces High Levels of Beta Interferon and Is Attenuated in Mice. *J. Virol.* **77**, 13257–13266 (2003).
  237. Wang, W. *et al.* RNA binding by the novel helical domain of the influenza virus NS1 protein requires its dimer structure and a small number of specific basic amino acids. *RNA* **5**, 195–205 (1999).
  238. Seitz, C., Frensing, T., Höper, D., Kochs, G. & Reichl, U. High yields of influenza A virus in Madin-Darby canine kidney cells are promoted by an insufficient interferon-induced antiviral state. *J. Gen. Virol.* **91**, 1754–1763 (2010).
  239. Garcia-Moreno, M. *et al.* System-wide Profiling of RNA-Binding Proteins Uncovers Key Regulators of Virus Infection. *Mol. Cell* 1–16 (2019). doi:10.1016/j.molcel.2019.01.017
  240. Sanchez, J. G. *et al.* TRIM25 Binds RNA to Modulate Cellular Anti-viral Defense. *J. Mol. Biol.* **430**, 5280–5293 (2018).
  241. Rhodes, D. A., De Bono, B. & Trowsdale, J. Relationship between SPRY and B30.2 protein domains. Evolution of a component of immune defence? *Immunology* **116**, 411–417 (2005).
  242. Williams, F. P., Haubrich, K., Perez-Borrajero, C. & Hennig, J. Emerging RNA-binding roles in the TRIM family of ubiquitin ligases. *Biol. Chem.* (2019). doi:10.1515/hsz-2019-0158
  243. Lin, H. *et al.* The long noncoding RNA Lnczc3h7a promotes a TRIM25-mediated RIG-I antiviral innate immune response. *Nat. Immunol.* (2019). doi:10.1038/s41590-019-0379-0
  244. Sato, W. *et al.* Efp promotes in vitro and in vivo growth of endometrial cancer cells along with the activation of nuclear factor- $\kappa$ B signaling. *PLoS One* **13**, (2018).
  245. Castanier, C. *et al.* MAVS ubiquitination by the E3 ligase TRIM25 and degradation by the proteasome is involved in type I interferon production after activation of the antiviral RIG-I-like receptors. *BMC Biol.* **10**, 44 (2012).
  246. O’Hagan, D. T., Ott, G. S., Van Nest, G., Rappuoli, R. & Del Giudice, G. The history of MF59.sup.[R] adjuvant : a phoenix that arose from the ashes. *Expert Rev. Vaccines* **12**, (2013).